Ministry of Higher Education & Scientiflic Research

University of Kerbala

College of Engineering

Building and Testing a Parabolic Trough Collector to Generate Steam

A Thesis

Submitted to the College of Engineering

University of Kerbala in Partial Fulfillment of the Requirements for the Degree of Master of Science in Mechanical Engineering

By

Ahmed Abdulrazaq Shaheed

(B.Sc. 2005)

Supervised By

Asst. Prof. Dr. Mohammed Hasan Abbood   Asst. Prof. Dr. Raoof Mohammed Radhi

January 2017   **ربيع الآخر 1439ه**

بِسْمِ ٱللَّهِ ٱلرَّحْمَٰنِ ٱلرَّحِيمِ

وَٱلشَّمْسُ تَجْرِى لِمُسْتَقَرٍّ لَّهَا ۚ ذَٰلِكَ تَقْدِيرُ ٱلْعَزِيزِ ٱلْعَلِيمِ ﴿٣٨﴾ وَٱلْقَمَرَ قَدَّرْنَٰهُ مَنَازِلَ حَتَّىٰ عَادَ كَٱلْعُرْجُونِ ٱلْقَدِيمِ ﴿٣٩﴾ لَا ٱلشَّمْسُ يَنۢبَغِى لَهَآ أَن تُدْرِكَ ٱلْقَمَرَ وَلَا ٱلَّيْلُ سَابِقُ ٱلنَّهَارِ ۚ وَكُلٌّ فِى فَلَكٍ يَسْبَحُونَ ﴿٤٠﴾

صدق الله العظيم

سورة يس

ACKNOWLEDGMENTS

Abstract

Three parabolic trough solar collectors (PTC) were constructed, operated and tested in order to generate hot water and steam at moderate temperatures. In this study, an experimental investigation for testing the performance of a PTC array (3.73 m^2 total aperture area) is presented. The model, which is made up of reflector surfaces, support structure with sun manual tracking and absorber pipes, was fabricated using a locally sourced material. The collectors are made of aluminium with the aim of having a lightweight and weather resistant. The design of the collectors considers unshading receivers, whereas sun manual tracker has been developed (using two-axis) to track the beam solar radiation. The experimental tests have been carried out in Najaf City climatic conditions (32.02º N, 44.33º E) during selective days of the month August. The data measured were collected for eight days, the 5th, 6th, 8th – 13th of Aug 2016. The tests were performed using the outdoor measurements to evaluate the useful heat gain and the instantaneous thermal efficiency. In the performance analysis of the PTC array, the effects of collector inlet temperature, ambient conditions, two types of a receiver and the variation in mass flow rate of the working fluid were investigated. The thermal performance of PTC was evaluated according to the Standard ASHRAE 93-1986 (RA 91) and the efficiency curve for the PTC was estimated. A peak efficiencies close to (50%, 18.8%) were obtained for solar collectors with evacuated and non-evacuated glass receiver respectively at higher flow rate. Steam was generated with a temperature excesses 152 ^{0}C and a pressure of 4barG. The collector efficiency equation obtained in the present work compares well with the other reported literature. The final results establish that the technical of using PTC is feasibility for applications requiring thermal energy at temperatures up to 152 ºC.

Table of Contents

Nomenclature

Latin Symbols

Symbol	Description	units
$h_{c,r-g}$	Convection Heat Transfer Coefficient between Receiver and Glass Cover	W/m².°C
$h_{r,g-a}$	Radiation Heat Transfer Coefficient between Glass and Ambient Air	W/m².°C
$h_{r,r-g}$	Radiation Heat Transfer Coefficient between Receiver and Glass Cover	W/m².°C
$h_{r,r-g}$	Radiation Heat Transfer Coefficient between Receiver and Glass Cover	W/m².°C
h_w	Wind Heat Transfer Coefficient	W/m².°C
A_g	Area of Glass Cover	m²
A_r	Area of Receiver	m²
D_g	Glass Cover Diameter	m
D_r	Receiver Diameter	m
F_R	Heat Removal Factor	-
I_b	Beam Radiation	W/m²
Q_u	Useful Heat Gain	W
T_a	Ambient Temperature	°C
$T_{f,i}$	Inlet Fluid Temperature to the Collector	°C
$T_{f,o}$	Exit Fluid Temperature from the Collector	°C
T_g	Temperature of the Glass Cover	°C
U_L	Heat Loss Coefficient	W/m².°C
$\dot{m}_f$	Mass Flow Rate	L/hr.
r_r	Rim Radius	m
w_a	Collector Aperture	m²
C_p	Specific Heat	kJ/kg.°C
I_{sc}	Solar Constant	W/m²
Ra	Rayleigh Number	-
Re	Reynolds Number	-

C	Collector Concentration Ratio	-
Nu	Nusselt Number	-
Pr	Prandtl Number	-
S	Absorbed Solar Radiation Per Unit Area	J/m^2
V	Velocity	m/s
f	Parabola Focal Length	m
k	Thermal Conductivity	W/m .$^\circ$C
r	Local Radius	m
$K(\theta)$	Incident Angle Modifier	-

Greek Symbols

ε_g	Emitance of Glass	-
ε_r	Emittance of Receiver	-
η_o	Optical Efficiency	-
η_{th}	Thermal Collector Efficiency	-
$\eta_{thi.}$	Thermal Instantaneous Efficiency	-
θ_m	Acceptance Half-Angle	Degree
θ_r	Rim Angle	Degree
ρ_m	Mirror Reflectance	-
τ_g	Transmittance of Glass	-
$\emptyset$	Latitude Angle	Degree
v	Kinematic Viscosity	m^2/s
α	Absorptance of Receiver	-
γ	Intercept Factor	-
δ	Solar Declination	Degree
θ	Angle of Incidence	Degree
μ	Dynamic Viscosity	kg/m. s
ρ	Density	kg/m^3

σ	Stefan Boltzman Constant	W/m^2.K^4

Abbreviation

barG	Bar gauge
PV	Photovoltaic
CSP	Concentrating Solar Power
PTC	Parabolic Trough Solar Collector
SEGS	Solar Electric Generating Systems
DSG	Direct Steam Generation
DISS	Direct Solar Steam
HTF	Heat Transfer Fluid
PSA	Plataforma Solar De Almería
A.C.M.P	Aluminum Composite Material Panels

Chapter One
Introduction

1.1 General

In the modern world, energy is the main necessity for real human culture. The country where more energy generates is more advanced than another. Energy is vital for execution any work. All of the energy resources employed today can be categorized into two collections; renewable and non-renewable. Renewable energy is coming from natural procedures, which are resupply constantly. In its various varieties, it derives directly from the sun.

Energy produced from the wind, solar, tidal, ocean, biomass, hydropower, geothermal resources, bio fuels and hydrogen represent renewable sources. Non-renewable energy is the energy resources that cannot return supply soon such as oil, coal, natural gas and petroleum. Renewable and non-renewable energy resources can be utilized to yield supplementary energy resources as electricity[1].

Within the last hundred years, fossil fuel has delivered almost all of our energy needs because they are much cheaper and far more convenient than the renewable energy resources. Another serious problem related to combustion of Non-renewable energy like fossil fuels has caused serious air pollution problems because of large amount of harmful gases into the atmosphere[2]. It has additionally led to global heating. The discharge of huge amounts of waste heat from the power plant has induced thermal pollution in waterways resulting in the devastation of several forms of plant and creature life. Regarding nuclear power plants, additionally, there is concern above the

probability of radioactivity being liberation into the atmosphere and long-term permanent of problems of the removal of radioactive wastes from these plants[3]. Therefore, the renewable energy can be used as an alternate energy resource.

1.2 Solar Technology

Solar energy is clean, unlimited and safe. Even when it is converted into electricity through photovoltaic or thermodynamic plants, it does not produce harmful emissions. Solar technology, for power generation, can be broadly classified into photovoltaic (PV) and concentrating solar power (CSP). In PV technologies, semiconductor materials are used in solar panels to convert photons in sunlight directly to electricity. Whereas, CSP technologies are those that concentrate the sun's energy to heat a working fluid (liquid, solid or gas) , it can then be used in a downstream process for electricity generation. A more economical method is using a concentrating solar power technology to meet a significant portion of the future energy demands in an environmentally clean and cost-effective way. In addition, CSP technology is a superb and a viable option as it is not sensitive to drought or to fuel price fluctuations as well as relying upon a secure and local resource: the Sun [4].

Solar concentrating thermal technologies including Parabolic Trough Collector (PTC), Linear Fresnel Reflector System, Power Tower or Central Receiver System, and Dish/Engine system which is one of the recent renewable energy sources that are widely used to provide a non-polluting and permanent energy.

In this thesis, the focus will be on the parabolic trough solar technology, which is the most established and proven technology available today for collecting solar energy.

1.3 Parabolic Trough Solar Collector Technology

Parabolic trough solar collector (PTSC) technology likes the one displayed in figure (1.1) is presently the best validated solar thermal reflector technology. It is a solar technology that turns solar beam irradiance into thermal energy in their linear concentrate device. PTSC utilizations can be split into two teams. The first developed is targeted solar power plants. Presently, several commercial reflectors for such utilizations have been effectively experienced and run. The temperatures achieved in those plants ranging from 300 to 400 ℃. The concentrating solar power plants with PTSC are linked to electric power cycles both directly and indirectly [5]. The next group is intended to supply thermal energy to utilizations that require temperature ranges between 85 and 250 ℃. These utilizations are mostly industrial process heating, such as cleanup, drying out, vaporization, distillation, pasteurization, sterilization, cooking food, amongst others, as well as utilizations with low-temperature heating demand and high intake rates (local warm water, space warming and swimming pond warming), and heat powered refrigeration and chilling [5].

Presently the term "medium temperature reflectors" is utilized to deal with reflectors working in the temperature range of 80 to 250 ℃. Among the goals of solar thermal industry is to build up reflectors that are suited to utilizations in this temperatures range. Until now a few experiences exist because of this temperature range [6]. It's quite common to find commercial processes that use warm water and steam with temperatures range between 80 and 180 ℃. Considering the possible decrease in the utilization of typical energy resources that caused a reduction in the carbon dioxide emissions, studies into solar heating systems that can perform these temperatures levels are of great relevance.

Figure (1.1): Parabolic Trough Collector [7]

1.4 Direct Steam Generation in Parabolic Trough Collector

Many of the PTSC power plants use special oils as a heat transfer fluid that is circulated through receiver pipes. The heated oil is utilized to generate steam by using heat exchangers. The primary features are to make solar power plants more commercially useful to decrease the costs and increase efficiencies. Today's PTSC power plant's heat exchangers raise the creating cost and reduce the efficiency due to losses of the heat transfer. To avoid these disadvantages outcome, new generation of plants are being created to produce steam directly in the reflectors without using a heat exchanger. This technique is named the direct steam generation.

1.5 Methods of Direct Steam Generation

Steam generation through parabolic trough collectors has been given by Kalogirou using three methods [8]:

1. The steam- flash method, in which pressurized water is reheated in the reflector and inflated to steam in a separate vessel, as shown schematically in figure (1.2)
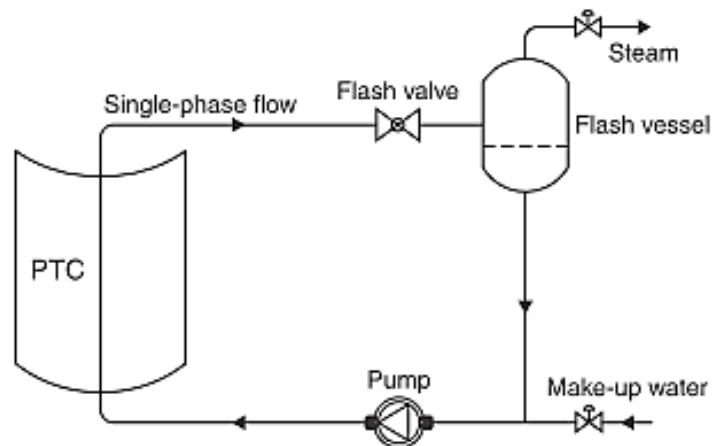
Figure (1.2): The Steam–flash Steam Generation Concept [8].

2. The direct method, in which two-phase flow is provided for the reflector tube so that steam is formed directly, as shown schematically in figure (1.3)

3. The unfired boiler method, in which a fluid is recirculated through the reflector and steam is formed through heat exchanger in unfired boiler, as shown schematically in figure (1.4)
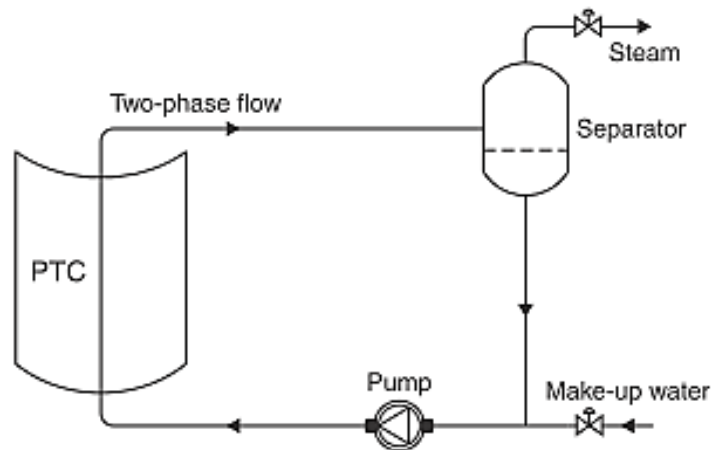
Figure (1.3): The Direct Steam Generation Concept [8].
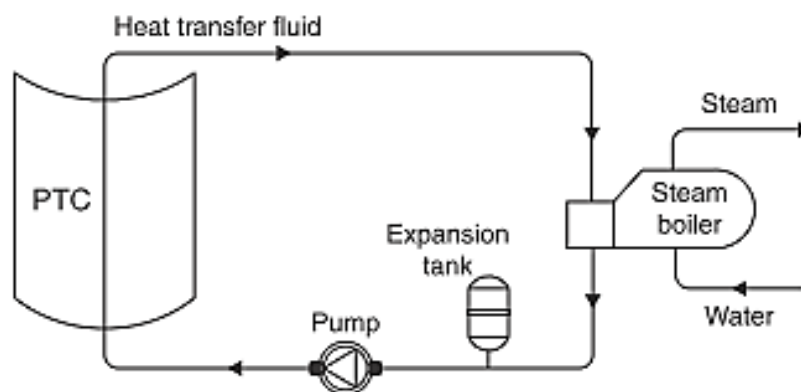
Figure (1.4): The Unfired Boiler Steam Generation Concept [8].

1.6 Direct Steam Generation in power plants

Power plants using direct steam generation possess the possibility for a greater efficiency and lower cost since there will be no heat exchangers for steam production. The parabolic trough collector solar power plants have dangers due to seeping oil leading to fires such as in the main one in Solar Electric Generating Systems where in fact the therminol container exploded

[9]. Therefore, in the direct steam generation, the heat transfer fluid is liquid/steam water and no oil is used. Direct steam generation system is green and much more reliable than traditional parabolic trough collector plants using oil as the heat transfer fluid. Since oil is removed, the plant design will be facile. Finally, the parabolic trough collector solar powered energy plant has a temperature limit of 400°C due to the oil, but in the direct steam generation, this limit can be exceeded leading to greater heat engine efficiencies.

In order to answer some of the concerns about DSG, the DISS (Direct Solar Steam) plant as displayed in figure (1.5) was introduced and an experiment plant built in Spain. This plant has a 0.1 km long reflector array and a 2000 kW capacity. Different procedure alternatives were analyzed in the plant with different pressures. The plant was also used to check starting and stoppage steps and experiment any risk of strain rate of the receiver pipe. The plant performed more than 3500 hrs. time from 1999 to 2001 [10].
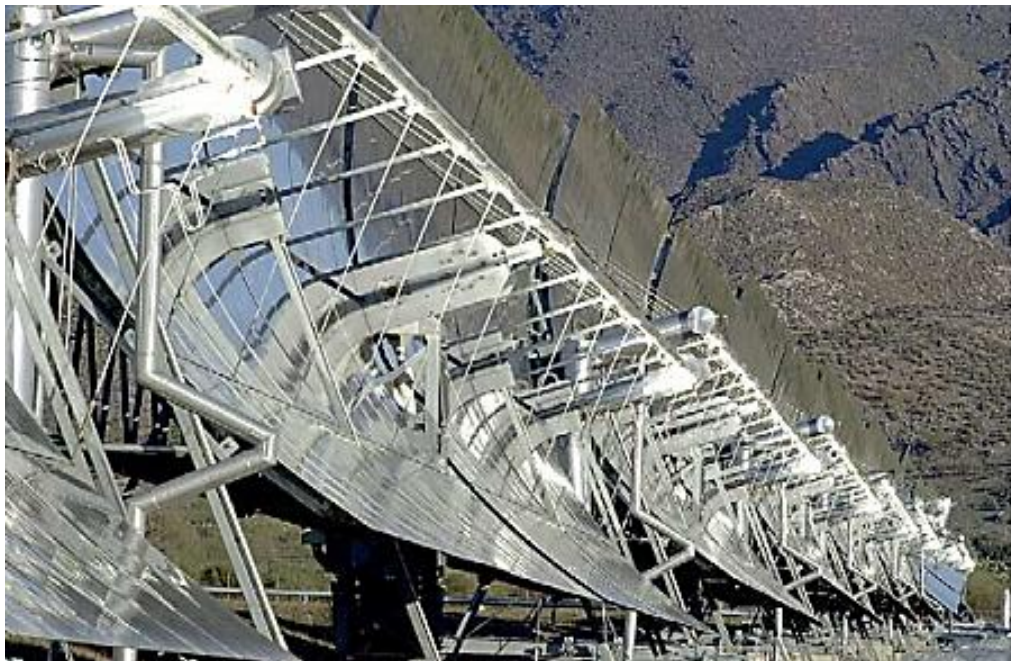
Figure (1.5): Direct Solar Steam Facility [5]

The direct solar steam plant was a milestone for the manufacturing of the direct steam generation solar power plant because the project demonstrated that a direct steam generation solar power plant is possible. The knowledge acquired by this project will be useful for the research workers to design a commercial measured direct steam generation solar power plant. The INDITEP project was introduced for that goal. In Ref. [11], a conceptual design of INDITEP is explained. The design is perfect for a 5 MWe direct steam generation solar power plant. The design includes seven reflector loops with ten reflectors for every loop as displayed in figure (1.6). For an individual loop of reflectors, the first eight reflectors are created for evaporating. The ultimate two reflectors are for superheating. Following the first eight reflectors, which is prior to the superheating section, there's a separator to split up liquid water and steam. Parting is important to get fully superheated vapor at the superheating portion of the reflector loop. There will be remaining saturated liquid water in the separator and that remaining liquid water is re-circulated through the reflector loop.
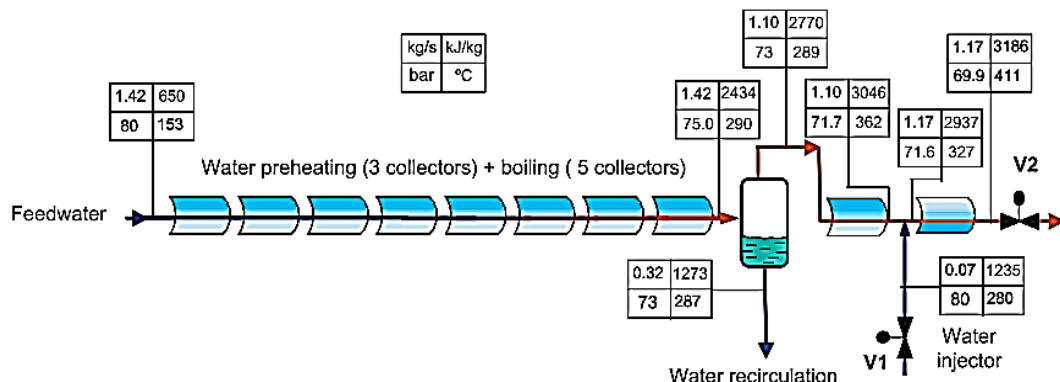
Figure (1.6): Schematic Representation of Solar Array in INDITEP Project [11]

1.7 The Aims of the Thesis

This study aims to

1. Building and testing a model of a parabolic trough solar collector system by using local market materials to generate medium-temperature steam (excess 152 ℃)

2. Examining the thermal performance of the PTC under various receiver tubes and various flow rates.

1.8 Organization of the study

This thesis consists of five chapters. They are briefly introduced as flows:

Chapter One presents a broad background of the parabolic trough technology, including methods of direct steam generation in PTC and its applications.

Chapter Two discusses the previous studies that have been carried out regarding the parabolic trough technology and scope of the present work.

Chapter Three presents a related calculations and the experimental setup of the PTC, and all equipment used in the test are presented in detail.

Chapter Four presents the results and discussion of PTC tests

Chapter Five gives a conclusion of the study along with some recommendations that may be followed for future study.

Chapter Two
Literature Survey

2.1 Introduction

A parabolic trough technology is nowadays the most extended solar system for electricity production or steam generation for industrial processes. The following is a summary of the previous experimental and theoretical work related to the present research in the field of a solar concentrator.

Odeh et al. 1998 [12] carried out a performance analysis of PTC with synthetic oil and water as working fluids. The formulations for the efficiency of solar parabolic trough collectors have been developed based on absorber wall temperature rather than fluid bulk temperature so it can be used to predict the performance of the system with any working fluid. The thermal performance of a trough collector using Syltherm 800 oil as the working fluid has been measured and is used in this study to develop a model of the thermal losses from the collector to evaluate the performance of direct steam generation collectors for different radiation conditions. The thermal losses from the trough collector have been described in terms absorber, emissivity, wind speed, absorber wall temperature and radiation level.

Zarza et al. 2001 [13] investigated updating the DISS (Direct Solar Steam) plant status, which was implemented at the Plataforma Solar de Almería (PSA), and explained operation and maintenance related experience (e.g. main problems confronted and solutions applied) for the plant. The Direct Solar Steam was operated for 2000 hr. from the year 1999 to 2000. The

most important conclusion derived from this is the certainty that direct solar steam generation is possible in parabolic trough collectors with horizontal absorber tubes. Regardless of the practical difficulties faced during this time age, varied experiments have been achieved and worthy experiences have been gained. This experiment during the test ought to notice that the major difficulties faced up until now weren't in the direct steam generation process itself; whatever the conventional equipment used for this.

Geyer et al. 2002 [14] developed a new design of PTC called (Euro Trough) through the development of a generation of solar concentrators and reduce cost. Two types of concentrates (ET 100 & ET 150) were designed and developed to utilize it to generate the steam required for the applications of solar thermal electric power generation. As the electric power generation system in California could complement the use of these models. The rehabilitation of this plant was actually in the years from 2000 to 2002 with using the same materials in the manufacture of the models, but they differ in the lengths of PTC in the area and the number of absorber tubes, with a length of the form (ET150) (148.5m) area ($817.5m^2$) while that of model (ET 100) was long (99.5m) and area ($545m^2$). 14% solar field cost reduction are anticipated due to weight reduction and collector extension to 150 meters.

Eck et al. 2003 [15] Performed experimental and theoretical investigations within the DISS (Direct Solar Steam). The test facility was implemented at the Plataforma Solar de Almerı´a (PSA) in 1997–8. The so-called PSA DISS test facility, was operated for more than 3000 hr. targeting at the optimization of the data regarding the direct steam generation process and the development of this procedure under real solar conditions. The major scientific results of the DISS project were the direct steam generation process is achievable in the PTC, and the recirculation process is the most attractive option for

commercial DSG collector fields. With these scientific results the main targets of the DISS project have been reached. Moreover, a deep understanding of the thermohydraulic behavior of the direct steam generation process in PTC has been executed. Based on the many experimental investigations models dealing with all areas of the direct steam generation process have been developed and implemented in design tools. These tools will be used for the detailed design of commercial DSG collector fields.

Singh et al. 2003 [16] investigated the performance of a PTC and the use of processed data to design a simulated model using the same meteorological data. The results indicated that there would be an equilibrium achieved between the increasing thermal losses with the increasing aperture area, and the increasing optical losses with the decreasing aperture area.

Zarza et al. 2004 [17] investigated the Direct Steam Generation (DSG) process within the DISS (Direct Solar Steam) test facility under real solar conditions. A new prototype of solar system with parabolic trough collectors was implemented at the Plataforma Solar de Almerı´a (PSA, South-East Spain); so-called PSA DISS test facility, to investigate the direct steam generation process under real solar conditions in the parabolic solar collector field. It was operated for more than 3000 hour. The three basic DSG options (i.e. Once through, Recirculation and Injection) have been inspected under real operating conditions in the project DISS. The feasibility of the DSG process in horizontal parabolic trough collectors has been established and and an important know how has been acquired by the project partners regarding the thermo-hydraulic parameters of the water/steam flow in DSG solar fields.

Brooks and Harms 2005 [18] developed a PTC similar in size to smaller-scale commercial modules for use in a South African solar thermal research program. The collector length is 5m, aperture width is 1.5m and rim angle is

82°.Two receivers were fabricated for comparative testing, including one enclosed in an evacuated glass cover. Peak efficiencies of 55.2% and 53.8% were obtained with the unshielded and glass-shielded receivers respectively.

Eck and Zarza 2006 [19] investigated the advantages, disadvantages, and design considerations of a steam cycle operated with saturated steam for the first time. They developed a new design of PTC called INDITEP project located near Seville, Spain (latitude: 37° 24´ N; longitude: 5° 58´ W) , the detailed engineering and design for the first DSG solar thermal power plant was performed for a size of 5 MW. Due to the economics of scale, the plant size was not chosen for cost-effective power generation. However, the size was selected to minimize the financial risks associated with large initial capital investments for potential investors. According to the investigation performed, the saturated steam option has a 4% higher annual net electricity production of the power plant. On the other hand, for the plant size analyzed, the initial investment required by the saturated steam option is of about 5% higher than that of the superheated steam option.

Arasu and Sornakumar 2006 [20] industrialized a PTC for warm water production. The performance of a PTC with warm water production system is studied through tests for one day in a summer season. The PTC works under clogged loop method by circulating the fluid through a well-mixed hot water storage tank. The difference between the water outlet temperature and the water temperature of storage tank are collected amid 9.30 and 16.00 h. The water temperature of storage tank is changed from 35 °C at 9.30 h to 73.84 °C at 16.00 h.

Ming et al. 2006 [21] industrialized lined up tracking PTC centered on tube receiver banding within an evacuated glass receiver, and obtained fundamental radiative and convective heat transfer and mass and energy

balance relations. The experiment is shows that when hot water at 165°C flows through a 6m by 2.3m Parabolic Trough Solar Collector with 900 w/m^2 solar insulation and 0 incident angles, the estimated collector efficiency is about 55%.

Krüger et al. 2008 [22] studied the solar thermal of PTC named solitem parabolic trough reflector-1800 to supply heat for desalination, cooling and electricity production. The finding revealed that thermal experiments of the reflector have exposed comparably low thermal loss but still important optical loss. Completely, the reflector is suitable for medium temperature utilization at 150 to 190°C.

Folaranmi 2009 [23] implemented design, built and operated of a PTC working on solar technology and created focused reflector, the radiation from the sunlight was focused on a black receiver placed at the concentration line of the collector where water is warmed to an extremely high temperature to produce steam. In addition, defines the sunlight tracking system device by manual tracking of the lever at the bottom of the PTC to capture solar energy. The complete PTC is installed on a hinged structure backed with a slotted lever for tracking the PTC to dissimilar angles so the sunlight is continuously directed to the reflector at various time of the day. On the average sunlight and cloud free times, the experiment yields provided high temperature over 200°C.

Hau and Soberanis 2011 [24] built a water heating system for testing with a constant flow limited and a maximum temperature of 55 ^{0}C using water as a working fluid. The performance of a parabolic trough collector (PTC) manufactured in Merida, Yucatán, Mexico, was evaluated under the ANSI/ASHRAE 93-1986 standard. It was found that the maximum efficiency of the collector was 5.43%, with a flow rate of 0.022 kg/s at a direct solar

irradiance with incidence angle 0. The evaluation methodology and design of the system for testing the collector is reported in this research.

Ruby et al. 2012 [25] carried out designing, building, working, and analyzing of a high temperature solar thermal system at a Frito-Lay snack food plant situated in Modesto, California. Within this plant, water at high temperature is generated by a focusing solar reflector, which in turns was utilized to generate around 300 Ib/In^2 (20 kg/cm^2) of steam. In this plant, the steam was utilized for cooking, which contains heating edible oil for cook and warming baking equipment. This steam is also converted into warm water for cleaning and disinfection procedures.

Zhang et al. 2012 [26] design a U-type natural circulation heat pipe system and applied to a PTC. The field experiments were performed to evaluate characteristics of system natural circulation and reliability for generating mid-temperature steam at three working of unfired boiler conditions (0.2 Mpa, 0.5 Mpa and 0.75 Mpa).Thermal performance of heat tube is studied experimentally. An in depth heat transfer examination is implemented on thermal conducts of the system, particularly the solar reflector. The outcomes reveal that the system can produce steam at medium temperature with a pressure up to 0.75 Mpa. The thermal efficiency is found to be 38.52% at pressure of 0.5 Mpa during the summer months.

Valenzuela et al. 2012 [27] performed a numerical study connected to the thermal-hydraulic behavior of solar reflectors to saturated steam generation for industrialized utilizations and heating utilizations considering two various types of PTC, which are available in the market. The first plant is called Capsol, which has an absorber tube with 15 mm inner diameter and the other reflector is called PolyTrough 1200, which has an absorber tube with 25 mm inner

diameter. The purpose of the research is to prove the viability of DSG in the PTC small-sized for industrialized utilizations heat applications demanding steam in the range of 200°C. The mass flow rate and the reflectors -loop length have been enhanced to reach a temperature rise in the reflectors of about 130°C, from 70-200°C, and above 0.5 steam fractions in the outlet. Sensitivity analysis has been implemented to estimate the influence of changeable inlet water pressure, temperatures and irradiance.

Reyes et al. 2012 [28] Implemented designing, building, and assessment of a PTC for warm water and steam production with a length of 4.88 m, an aperture area of 5.8 m^2, and a rim angle of 45. It is designed with an unshielded receiver and without a glass cover in order to reduce both production and transportation costs. The optical efficiency of the reflector is reported. Aforementioned efficiency relies on the optical characteristic of the materials including, the different shortcoming ascending from the structure of the reflector and the geometry of the reflector. The thermal performance of the parabolic trough collector was evaluated as stated by the Standard ASHRAE 93-1986 (RA 91). Peak efficiencies close to 60% were obtained.

Zhang et al. 2013 [29] implemented an experiential research of the heat losses from vacuum U-type tube with a transparent glass cover that installed in a parabolic trough collector natural circulation for producing steam at medium-temperatures. Reflectors experiments were showed to calculate overall heat losses of the tube. Effects of structural features, wind, irradiance, and U-type glazing receiver on the heat losses was examined. The thermal efficiency of the glazing tube was found to be around 79% and 47% in calm and windy days, respectively, at an experiment temperature of around 100 °C, at which the thermal efficiency come to be 79% and 66%, respectively, when

considering the glazing receiver element. The heat losses were increased from 0.183 to 0.255 kW per receiver for the two cases tested.

Alguacil et al. 2014 [30] built, operated, and evaluated a demonstration plant, which used direct steam generation (DSG) in a PTC. So as to attain higher temperatures. The first level warming until 450 ºC and the next level warming until 550 ºC. The model is situated in Seville (Spain) and it yields about 8 MWth of thermal electric power. The project is compound of three major stages; the evaporator reflectors with three arrangement annulus of 800m length, the superheated reflectors with two arrangement annulus of 200m length and the balancing of the project system compound of a laminar valve and an air-cooled condenser. The shown project has been worked and estimated for one year; the main technological tests of the direct steam generation PTC plants such as receiver pipe feasibility, collector interconnection viability and the control stability have been studied and proved in the showing project.

Chiad et al. 2014 [31] performed an experimental study for improving the performance of a parabolic trough collector in terms of minimizing the heating loss, moving of the sun tracker device and efficiencies. The PTC is made from glazing reflector to create the trough (0.8 × 1.8 m) and evacuated glass as receiver placed in the focal line of trough. The performance of parabolic trough collector is assessed using outdoors experimental measurements comprising the energy gained by the storage tank, the useful heating gain and thermal instantaneous efficiency. The water temperature of storage tank varied from 25 ˚C at 9:30h to 94 ˚C at 13:30h. The experimental result shows the average thermal efficiency was 50%, which is fairly acceptable assessment results of a PTC locally.

Al Asfar et al. 2014 [32] designed, constructed and tested a parabolic trough solar collector to assess its performance. The length of the PTC was

6m with an aperture width of 1.67m. The collector's sun tracking was adjusted manually. The peak thermal efficiency obtained during the tests was 22.4%. Steam was generated with a temperature up to 123 ^{0}C and a pressure of 2 bar.

Tayade et al. 2015 [33] investigated the performance of a new parabolic trough collector with hot water generation system through experiments over one full day in a winter period. The design and fabrication of PTC solar warming was performed. The PTC, which was made from collector, collector support, receiver tube and a stand with manual tracking design, was made-up by locally sourced materials for countryside utilizations viewpoint. The thermal performance of the PTC has been evaluated through the months of November and December (winter weather) 2014 at Chandrapur (19.95°N latitude, 79.3°E longitude). From the result, it has been seen that the PTC is a good option through winter weather to decrease the heating cost.

Yilmaz et al. 2015 [34] presented an experimental investigation for testing the performance of a PTC array (10.2 m^2 total aperture area) at moderate temperatures. The tests were performed using the outdoor measurements to evaluate the useful heat gain and the instantaneous thermal efficiency. The steady state and dynamic tests were carried out in a summer season of Gaziantep. The peak thermal efficiency for the PTC array was estimated as 57% while the optical efficiency is at the level of 56%. Moreover, the efficiency tests were performed in a temperature range from 50°C to 200 ^{0}C, and mass flow rate of 0.1 kg/s to 0.5kg/s, respectively. The performance tests show that the obtained characteristic curve of the tested collector is considerably favorable for Industrial Process Heat (IPH) applications requiring thermal energy need less than 200 ^{0}C.

Jamadi 2016 [35] Performed an attempt to improve the solar water heating system with a parabolic trough collector by changing the oil mass flow rates.

The thermal behavior of the PTC was evaluated under conditions of three variations in oil mass flow rates. The impact of effective parameters such as time, mass flow rate) on thermal efficiency was investigated. The results showed that the reflector efficiency was improved by increasing the flow rate. When there is the greatest flow rate, it has the maximum efficiency.

2.2 Summary of the Current Study:

In this study, a three parabolic trough concentrating solar collectors were constructed, operated and tested in order to generate hot water and steam at moderate temperatures. Table (2.1) presents a summary of the previous experimental and theoretical work related to the present research.

Table (2.1) Summary of Some Literature Review Related to the Present Work

Authors	Title	Objective	Results
Arasu and Sornakumar 2006	Performance characteristics of the solar parabolic trough collector with hot water generation system	The performance of a new parabolic trough collector with hot wa-ter generation system is investigated through experiments over one full day in summer period.	The storage tank water temperature is increased from 35 °C at 9.30 h to 73.84 °C at 16.00 h.
Zhang et al. 2012	An experimental investigation of a natural circulation heat pipe system applied to a parabolic trough solar collector steam generation system	Design a U-type nat-ural circulation heat pipe system and applied to a para-bolic trough solar collector for generat-ing mid-temperature steam at three work-ing of unfired boiler conditions (0.2, 0.5 and 0.75) Mpa.	The system can generate mid-temperature steam of a pres-sure up to 0.75 Mpa. The thermal efficiency is found to be 38.52% at pres-sure of 0.5 Mpa.

Venegas-Reyes et al. 2012	Design, construction, and testing of a parabolic trough solar concentrator for hot water and low enthalpy steam generation	Design, construction, and evaluation of a solar parabolic trough concentrator (PTC) for hot water and low enthalpy steam generation.	Peak efficiencies close to 60% were obtained.
Jamil Al Asfar et al. 2014	Design and performance assessment of a parabolic trough collector	Designed, constructed and tested a parabolic trough solar collector to assess its performance.	The peak thermal efficiency obtained was 22.4%. Steam was generated with temperatures up to 123 ^{0}C and a pressure of 2 bar.
Yılmaz et al. 2015	Performance testing of a parabolic trough collector array	Presented an experimental investigation for testing the performance of a PTC array at moderate temperatures.	The peak thermal efficiency for the PTC array was estimated as 57% while the optical efficiency is in the level of 56%.
Present work	Building and Testing a Parabolic Trough Collector to Generate Steam	A three parabolic trough concentrating solar collectors were constructed, operated and tested in order to generate hot water and steam at moderate temperatures.	The peak thermal efficiency obtained during the tests was 50% for solar collectors with evacuated glass receiver at higher flow rate. Steam was generated with temperatures excess 152 ºC.

2.3 Scope of the Present Work

From all of above, it can be concluded that solar energy can be regarded as an attractive renewable source of thermal energy. In addition, the large magnitude of solar energy available with its well established harnessing technology makes it a highly appealing energy source for so many commercial and industrial applications.

The personal desire to study such thermal engineering field rose from being an engineer employee in one of government industrial firm, and as I'm aware of one of the important operational needs in this firm were the specific steam supply requirements. So I felt that it will be a good practice to fulfill such requirement by employing sustainable source of thermal energy, and thus, solar energy seems to be an appropriate solution. Therefore, this project is an attempt to study and examine such method of steam raising process by using solar thermal energy. Thereafter, an appropriate scale unit can be designed for the exact needs and requirement of the industrial firm steam supply in terms of both quality and quantity.

The scope of this study is to construct, operate and test three parabolic trough concentrating (PTC) aluminum solar collectors in an extensive experimental investigation and verification program to assess steam generating capability at moderate temperatures. The PTC performance analysis will be related to the collector inlet temperature, ambient conditions, type of receiver and the working fluid mass flow rate variation.

Part one Related Calculations

In the following part, the mathematical correlations relating to the optical and thermal analysis of the parabolic trough collector are shown in detail below:

3.1 Geometry of Parabolic Trough Solar Collector

Parabolic Trough Solar Collector (PTC), which is also called cylindrical-parabolic collector, employs linear imaging concentration. These collectors are comprised of a cylindrical concentrator of parabolic cross – sectional shape (reflector), and a circular shape (receiver) located along the focal line of the parabola. A cross section view of a receiver and a reflector, shown in figure (3.1), shows several important factors.

Figure(3.1): Cross-section of a parabolic trough collector with circular receiver [8].

When the solar incident beam radiation is incident on the reflector at the rim, the mirror radius has a maximum value at r_r ,also when incident radiation hits the reflector at the rim collector, it makes an angle which is known as rim angle, θ_r that is given by [36]

$$\theta_r = \sin^{-1}\left[\frac{(w_a)}{2r_r}\right] \tag{3.1}$$

For any point of the parabolic reflector the local mirror radius r, shown in figure (3.1) can be determined by the following equation [8]:

$$r = \frac{2f}{1 + \cos\theta} \tag{3.2}$$

θ is the angle between the reflected beam at the focus and the collector axis, f is the Parabola focal length. as θ varies between 0 to rim angle, θ_r,Thus, the radius, r, also varies from the focal length, f, and r_r [8].

Equation (3.2) at the rim angle, θ_r , become:

$$r_r = \frac{2f}{1 + \cos\theta_r} \tag{3.3}$$

For specular reflectors of perfect position, the size of the tube (diameter D_r) required to intercept all the solar image can be found from trigonometry and known by:

$$D_r = 2r_r \sin\theta_m \tag{3.4}$$

Where an incident beam of solar radiation is a cone with an angular width of 0.53 (i.e., a half-angle θ_m of 0.267°) [36].

The aperture of the parabola is another important factor which is related to the rim angle and parabola focal length, and it is given by:

$$w_a = 4f \tan(\frac{\theta_r}{2}) \qquad (3.5)$$

The concentration ratio C, which is defined as the ratio of the aperture area to the area of the absorber [8] is presented in the following equation:

$$C = \frac{effective\ aperture\ area}{absorber\ area} = \frac{w_a}{\pi D_r} \qquad (3.6)$$

3.2 Optical Analysis of Parabolic Trough Collectors

In ideal conditions, 100% of the incident solar energy is reflected by the concentrator and absorbed by the absorber. However, in reality, the reflector does not reflect all solar radiation due to imperfections of the reflector causing some optical losses. The optical efficiency relies on many factors such as tracking error, geometrical error, and surface imperfections.

3.2.1 Optical Efficiency

As mentioned before, optical efficiency is defined as the ratio of the energy absorbed by the tube receiver to the energy fallen on the reflector aperture. [37]:

$$\eta_o = \frac{S}{I_b} \qquad (3.7)$$

With all of the modifiers taken into account, the absorbed radiation, S, or the actual amount of radiation on the receiver is calculated by [37], [38]

$$S = I_b \, (\rho_m \, \tau_g \, \alpha \, \gamma) \, K(\theta) \qquad\qquad (3.8)$$

Where I_b , is the beam radiation, ρ_m is the mirror reflectance, τ_g is the glass envelope transmittance, α is the absorber surface absorptance, γ is the intercept factor and $K(\theta)$ is incident angle modifier.

3.2.2 Incidence Angle Modifier

An incidence angle modifier $K(\theta)$ can be used to account for deviations from the normal of the angle of incidence of the radiation on the aperture [43]. Here, θ is defined as the angle between the beam radiation on a reflector and the normal to that collector, it is equal to zero at continuously tracking about two axes [36]. Reflector performance is often provided to the upright radiation that is direct to the aperture area. The significant effect of the position of radiation in minimizing the straight radiation on the aperture area is containing the cosine factor .There are additional losses connected to the position of radiation because of the difference between the reflection and wine glass cover absorption with the position of radiation. The result of these losses on the reflector performance is assessed by the incidence modifier $K(\theta)$. The incidence modifier is known as an empirical fit to experimental data for a confirmed reflector kind, which is referred to as a polynomial function of the infinite value of θ [39]

$$K(\theta) = \; 1 + b_1 \,.\theta \; + b_2.\, \theta^2 \; + b_3.\theta^3 \qquad\qquad (3.9)$$

As mention above, when the collector is continuously tracking about two axes to minimize the angle of incidence, the incident angle modifier is equal to unity.

3.2.3 Intercept Factor

Another factor affecting the optical efficiency is called the intercept factor (γ). It is defined as the fraction of incident solar flux that is intercepted by the concentrator. Ideally, the mirror and receiver are aligned perfectly and the tracking drive system is perfect and the mirror surface is clean without surface imperfections. Values of (γ) greater than 0.9 are common [36].

The optical efficiency η_o and the factors (ρ_m, τ_g, α, γ) of PTC for the present study are reported in Table (3.1). It is vital to point out that the optical efficiency η_o was performed by considering the angle of incidence θ as equal to zero (i.e., K(θ) equal to unity).

Table (3.1): The Optical Efficiency and the Geometric Parameters of the PTC.

Parameters	%
η_o	0.55
ρ_m	0.80 [40]
τ_g	0.89 [41]
α	0.87 [41]
γ	0.90 [36]

3.3 Thermal Analysis of Parabolic Trough Collectors

In a thermal transfer system, an operating fluid is utilized to draw out energy from the tube. The thermal performance of PTC depends upon their thermal efficiency, which is thought as the percentage of the useful energy sent to the energy fallen on the reflector aperture. The thermal loss for a PTC is from the tube to ambient [38], [42].

3.3.1 The Heat Loss Coefficient

Thermal losses from the tube must be calculated in expressions of the heat loss coefficient U_L, which is based on the area of the tube. For a non-evacuated glass tube, the loss coefficient considering convection, radiation and conduction is:

$$U_L = \left[\frac{A_r}{A_g\,(h_w + h_{r,g-a})} + \frac{1}{h_{r,r-g} + h_{c,r-g}} \right]^{-1} \qquad (3.10)$$

To decrease the heat loss, a centric glass pipe is used to cover the tube. The space between the tube and the glass envelope is generally evacuated, in which status the convection losses are negligible. In this status, U_L, based on the tube area A_r, is :

$$U_L = \left[\frac{A_r}{A_g\,(h_w + h_{r,g-a})} + \frac{1}{h_{r,r-g}} \right]^{-1} \qquad (3.11)$$

Where: A_r external area of receiver (absorber) tube and A_g external area of the glass cover.

The convection heat transfer coefficient between the glass and ambient air which is due to the wind can be evaluated as

$$h_{c,g-a} = h_w = \frac{Nu\ k}{D_g} \qquad (3.12)$$

Where (Nu) is the Nusselt number of air, defined by two equations [8], [38]:

$$Nu = 0.4 + 0.54\ (\text{Re})^{0.52} \qquad \text{For } 0.1 < \text{Re} < 1000 \qquad (3.13)$$

$$Nu = 0.3\ (\text{Re})^{0.6} \qquad \text{For } 1000 < \text{Re} < 50{,}000 \qquad (3.14)$$

Where Re is the Reynolds number of air, calculated by the following equation:

$$Re = \frac{\rho V D_g}{\mu} \tag{3.15}$$

The radiation heat transfer coefficients between the glass cover and the ambient ($h_{r,g-a}$) and between the receiver tube and glass cover ($h_{r,r-g}$) are given by the following equations

$$h_{r,g-a} = \varepsilon_g\, \sigma\, \left(T_g + T_a\right)\left(T_g^{\,2} + T_a^{\,2}\right) \tag{3.16}$$

$$h_{r,r-g} = \frac{\sigma\,\left(T_r + T_g\right)\left(T_r^{\,2} + T_g^{\,2}\right)}{\frac{1}{\varepsilon_r} + \frac{A_r}{A_g}\left(\frac{1}{\varepsilon_g} - 1\right)} \tag{3.17}$$

To evaluate the convection heat transfer coefficient between the receiver tube and glass cover $h_{c,r-g}$ (in case air is exist between the receiver tube and glass cover), the properties of air should be evaluated at the film temperature

$$T_f = \frac{T_r + T_g}{2} \tag{3.18}$$

From the equation above, the temperature of the glass envelope, T_g, is necessary. This temperature is closer to the surrounding temperature than the tube temperature and is given by:

$$T_g = \frac{A_r h_{r,r-g} T_r + A_g \left(h_{r,g-a} + h_w\right) T_a}{A_r h_{r,r-g} + A_g \left(h_{r,g-a} + h_w\right)} \tag{3.19}$$

Thus, the convection heat transfer coefficient between the receiver tube and glass cover becomes

$$h_{c,r-g} = \frac{Nu \; k}{D_r} \qquad (3.20)$$

Where *Nu* is the natural convection Nusselt number for air that is exist in the space between the receiver and glass cover. This Nu number can be determined as

$$Nu = \left\{ 0.6 + \frac{0.387 \, (Ra_D)^{1/6}}{[1 + (0.559/Pr)^{9/16}]^{8/27}} \right\}^2 \qquad (3.21)$$

Ra Represent the Rayleigh number given by

$$Ra = \frac{g \, \beta \, (T_r - T_g) \, D_r^3}{v^2} \, Pr \qquad (3.22)$$

3.3.2 Heat Removal Factor

The heat removal factor or correction factor, F_R, can be interpreted as the ratio of the actual useful energy gain of a collector to the useful gain if the whole collector surface were at the temperature of the fluid entering the collector [8]. This factor having a value between (0 to 1). The quantity F_R is the same as the effectiveness of a conventional heat exchanger, which is thought as the percentage of the real heat transfer to the utmost potential heating transfer. The maximum potential useful energy gain in a solar reflector take places when the complete reflector reaches the inlet fluid temperatures; heat loss to the environment are then at the very least. It's value is governed by the working fluid flow rate and it's properties as well as the thermal properties of the receiver material [36], [43].

$$F_R = \frac{m_f^{\cdot}\, c_p\left(T_{f,o} - T_{f,i}\right)}{A_c\left[S - U_L\left(T_{f,i} - T_a\right)\right]} \qquad (3.23)$$

3.3.3 Thermal Efficiency

The instantaneous thermal efficiency η_{th} of a solar reflector may be computed from the energy balance on the tube. The useful heat gain, Q_u, supplied by the tube can be inscribed in expressions of optical and thermal loss, where optical losses are exemplified by the optical efficiency, η_o [42], [44]

$$Q_u = \eta_o I_b A_a - U_L\left(T_r - T_a\right) A_r \qquad (3.24)$$

where A_a is the unshaded area of the concentrator aperture and A_r is the area of the receiver ($\pi D_{r,o} L$ for the cylindrical absorber) [36].

Note that, because concentrating collectors can only utilize a beam radiation, I_b instead of the total radiation, I_{bt}, used in the flat plate collectors.

Since the receiver surface temperature is difficult to determine, it is convenient to express the Q_u in terms of the inlet fluid temperature to the collector by means of heat removal factor F_R as [8]:

$$Q_u = A_a F_R \left[S - \frac{U_L\left(T_{f,i} - T_a\right)}{C}\right] \qquad (3.25)$$

The useful heat associated with the flow rate can be defined on the base of fluid difference temperatures as:

$$Q_u = m^{\cdot} c_p \left(T_{f,o} - T_{f,i}\right) \qquad (3.26)$$

The thermal efficiency of the solar thermal reflector can be easily defined as the ratio of useful heat Q_u, supplied per A_a, and the radiation, I_b, which is fallen on the aperture reflector.

$$\eta_{th} = \frac{Q_u}{A_a I_b} \tag{3.27}$$

The thermal instantaneous efficiency of the collector can now be re-written against the temperature rise of fluid, $\left(T_{f,o} - T_{f,i}\right)$ by substituting Eq. (3.26) into Eq. (3.27) [41], [42], η_{th} now becomes:

$$\eta_{th} = \frac{m^{\cdot} C_p \left(T_{f,o} - T_{f,i}\right)}{A_a I_b} \tag{3.28}$$

Inserting the value of Q_u from Eq. (3.25) into Eq. (3.27), the thermal collector efficiency becomes [8], [36]:

$$\eta_{th} = F_R \left[\eta_o - \frac{U_L \left(T_{f,i} - T_a\right)}{I_b C} \right] \tag{3.29}$$

The thermal efficiency depends upon two types of quantities namely; the concentrator design parameters and the parameters characterizing the operating conditions. The optical efficiency, heat loss coefficient and heat removal factor are the design dependent parameters while the solar flux, inlet fluid temperature and the ambient temperature define the operating conditions [42].

Part Two Experimental Work

A parabolic trough is a concentrating solar collector in which the reflecting surface is bent in the form of a parabola. The energy of beam radiation falling on the trough entering the collector parallel to its plane of symmetry is concentrated along its focal line and converted to thermal energy, where a receiver tube is installed. The mirror is oriented so that solar radiation, which it reflects, is concentrated on the tube. The tube contains a heat transfer fluid to which heat is transferred for heating to a high temperature by the energy of the solar radiation. The experimental test rig, which consists of a parabolic trough solar concentrator (PTC) set-up, has been constructed, operated and tested to demonstrate its ability for steam generation. Fabrication of several types of equipment needed for collector testing was also done, e.g. fabrication of inserted copper pipes, storage tank and manual tracking system.

3.4 Description of Parabolic Trough Collector System

A parabolic trough solar collector model for the concentration solar radiation has been fabricated to generate steam as shown in the plate (4.1). The experimental set-up used in this study consists of a locally fabricated parts of three parabolic troughs solar collector with a total aperture area of 3.73 m². The collectors are arranged in series so that the heat transfer fluid (HTF) gains heat gradually as it flows through the tubes in a sequential manner. In addition, the collectors are continuously oriented directly toward the beam radiation to achieve a maximum efficiency. The PTC system mainly consists of three collectors (reflectors), inserted copper pipes (absorber), evacuated glass tube, storage tank, centrifugal pump, support structure and other accessories.

Plate (4.1): The PTC System

3.5 Fabrication of the PTC System Parts

3.5.1 The Support Structure

The support structure for this model contains two main mechanical groups: stationary and moving base. They represent a metal support frame and manual tracking for the model at the same time. The necessary data for describing the support structure are shown in appendix (A)

3.5.1.1 The Stationary Base

The Stationary base structure of this model has been fabricated to undergo, support and rotate the model at which is composite of a rectangular steel pipe welded together in the form of a square frame and fixed on concrete ground base by anchor bolt. This base consists of a stationary steel pipe that is vertically welded in the center of the base with 2.5″ diameter and 13cm length in order to fix the moving base on this base, see appendix A for details.

3.5.1.2 The Moving Base

The thought of the moving base design has been placed to afford the hard climate conditions and attain the bearing and supporting needed through the solar energy system operation as well as carrying out the functional allocations that are to be used by the moving this base. The rectangular and square steel pipes have been used to forming this base because they have maximum bending and shearing stress. The moving base composites of two bases, axial and tilting motion bases.

3.5.1.2a The Axial Motion Base

This part will satisfy an axial motion for a model about 360° horizontally. A metal base has been fabricated to achieve this axial motion. This base composites of a set of a rectangular steel pipe welded in the form of (I) frame, and it consists of a cylindrical hole that is drill in the center of base frame. The axial motion, which is in charge of the horizontal movement, was fixed on the central stationary base tube through the hole in moving base, see appendix A for details.

3.5.1.2b The Tilting Motion Base

This part will enable the tilting of model up to 60 degree with the horizon. A metal base has been fabricated from two square steel pipes that are made in the form of tow arcs to achieve this tilting motion. Moreover, the metal arcs linked together by another square steel pipe. The arcs are then used to fix two parallel rectangular steel pipes, which in turn used to fix the collectors, storage tank, pump and other accessories. These two arcs are mounted and sliding above the axial motion base, and hence leading to implementing the function of the tilting motion properly and successfully, see appendix A for details.

3.5.2 Parabolic Trough Collector

The function of this part is to reflect and concentrate the parallel solar rays on the receiver to achieve the focus line finally. In order to decrease the structure expenses, commercially obtainable "off-the-shelf" aluminium composite material panels (A.C.M.P) were used to forming the PTC because it has a lightweight, weather resistant, and ease of forming as shown in figure (4.1). The (A.C.M.P) consists of two 0.5mm thick aluminium cover sheets and a 3 mm core made of polyethylene. To find the aperture width of the PTC as part of the design of the PTC, the curve length of the reflective surface is considered. This dimension is agreed with the width of the aluminium panel. The necessary data for describing the PTC are shown in appendix (A).

The parabolic curve length was drawn by using a Parabola Calculator Program as shown in figure (4.2) to provide the required dimensions and create the parabolic shape. The aperture width (diameter of a trough) w_a of 104 cm and depth of trough of 29 cm were introduced into the program to get the following results: a curve length of 122 cm and a focal distance f of 23.31cm. Then, the mirror plates are curved into parabolic shape by using

35

a metal sheet-bending machine. The parabola drawing was checked for consistency with the following equation [36]

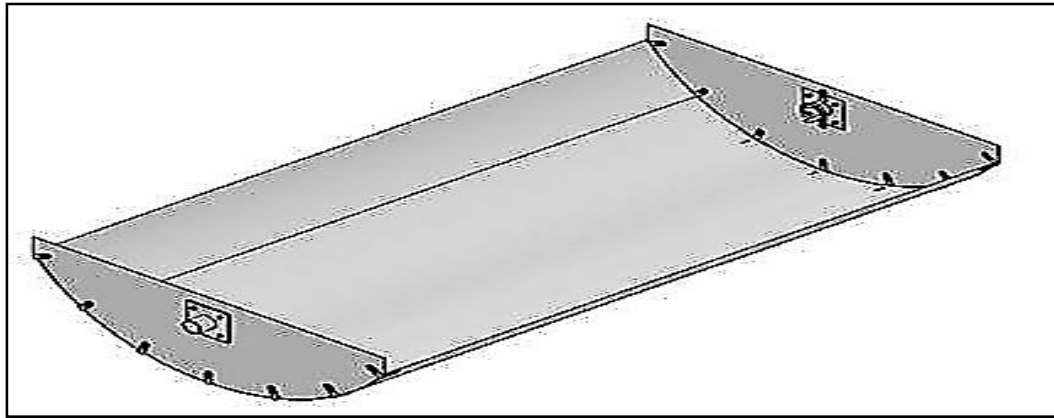$$x^2 = 4fy \qquad\qquad (4.1)$$
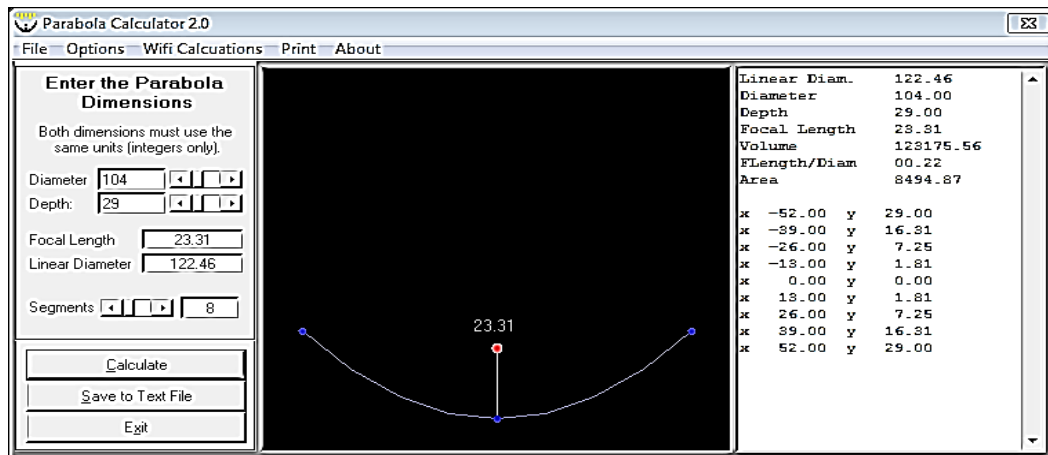

Figure (4.1): Parabolic Trough Collector

Figure (4.2): Parabola Calculator Program

The characteristics of parabolic trough collector parts specifications are shown in table (4.1)

Table (4.1): Characteristics of Parabolic Trough Collector Parts Specifications:

ITEM	Value/Type
Collector aperture width	104cm
The effective aperture width	75cm
Collector length	180cm
Parabolic curvature	122cm
Total Collector aperture area	3.73m^2
Mirror material	Aluminium composite panels
Rim angle	77.72
Focal distance	23.31cm
Glass envelope external diameter	5.8cm
Receiver external diameter	4.7cm
Inlet and outlet absorber material	Copper painted black
Copper pipe diameter	5/8″
Mode of tracking	Two axis
Concentration ratio	4.68

3.5.3 Edge Ribs of the Collector

Two edge ribs for each trough have been fabricated by using the aluminium composite material panel. The ribs are given by the shape of the parabolic profile and fixing with seven steel angles up to form of PTC structure. The rib has a circular hole that is drilled in it to hold the glass receiver. This hole is concentric with the hole placed in tilting base structure for each PTC and in this point the parabola focus coincides with the rotation axis of PTC structure, maintaining the absorber tube and rotation without translational. Moreover, the coupling between PTC structure and the support structure was made using a 2″ diameter steel tube that is fixed on each rib. The copper absorber pipe was inserted through this steel tube and passing into the glass receiver tube, see appendix A for details.

3.5.4 Glass receiver

The glass receiver comprises two coaxial borosilicate glass pipes with one open end and another sealed as shown in the plate (4.2). The exterior diameter is 5.8cm and length of the cover glass tube is 180 cm, the interior diameter is 4.7 cm and length of absorbing glass tube is 172 cm. The thickness of the interior and exterior tubes is 1.6 mm. Selective coating (aluminium nitrite) paint is used to coat the outer surface of the interior tube in order to increase the absorptivity. The spacing between the two tubes is evacuated from the air to reduce the heat losses. The receiver has been placed at the focal line of the parabola and fixed on two edge ribs of the trough. Copper pipes, which are used to passing the working fluid, have been inserted in the glass receiver. The space between the two tubes allows the passing of the reflected radiation through it and reaching the inner tube. Thus, the absorbed solar energy is converted to heat and transmitted to the copper pipes then it transferred to the fluid. In the present work, the glass receiver of the two cases , which is evacuated and non-evacuated, are used in order to study it's effect in the overall performance of the system as shown in the plate (4.2).
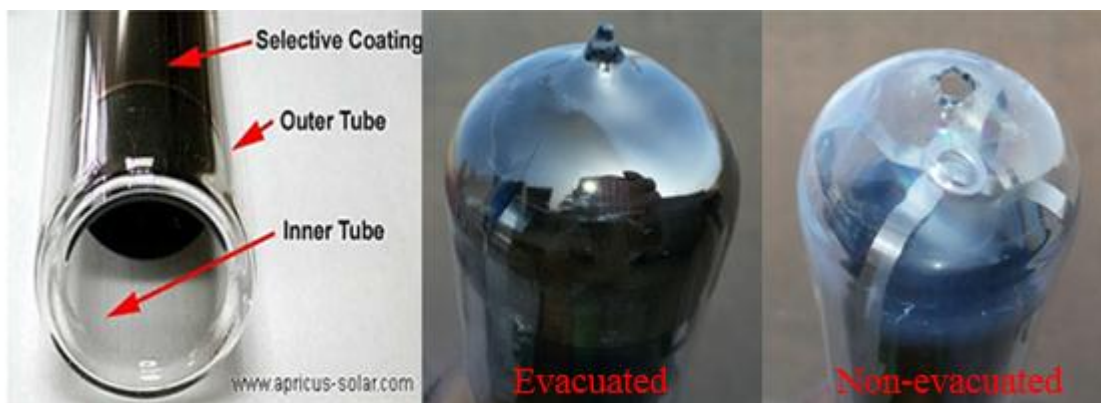
Plate (4.2): Glass Receiver, Evacuated and Non-evacuated

3.5.5 The Absorber Pipes

The absorber pipes for each collector are composed of enclosed triple copper pipe with an outer diameter of 5/8″ and coated with black paint to absorb the heat. The enclosed pipes have been collected and welded together in one of their ends while their other ends are separate. The enclosed pipes used to entering and exiting fluid in the same time as shown in the plate (4.3). On another hand, the absorber pipes were inserted inside the glass receiver tube, which has a 44 mm inner diameter. The fiberglass bung placed at the open end of the glazing receiver and tight roll around two copper pipes to seal the open end of the glass tube and it used to prevent convective flow occurring between the annular and double-glazing vacuum tubes. The copper pipes are supported inside the glass tube by using a Teflon at the near and distal ends of the glass tube to prevent contact between the copper pipes and glass structure.

Plate (4.3): Copper Inserted Pipes

3.5.6 Storage Tank

The storage tank used in this system is shown in the plate (4.4). The storage tank has dimensions of 39cm x 54cm diameter and height respectively. It has the ability of holding a maximum amount of water of 35 liters. The insulation used in this tank was a spray foam with a thickness of 4 cm in order to maintain the required working fluid temperature and to reduce the heat losses storage thermal energy as low as possible. Furthermore, the storage tank is fixed on the tilting motion base and connecting with the pipe coming from the troughs to the bottom left end (inlet to tank), while the bottom right end (outlet from the tank) is connected with the pipe going to the pump. Two holes have been fabricated in the upper part of the tank to use them for measuring the pressure and temperature.

Plate (4.4): Storage Tank

3.5.7 Connecting Pipes

The Connecting pipes consist of many hoses that connect all the collectors, storage tank and pump together. The type of hoses material chosen for this system was a synthetic rubber bald with an inner and outer diameter of 16mm and 26mm respectively. The rubber hoses can be used with a large variety of working fluid, and it can provide corrosion resistance for both chemical and weather reactions. In addition, this rubber is flexible that allows the easy connection of the parts together. Therefore, a synthetic rubber is a very suitable choice for this application. These hoses have been covered by using an air conditioning rubber insulation pipe in order to reduce the heat losses to the atmosphere.

Figure (4.3): Connecting pipes

3.6 Apparatus and Instrumentation

The experimental instruments, which has been used to investigate the performance of the system, can be classified into:

3.6.1 Thermocouples

Thermocouples (type-K) are used in this system and it have a range between -200 to +1372˚C. The position of thermocouples showed in schematic diagram of experimental setup figure (4.8) as follows:

A- Two thermocouples (1 and 2) are connected to the absorber pipes of the first collector to measure the inlet and outlet fluid temperatures.

B- One thermocouple (3) is connected to the absorber pipes of the second collector to measure the outlet fluid temperature.

C- One thermocouple (4) is connected to the absorber pipes of the third collector to measure the outlet fluid temperature.

D- Two thermocouples (5 and 7) are connected to the inlet and outlet port of the storage tank to measure the inlet and outlet fluid temperatures.

E- One thermocouple (6) is connected to the upper port of the storage tank to measure the fluid temperatures.

Thermometer selected for this system is Yokogawa digital thermocouple thermometer (2324 A). It is a portable and multi thermometer, which has a push button keypad, and it offers a wide range of functions. The thermometer is calibrated in the central organization for standardization and quality, see appendix D for details.

3.6.2 Pressure Gauge

The pressure gauge, which is fixed on the storage tank, is used to measure the pressure inside the system. A bourdon Pressure gauge is selected for measuring the pressure inside this system. The Pressure gauge is calibrated in the central organization for standardization and quality, see appendix D for details.

3.6.3 Solar Power Radiation Meter

The solar power meter selected for this application is LCD digital handheld solar power meter (TES 1333) shown in the plate (4.5). The solar power meter is calibrated in the Alternate and Renewable Energy Research Unit that is located in the Technical Engineering College of Najaf. This device has multi options, which are listed below

- Select either w/m² or Btu / (ft²*h) units

- Range of solar radiation 0.1 – 2000 W/m²

- Accuracy of   +/_ 10 W/m²

- Resolution   +/_ 0.1 W/m²

- Calibration   user recalibration available

- Data Hold   CU/ MAX / AVG modes

3.6.4 Wind Speed Meter

The Anemometer selected for this application is LCD Digital Hand-held wind speed meter as shown in plate (4.5). This device has multi options, which are listed below

- Measure wind speed and temperature.

- Wind speed range: 0-30m/s

- Current/max/average wind speed-reading.

- Wind speed unit: m/s, km/hr., ft/min, Knots, mph.

Plate (4.5): Solar Power Radiation and Wind Speed Meter

3.6.5 Flow Meter

The flow meter used in this system is Rotameter (variable area meter). The technique for measuring flow in this device is accomplished by a freely moving float finding equilibrium in a tapered tube. The flow rate is then read from a scale on the tube.

3.6.6 Pump

In order to run tests, a pump is required to circulate heat transfer fluid from the storage tank to the PTC. The pump must be capable of withstanding high temperatures due to the high fluid temperature. A water pump is used, a peripheral pump, which is placed at the outlet of the storage tank. This pump is fixed on a tilting motion base. The maximum volumetric flow rate is 35 liters per minute (LPM) and a head of 32m. In addition, the maximum power usage is 0.5 HP, which is provided by 220 volt AC.

3.7 Experimental Setup and Procedure

The experimental setup used for testing the PTC system is shown schematically in figure (4.4). It contains (1) three PTC, (2) a 35 -liter storage tank, (3) pump and (4) support structure with manual tracking

First of all, it is very important to clean the reflector (mirrors) from any accumulated dust or dirt. Then, the storage tank is filled up from the main water supply. The water recirculation is an open one, thus, the system with the storage tank is filled with 40 liter of water. The storage tank connection with the troughs system is established by connecting the tank inlet to the troughs outlet and the tank outlet to troughs inlet. Afterward, the tracking system of all troughs is guided and adjusted so that the sun is directly over the troughs. Water is pumped from the storage tank to the PTC. The flow meter placed after the pump measures the flow rate of the water passing through the

pipes. After water collects heat and gets hot, it returns to the storage tank. The cycle continued repeatedly throughout the test period until steam production is achieved. In the meantime, the fluid temperatures in the locations mentioned in the schematic diagram (the points 1 to 7), ambient temperature, wind speed, pressure of HTF and solar irradiance intensity are continuously recorded during the test periods.
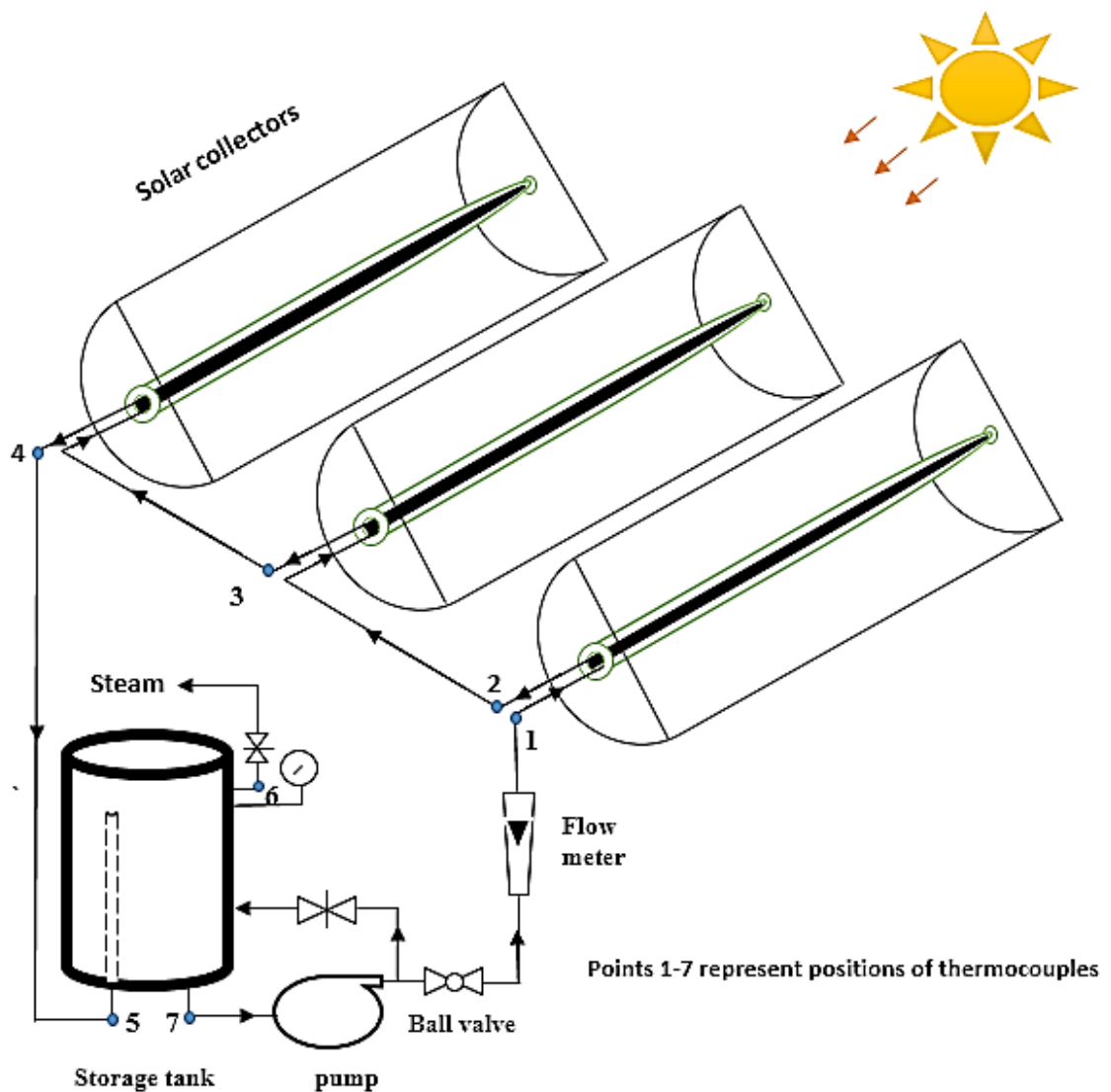

Figure (4.4): Schematic Diagram of Experimental Setup

Chapter Four
Results and Discussion

5.1 Introduction

In this chapter, experimental investigation was carried out to generate a steam at a medium- temperature (with temperature exceeds 152°C and a pressure of 4barG) using PTC system. The effects of various parameters on the performance of the PTC are analyzed. Thermal performance of PTC was obtained from the measured data. The data was collected for eight clear-sky days in August at different flow rates by using evacuated and non-evacuated glass receiver. In the performance analysis of the PTC, the effects of fluid inlet temperature, ambient conditions, two types of receiver and the variation in mass flow rate of the working fluid were investigated.

5.2 Variation of Temperatures Difference

5.2.1 For Evacuated Glass Receiver

The data measured are collected for four days under similar weather conditions (5th, 6th, 8th and 9th of August 2016) from 9:00 am to 13:00 pm. The experimental tests have been chosen for measuring all necessary data to analyze the performance of the PTC with an evacuated glass receiver. T_{amb}, inlet temperature, outlet temperature and pressure represent the ambient temperature, the inlet temperature of water to the first collector, the outlet temperature of water from the third collector, and pressure of the tank, respectively. Different flow rates of water (100 L/hr., 300 L/hr., 500 L/hr., and 650 L/hr.) have been implemented for these experiment days. The necessary data for describing the PTC system are shown in appendix B.

It is observed from figure (5.1 a ,b ,c & d) that the inlet and outlet water temperatures to/from the collector increase with the time passing in the form of two parallel lines for all values of the water flow rate and continue to rise until the end of the experiments. This phenomenon can be attributed to the fact that received solar radiation is directly fall to the collectors due to tracing of the collectors directly and continuously toward the beam radiation.

Moreover, as the mass flow rate through the reflector increases, the temperatures difference through the collectors decreases as shown in figure (5.2). For example, when the flow rates are 100 L/hr., 300 L/hr., 500 L/hr. and 650 L/hr., the temperatures difference varies in the range from 0.7 to 6.7 ˚C, 0.5 to 3.79˚C, 0.4 to 2.4˚C, and 0.4 to 2˚C, respectively. Thus, the temperatures difference increases with the decrease in the mass flow rate.
This phenomenon can be attributed to the fact, whichever fluid moved slower, it could gain a greater amount of heat from the solar rays. Therefore, for the lowest water mass flow, the outlet water temperature revealed the highest value.

On the other hand, the pressure values in the PTC system were measured during the experiment period through the gauge pressure that is fixed on the storage tank. The pressure will continuously increase with the increase in the temperature of the system until reach to 4bar, where the relieve valve is opened.

Due to the pressure drop across the relieve valve and the temperature maintain constant, the process of steam generation has been achieved when the flow rate inside the system was at the highest value (650 L/hr.) as shown by the arrow in figure (5.1d), where the temperature is about 152.7 ˚C at a pressure of 4bar. For further details, see appendix B.
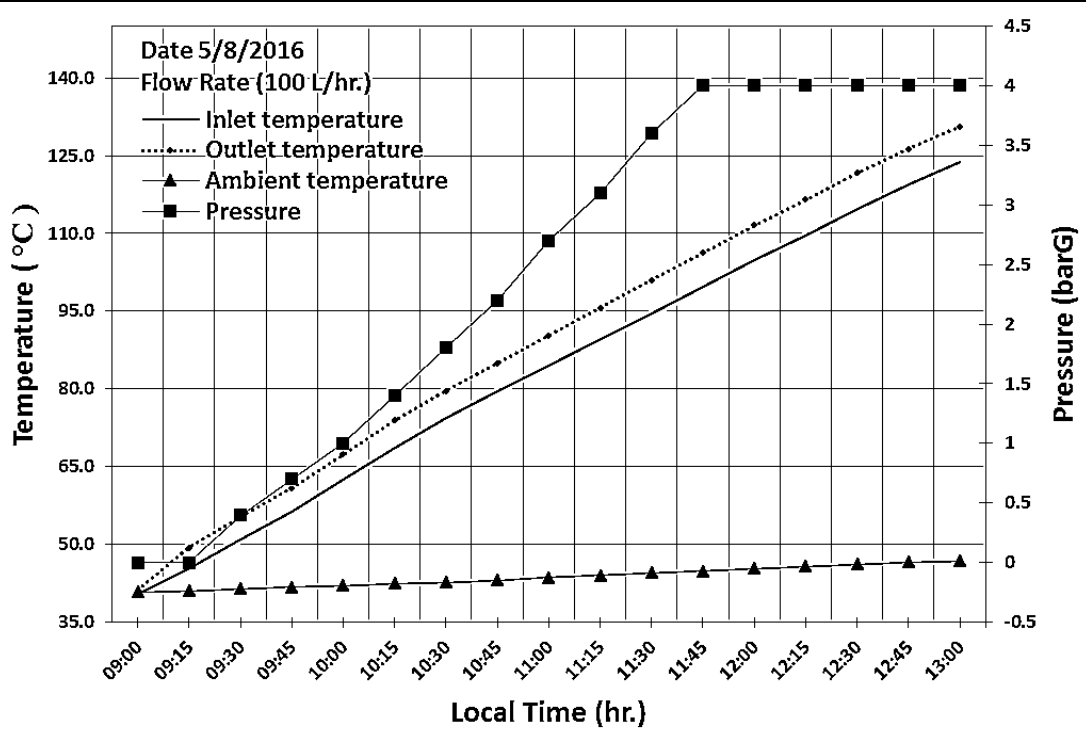
(a)
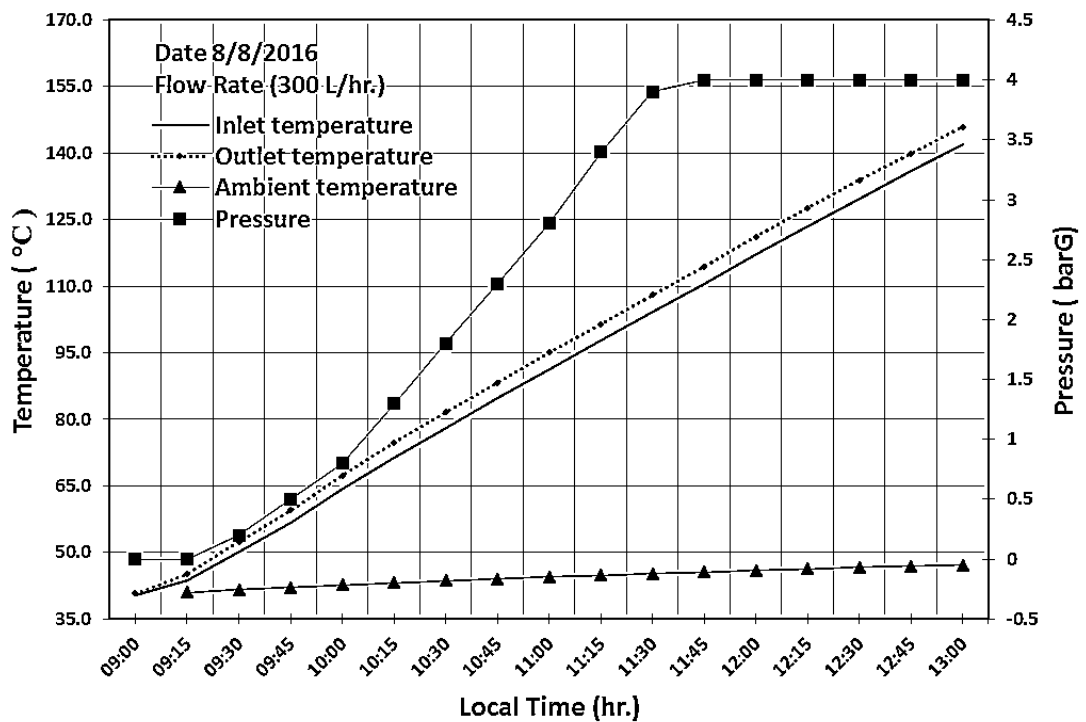
(b)

Figure (5.1): The Inlet and Outlet Water Temperatures of Collectors, the Ambient Temperature and the Pressure of Tank with Respect to Local Time for an Evacuated Glass Receiver

(c)

(d)

Figure (5.1): Contd.

49

Figure (5.2): The Temperatures Difference of Water Through the Collectors with Respect to Local Time.

5.2.2 For Non-evacuated Glass Receiver

The experiments on the PTC using a non-evacuated glass receiver are carried out during four clear sky days (10th to 13th of August 2016) from 9:00 am to 13:00 pm. The ambient temperature, the inlet and outlet water temperatures, the pressure of the storage tank and the temperatures difference through the collectors are shown in figure (5.3 a, b, c & d). Different values of flow rate of the water (100 L/hr., 300 L/hr., 500 L/hr., and 650 L/hr.) have been implemented for these experiment days. The necessary measuring data for these experiment days are shown in appendix C.

It is clearly seen from Figure (5.3 a, b, c & d); that the temperatures increase with the time passing in the form of two parallel lines for all values of the flow rate and continue to rise until the end of the experiments. This

phenomenon can be attributed to the fact that the received solar radiation is directly fall to the collectors due to tracing of the collectors directly and continuously toward the beam radiation.

In terms of the temperature difference between the inlet and the outlet of the collectors as shown in figure (5.4), the temperature difference is a function of solar intensity; it starts to increase with the sunshine until the afternoon, where it then starts to decrease due to the decrease in solar intensity.

It can also seem in figure (5.4) when the flow rate is low; the temperatures difference is the highest. While, when the flow rate is high, the temperatures difference is the lowest. For example when the flow rates are 100L/hr., 300L/hr., 500 L/hr. and 650 L/hr., the temperatures difference varies in range between 0.4 to 2.4°C, 0.4 to 1.4°C, 0.3 to 0.9°C, and 0.3 to 0.7°C, respectively. Thus, the temperatures difference increases with the decrease in the mass flow rate.

This behavior is the same as of that was mentioned previously using an evacuated glass receiver. However, the temperatures difference through the collectors is lower than that of the evacuated receiver.

This because the evacuation of the air reduces the convection and radiation losses, therefore, the primary function of the evacuated receiver is to absorb and transfer the concentrated energy to the fluid flowing through it, and its temperature will become considerably higher than that of a non-evacuated receiver.
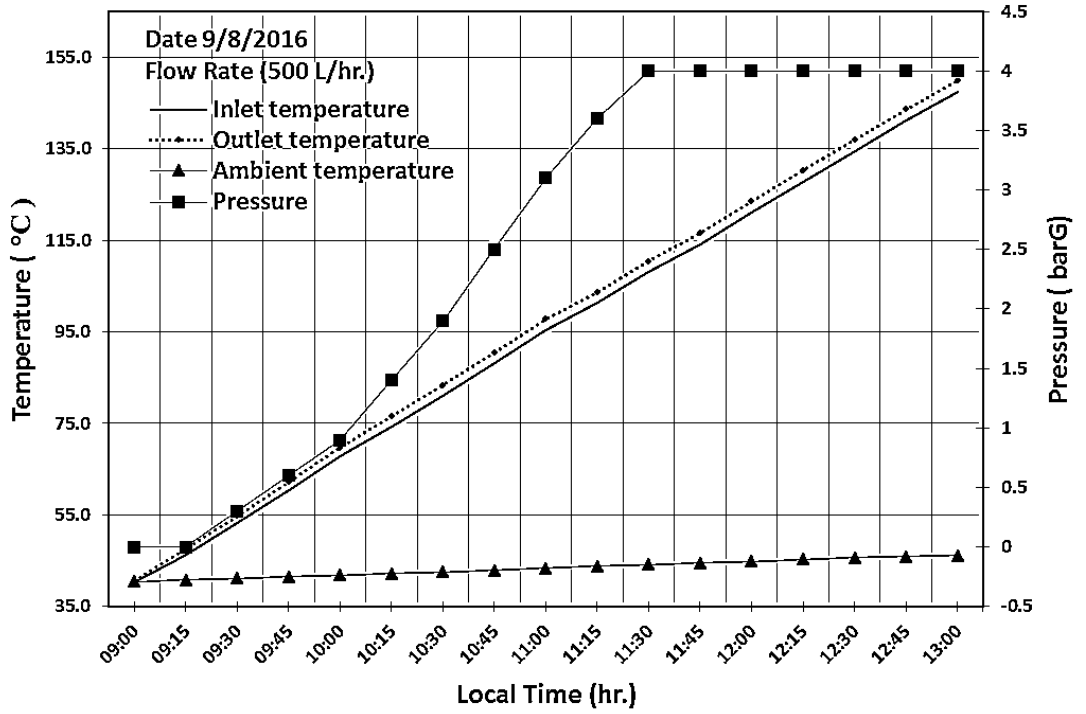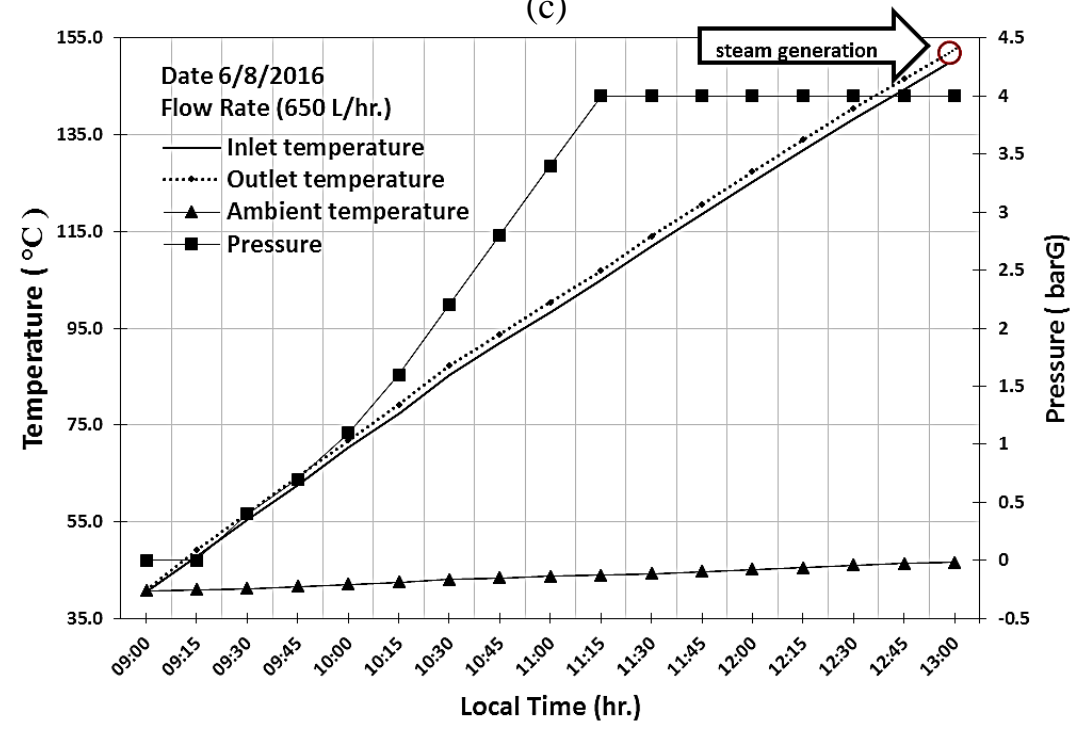
51
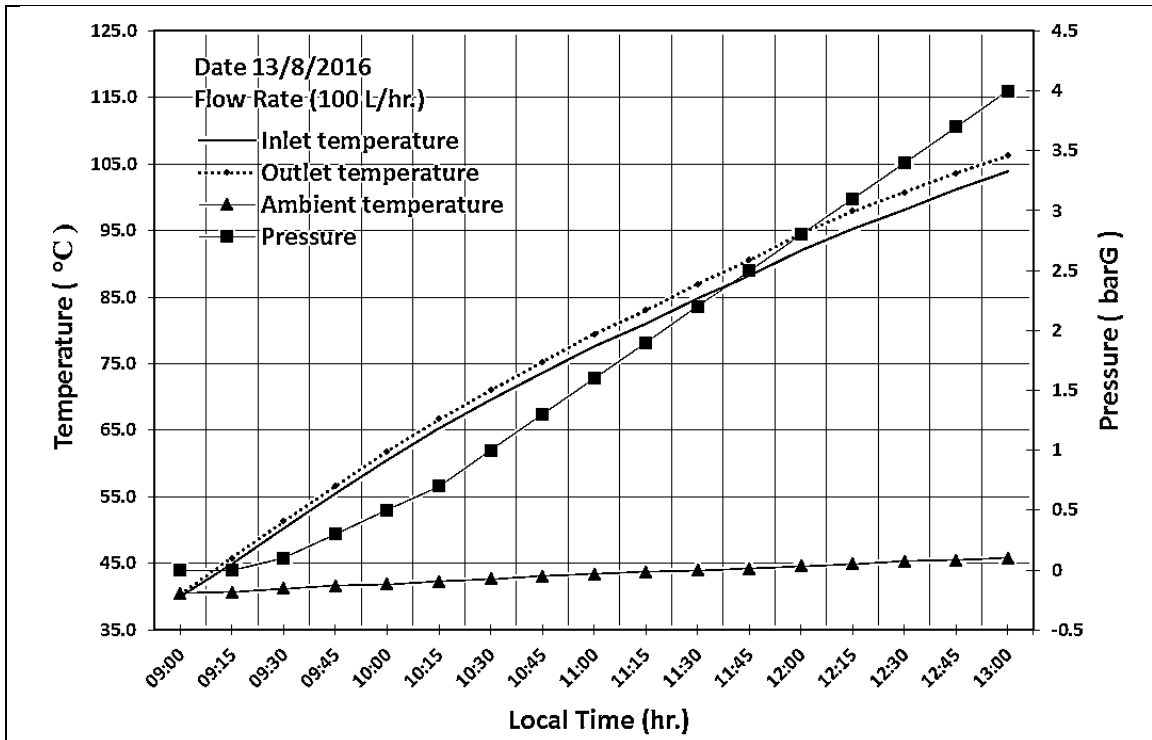
(a)
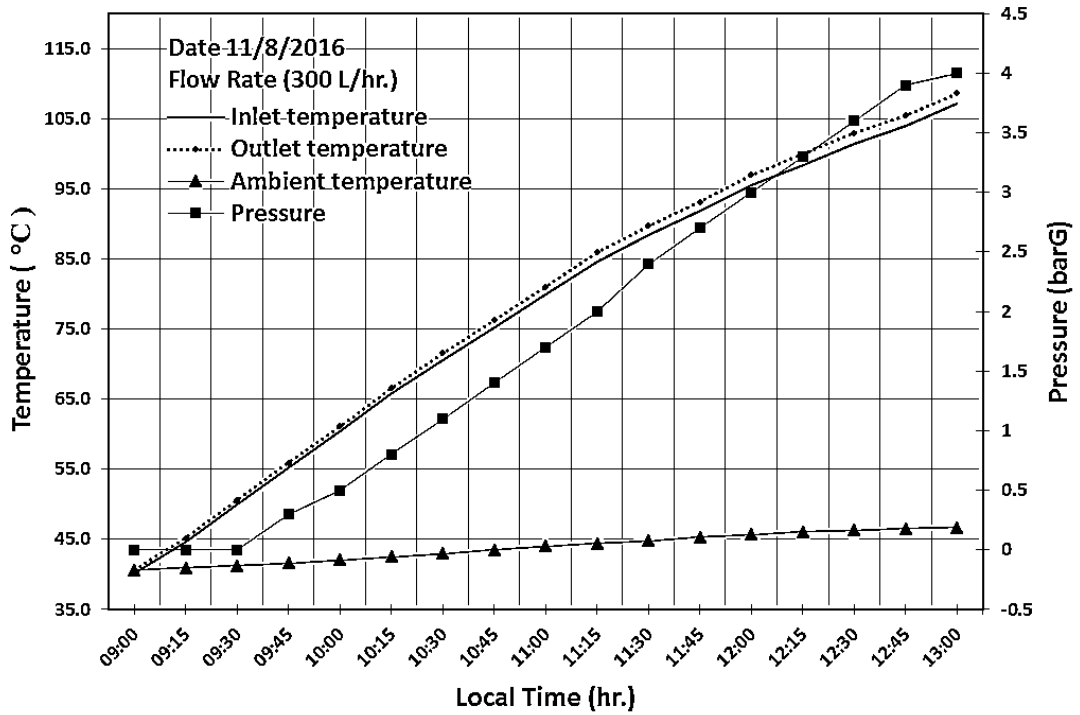
(b)

Figure (5.3): The Inlet and Outlet Water Temperatures of Collectors, the
Ambient Temperature and the Pressure of Tank with Respect to Local
Time for A non-evacuated Glass Receiver.
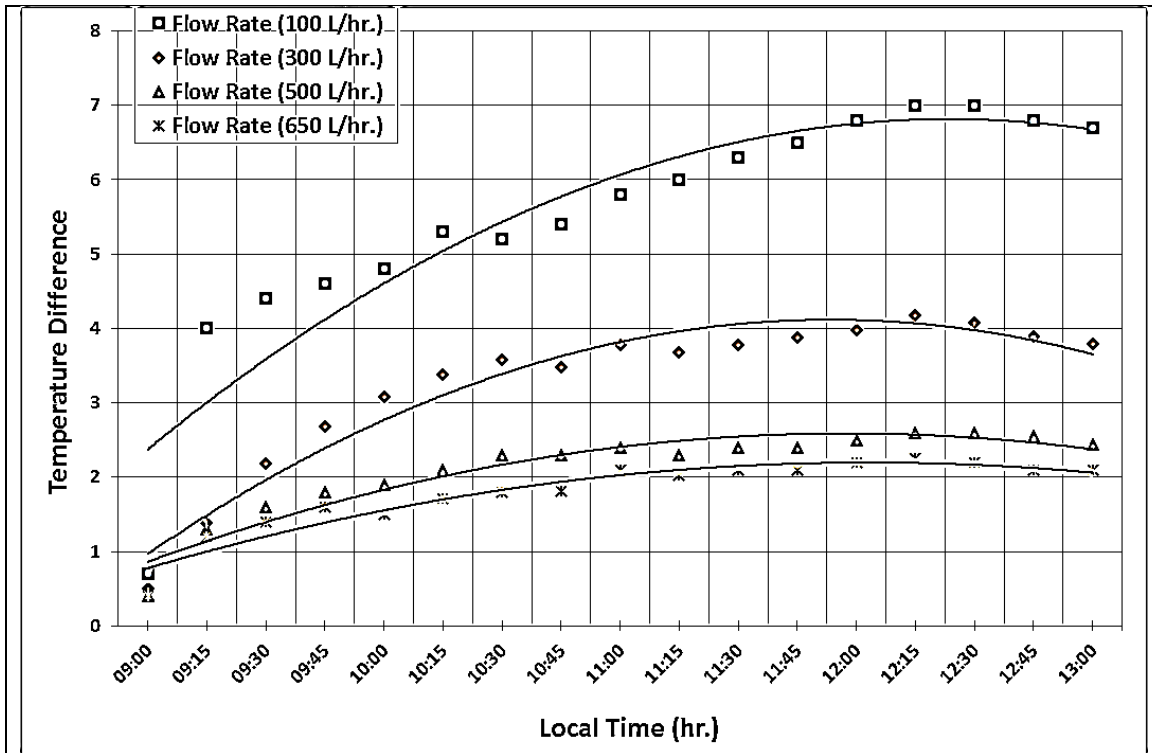
52

(c)

(d)

Figure (5.3): Contd.

53

Figure (5.4): The Temperatures Difference of Water through the
Collectors with Respect to Local Time.
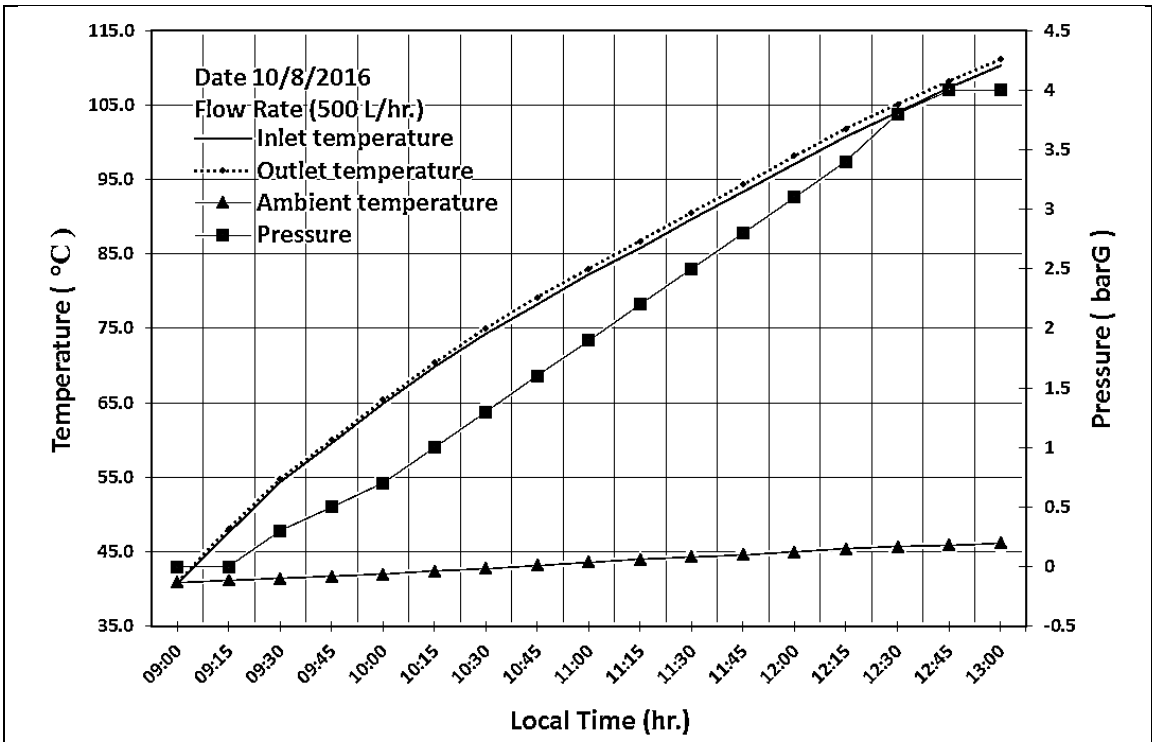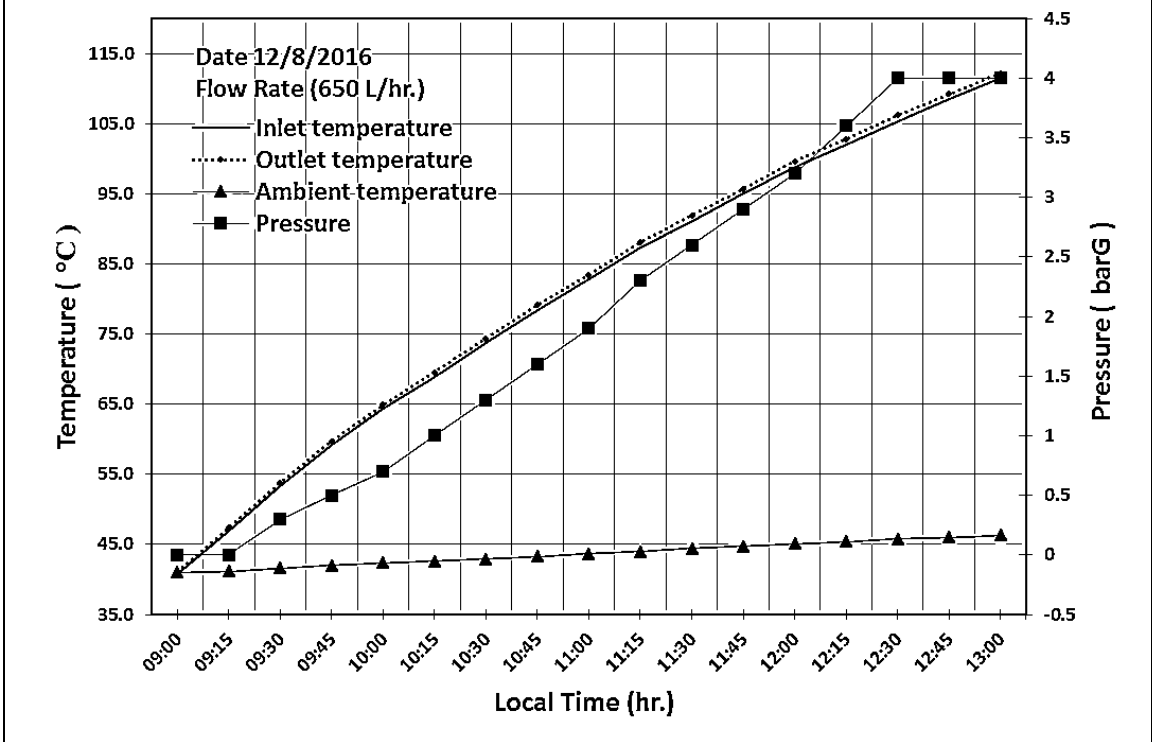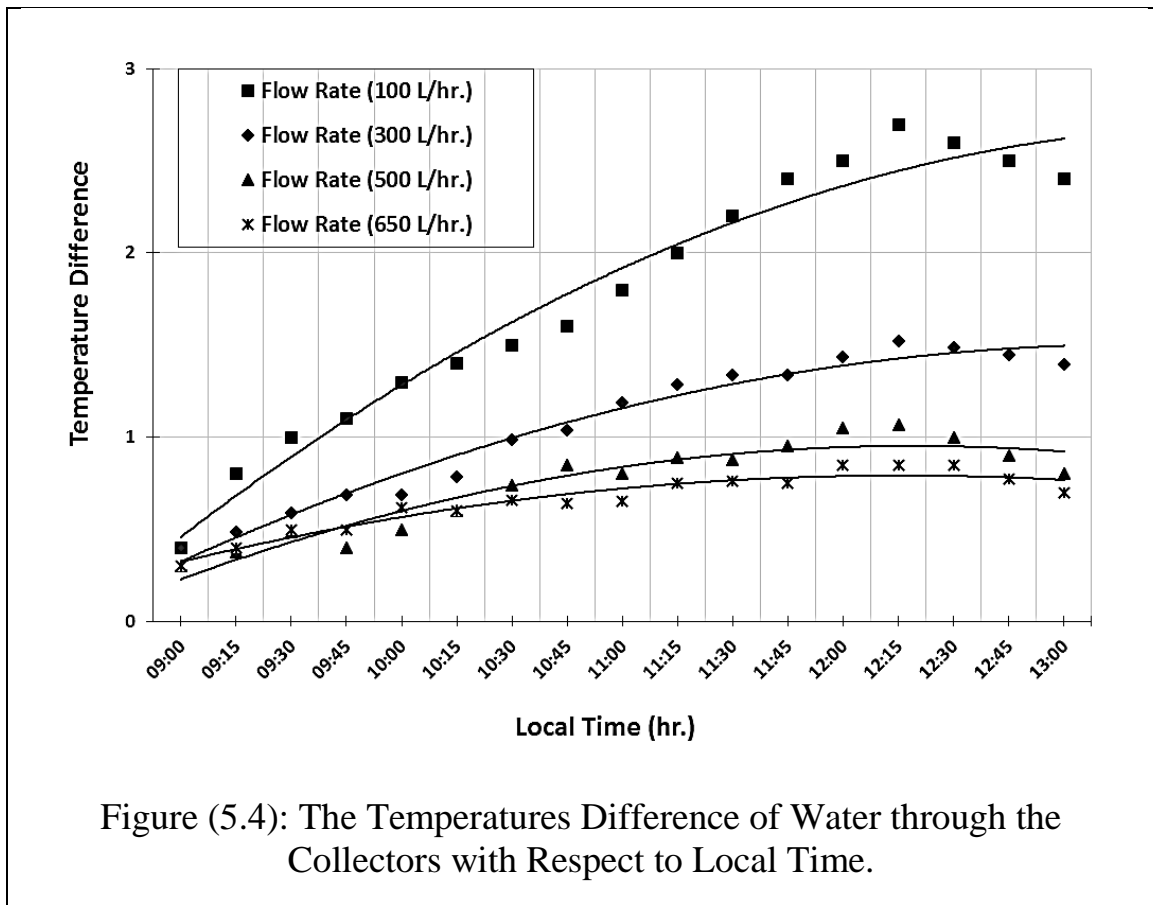
5.3 Useful Heat Gain

The useful gained heat Q_u is determined from the measured inlet and outlet temperatures of PTC, mass flow rate, and specific heat of water as demonstrated in equation (3.25). The temperature data were measured for eight days, and the experiments were carried out from 9:00 am to 13:00 pm.

Figure (5.5 a&b) shows the relation between the variation of beam solar radiation, I_b, and the useful heat gain, Q_u with respect to time, for evacuated and non-evacuated glass receiver at a flow rate of 650 L/hr. . At the beginning of the experiment, the gained heat is low due to the low solar intensity, then, as time passes, it starts to significantly increase until reaching the peak values at noontime (12:15 P.M.); then, it starts to decrease gradually as the time

54

passes. It is clearly seen from figure (5.5 a&b) that the heat gain increases with the increase in the solar irradiance. In addition, the useful heat gain decreases as a result of the decreased solar intensity until the end of the experiment. This phenomenon can be attributed to the fact that the energy collected is impressed by the solar irradiance rate. Similar behavior was seen for the other experiments days.

On the other hand, it is observed from figure (5.6 a&b) that the useful heat gain increases with the increase of the feed water flow rate. For example, when the flow rates are 100 L/hr., 300L/hr., 500 L/hr. and 650 L/hr., the useful heat gain varies in the range between 0.08 to 0.93 kW, 0.17 to 1.48 kW, 0.23 to 1.54 kW, and 0.3 to 1.73 kW, respectively, by using an evacuated glass receiver. In contrast, the useful heat gain varies from 0.046 to 0.33 kW, 0.14 to 0.53 kW, 0.17 to 0.62 kW, and 0.22 to 0.65 kW when the feed water flow rates are 100 L/hr., 300 L/hr., 500 L/hr. and 650L/hr., respectively, by using a non-evacuated glass receiver. In addition, the useful heat gain increases with increasing of the flow rate in spite of the decreasing in the temperatures difference through the collectors.

This phenomenon can be attributed to the known fact that heat losses inherently influences on the average absorber temperature, this lead to lower losses because the average absorber temperatures are lower and there's a corresponding increase in the useful heat gain. Moreover, it can also be seen that the useful heat gain of the system with an evacuated glass receiver is better than that with a non-evacuated glass receiver for the same flow rates. This because the evacuation of the air reduces the convection and radiation losses, therefore the absorbed energy by evacuated glass receiver is the highest.
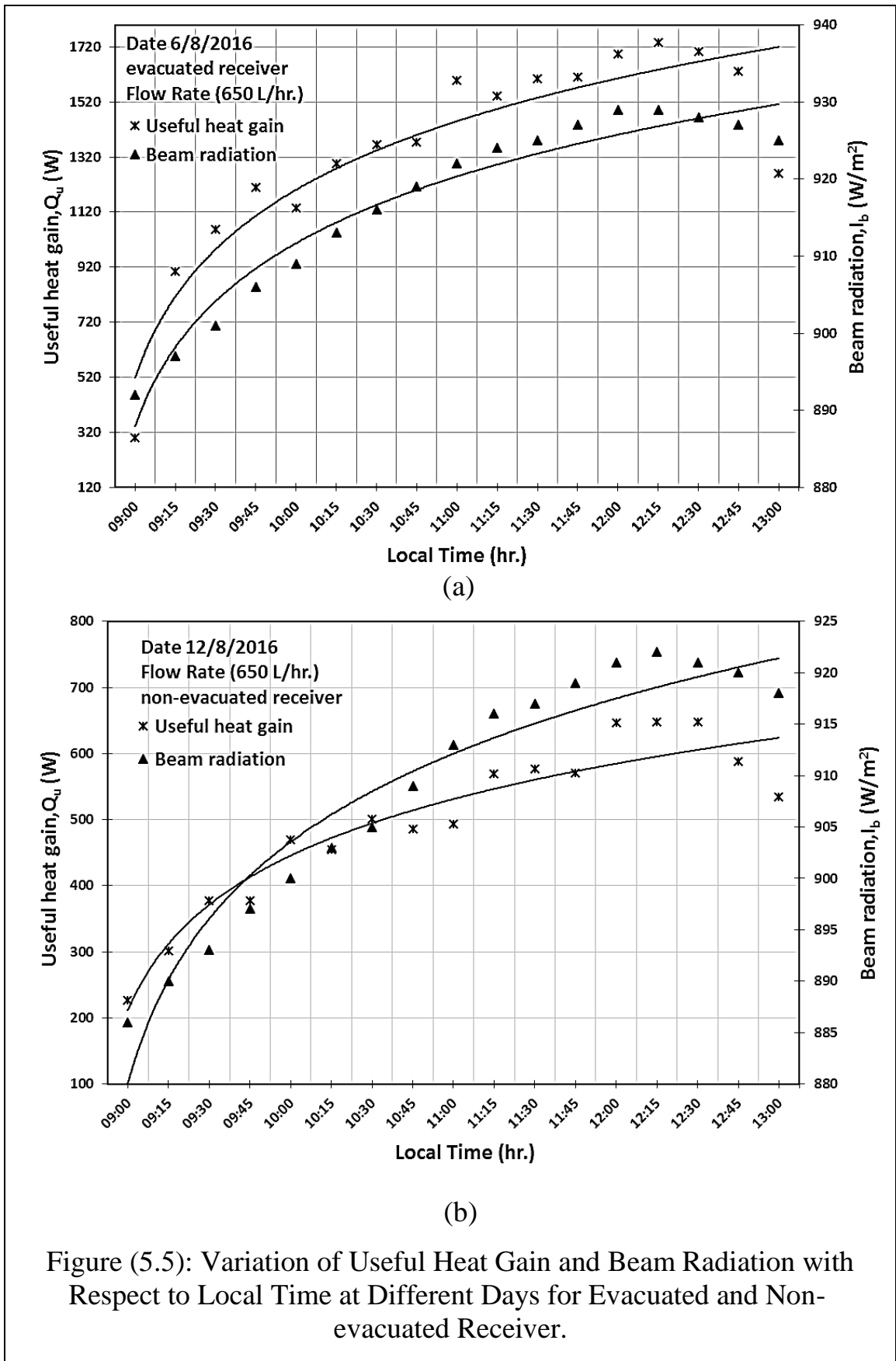
Figure (5.5): Variation of Useful Heat Gain and Beam Radiation with Respect to Local Time at Different Days for Evacuated and Non-evacuated Receiver.

(a)

(b)
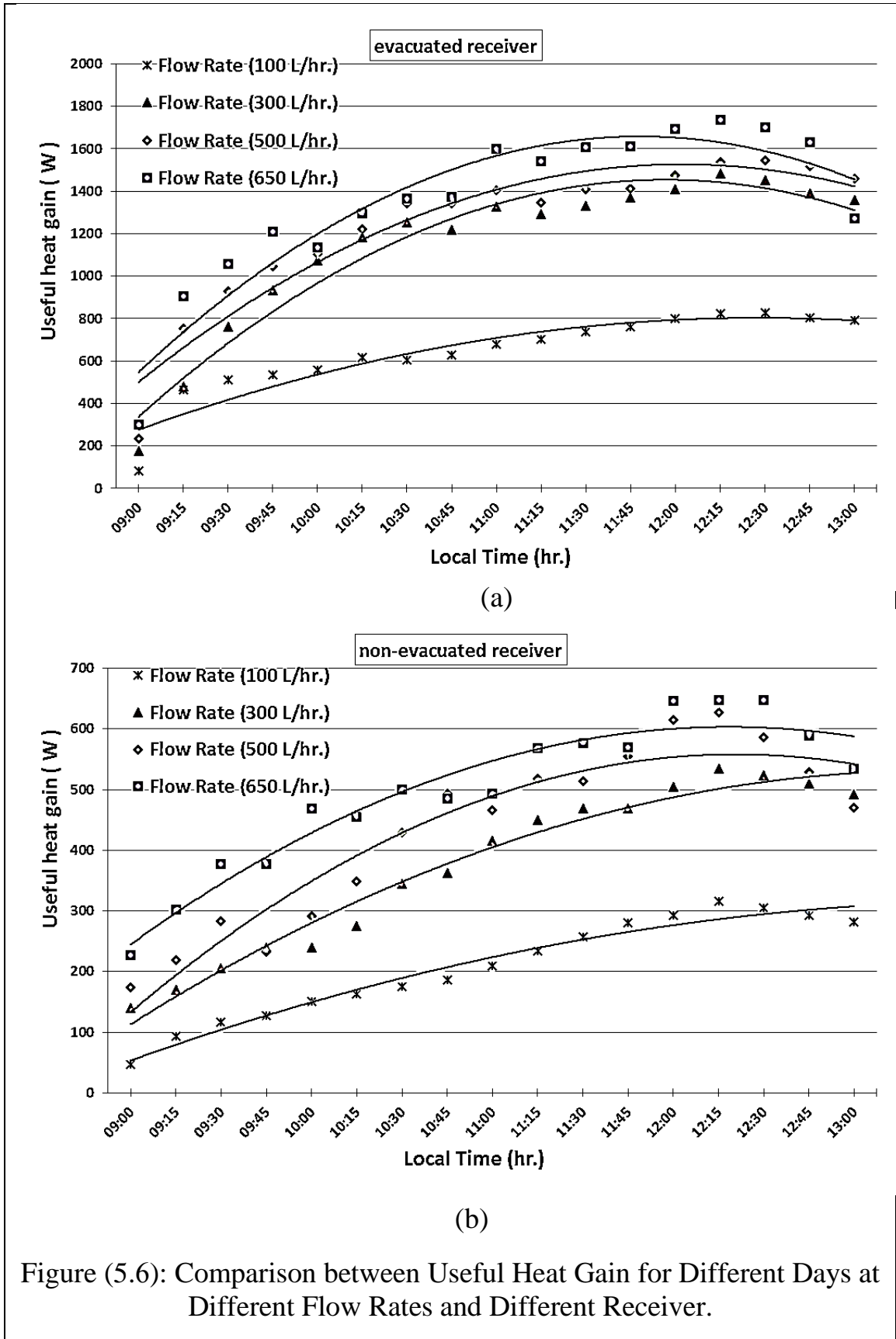
Figure (5.6): Comparison between Useful Heat Gain for Different Days at Different Flow Rates and Different Receiver.

57

5.4 Thermal Performance of the PTC

The thermal performance of the PTC was assessed experimentally by ASHRAE 93-1986 (RA 91) standard. The intent of the standard is to supply test procedures for evaluating the thermal performance of solar reflectors that use single-phase fluids and have no significant internal energy storage. This technique is well famed to get the thermal efficiency for comparison purpose with other solar reflectors.

5.4.1 Thermal Instantaneous Efficiency

The beam solar radiation, useful heat gain and aperture area were applied to the equation (3.26) to determine the thermal efficiency, η_{thi}. To investigate the performance of the PTC, all the experiments were carried out between 9:00 am and 13:00 pm and the required data were measured at quarter-hour intervals.

Figure (5.7 a&b) shows the relation between the variation of the thermal instantaneous efficiency, η_{thi}, and the beam solar radiation, I_b for an evacuated/a non-evacuated glass receiver at a flow rate of 650 L/hr. It can be observed that the thermal efficiency of the collector first starts to increase as the solar radiation increases until it reaches a maximum value around noontime (12:15 p.m.) and it then starts to decrease gradually as the time passes due to the decrease in solar radiation. Thus, the thermal efficiency increases with the increase in solar radiation.

Generally, it is noted that the overall pattern of the variance of efficiency over day is equivalent to that of the useful heat gain because the worth of efficiency is determined by both the incident beam radiation and the useful heat gain.

On the other hand, it can be concluded from figure (5.8 a&b) that the thermal efficiency increases with the increase in feed water flow rate. For example when the flow rates are 100 L/hr., 300 L/hr., 500 L/hr. and 650 L/hr., the thermal efficiency, η_{thi}, varies in range between 0.02 to 0.27, 0.05 to 0.43, 0.07 to 0.45, and 0.09 to 0.5 kW, respectively, using an evacuated glass receiver. In contrast, the thermal efficiency varies from 0.01 to 0.1, 0.04 to 0.15, 0.05 to 0.18, and 0.07 to 0.19, when the feed water flow rates are 100 L/hr., 300 L/hr., 500 L/hr. and 650 L/hr., respectively, using a non-evacuated glass receiver. Thus, the thermal efficiency increases with the increase in the mass flow rate.

This phenomenon can be elucidated by the fact that higher heat is gained and absorbed at a higher water flow rate, which in turns decrease the heat losses because the average absorber temperatures are lower and hence increasing the useful heat gain and the thermal efficiency. It can also be seen that the thermal efficiency of the system is better with an evacuated glass receiver than that with a non-evacuated glass receiver for the same flow rates.
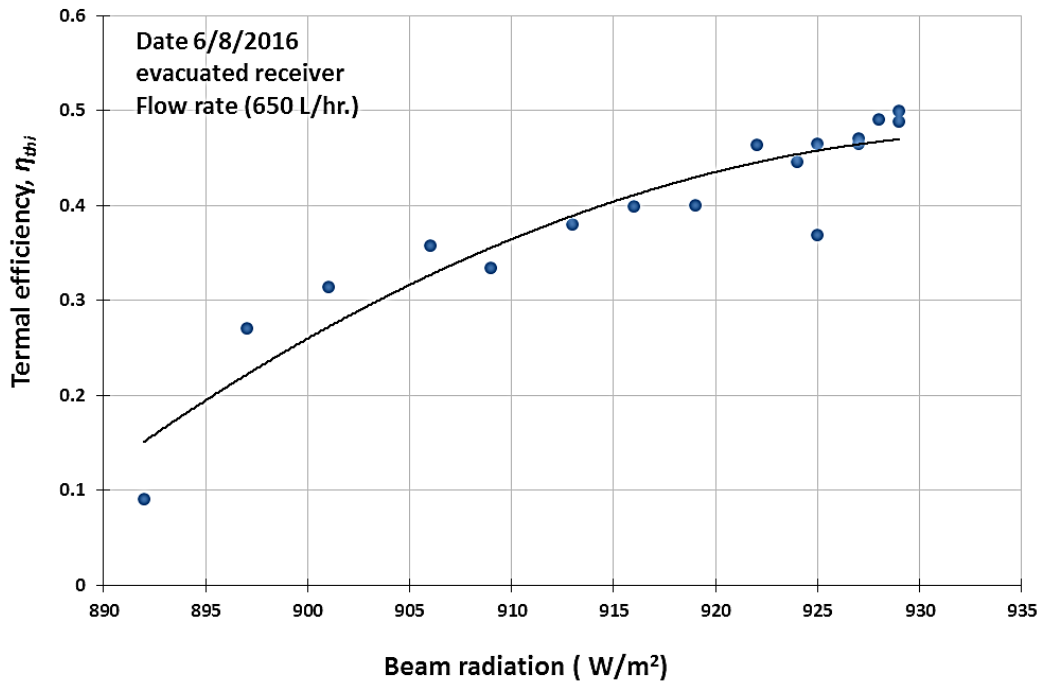
(a)
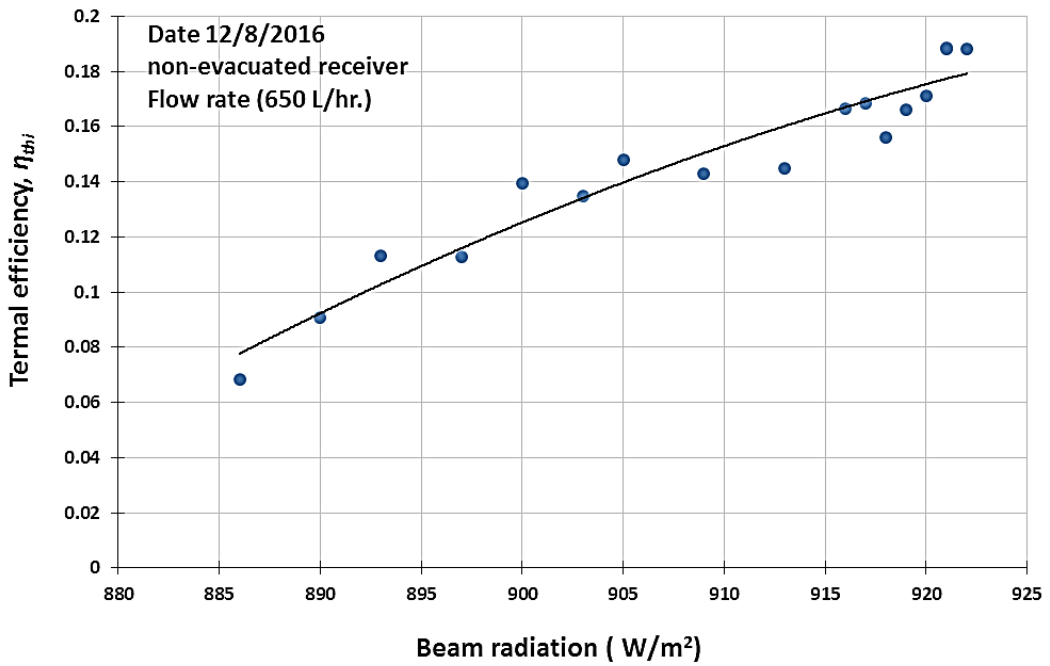
(b)

Figure (5.7): Variation of Thermal Efficiency with Solar Beam Radiation at Different Days for Evacuated and Non-evacuated Receiver.
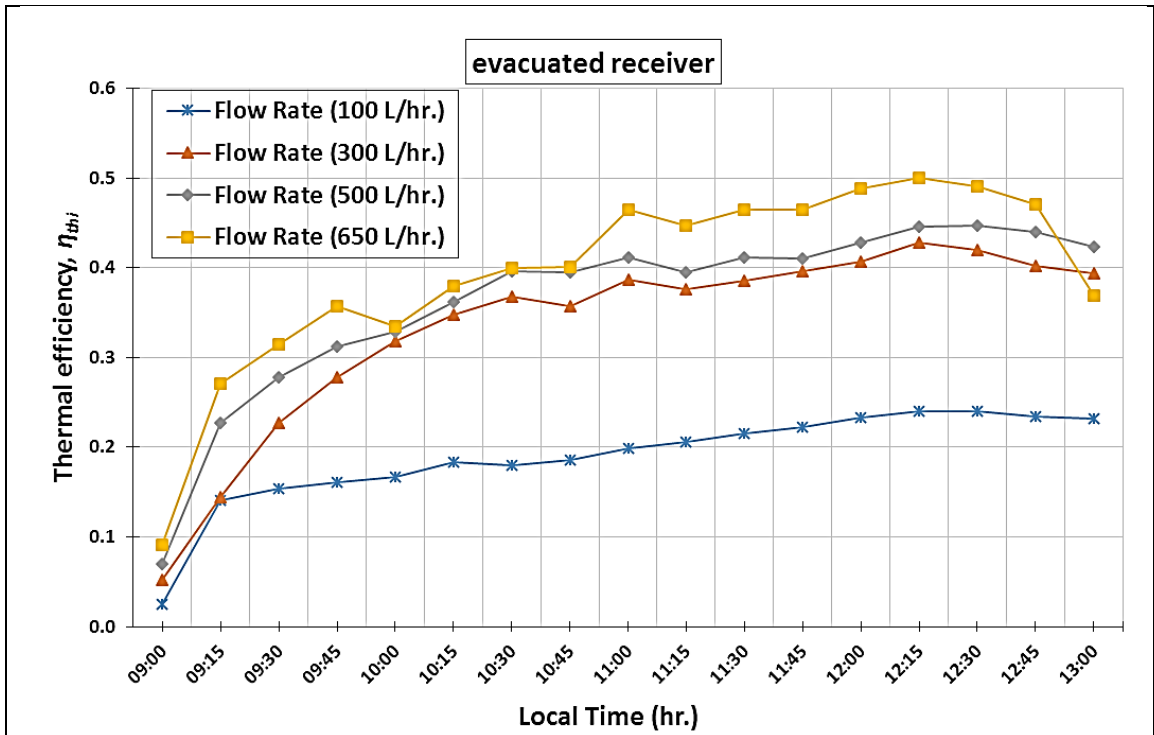
(a)
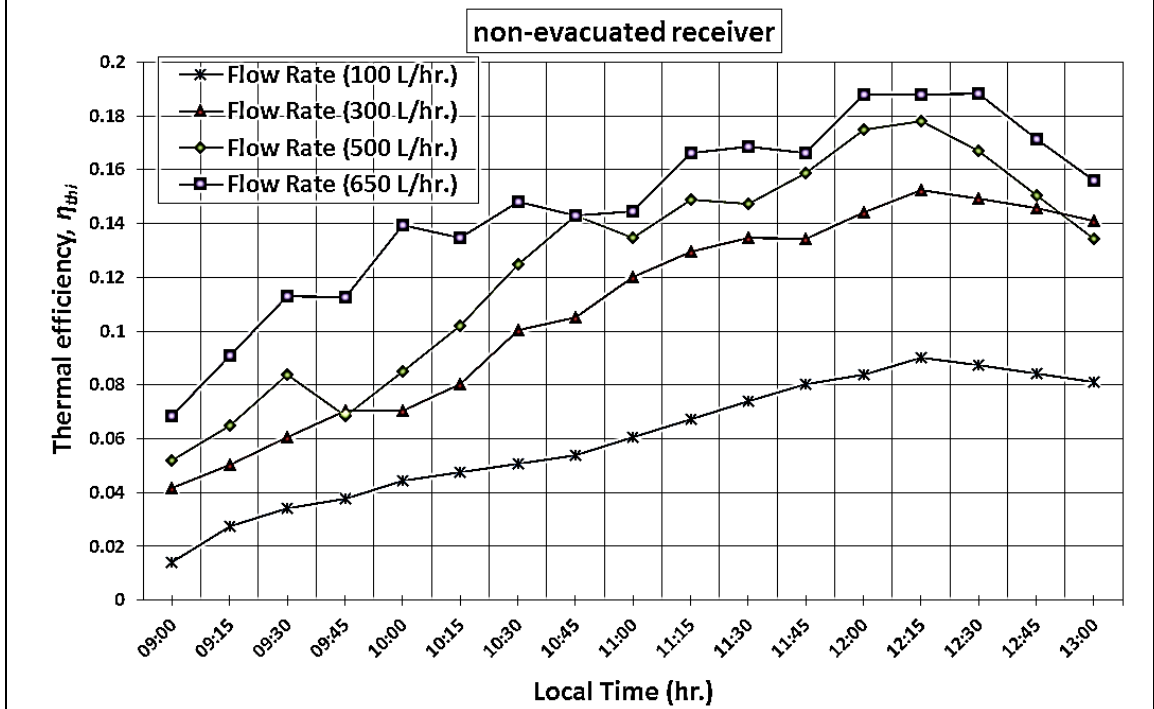
(b)

Figure (5.8): Comparison between Thermal Efficiency for Different Days at Different Flow Rates and Different Receiver.

61

5.4.2 Thermal Collector Efficiency

The instantaneous thermal efficiency η_{thi} was evaluated previously by using the equation (3.28). While the thermal collector efficiency η_{th} of the concentrators through the First Law is given as demonstrated in Eq. (3.29). The form is had by the thermal collector efficiency equation of $y = b + mx$, which can help experimentally to obtain the heat removal factor F_R and the overall heat loss coefficient U_L. Linear models of thermal efficiency were enforced on the experimental data corresponding to Equation (3.29), where $F_R U_L/C$ is the slope of the line and $F_R \eta_o$ is the y-intercept. It's important to point that for a reflector working under steady radiation and flow rate, $F_R \eta_o$ and $F_R U_L/C$ are nearly constant. Therefore, Equation (3.29) plots as a direct line over a graph of efficiency versus the heat loss parameter $\Delta T/I_b$. The performance curve of the PTC of the present work is derived from a series of test days conducted at different values of water flow rate that are passing in evacuated and non-evacuated glass receivers in two cases.

The efficiency curves for evacuated and non-evacuated glass receivers are shown in figure (5.9 a&b). The details show the thermal instantaneous efficiency and a direct line of best fit can be drawn between those points to get the thermal efficiencies for the solar concentrators.

The peak values for the thermal reflector efficiency are nearly 50% and 18.8% for both the evacuated and non-evacuated glass receiver, respectively. It is noted clearly, that the peak collector efficiency occurs at the higher flow rate in both cases. This phenomenon can be attributed to the fact that higher heat is gained and absorbed at the higher values of feed water flow rate. By increasing the feed water flow rate the heat removal factor will be increased, leading to a significant increase in the collector efficiency.
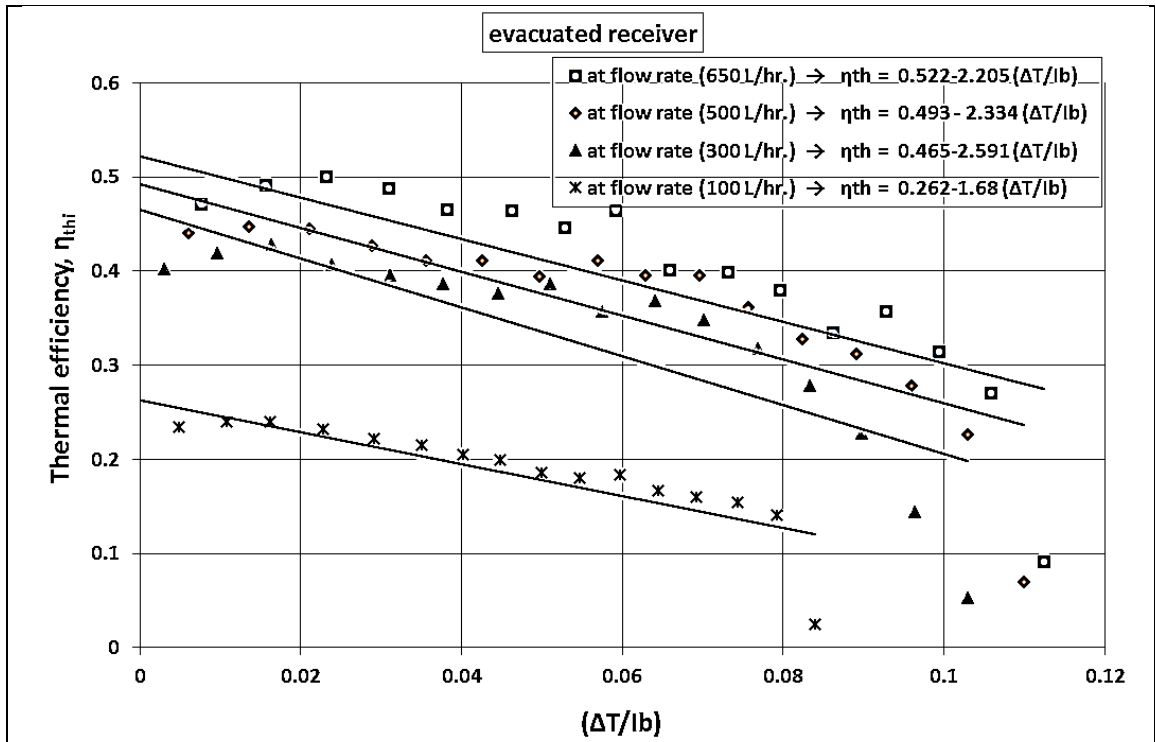
(a)
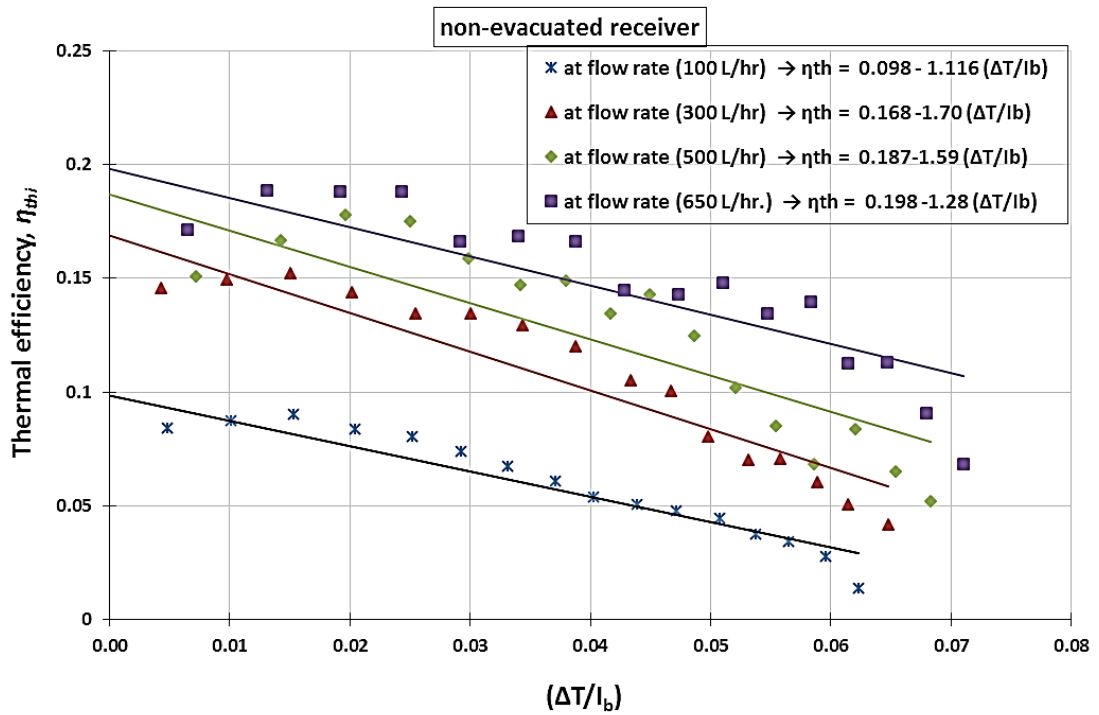
(b)

Figure (5.9): Thermal Efficiency Data and Fit Curves for Different Days at Different Flow Rates and Different Receiver.

63

Moreover, the thermal efficiency using evacuated receiver increasing steadily compared with that using non-evacuated glass receiver. Thus, thermal efficiency indicates a beneficial effect when the receiver is evacuated. The values of the heat removal factor F_R, the overall heat loss coefficient U_L, and thermal efficiency η_{th} are reported in table (5.1). Moreover, the efficiency curves which may have been reported in the literature for this kind of solar reflectors are shown in table (5.2).

Table (5.1): Thermal Performance of the PTC for the present work

Flow rate (L/hr.)	Receiver type	Thermal efficiency equation	F_R	U_L (W/m2 k)
100	Evacuated	$\eta_{th} = 0.262 - 1.68\,(\Delta T/I_b)$	0.47	16.5
	N-Evacuated	$\eta_{th} = 0.098 - 1.116\,(\Delta T/I_b)$	0.18	29.3
300	Evacuated	$\eta_{th} = 0.465 - 2.591\,(\Delta T/I_b)$	0.84	14.34
	N-Evacuated	$\eta_{th} = 0.168 - 1.70\,(\Delta T/I_b)$	0.30	26
500	Evacuated	$\eta_{th} = 0.493 - 2.334\,(\Delta T/I_b)$	0.89	12.1
	N-Evacuated	$\eta_{th} = 0.187 - 1.59\,(\Delta T/I_b)$	0.34	21.8
650	Evacuated	$\eta_{th} = 0.522 - 2.205\,(\Delta T/I_b)$	0.95	10.8
	N-Evacuated	$\eta_{th} = 0.198 - 1.28\,(\Delta T/I_b)$	0.36	16.6

Table (5.2): Thermal efficiency for different types of PTC.

Efficiency equation	Flow rate	Refs.
$\eta_{th} = 0.6128 - 2.3025\,(\Delta T/I_b)$	240L/hr.	[45]
$\eta_{th} = 0.69 - 0.390\,(\Delta T/I_b)$	60L/hr.	[46], [47]]
$\eta_{th} = 0.5430 - 0.189\,(\Delta T/I_b)$	0.022kg/s	[24]
$\eta_{th} = 0.5884 - 2.3014\,(\Delta T/I_b)$	300L/hr.	[28]
$\eta_{th} = 0.6052 - 2.252\,(\Delta T/I_b)$	360L/hr.	[28]
$\eta_{th} = 0.5214 - 0.1006\,(\Delta T/I_b)$	0.3kg/s	[34]

Chapter Five
Conclusions and Recommendations

6.1 Conclusions

In this research, an experimental investigation has been accompanied by the experimental study of the thermal performance of PTC in order to generate steam at a medium-temperature. The main investigated parameters were the inlet temperature of the system, the outlet temperature of the system, different flow rates at different days, heat gain, instantaneous thermal efficiency, collector efficiency η, solar beam radiation, ambient temperature and the receiver type. At the end of the experiments, the following important conclusions were drawn out :-

1. The temperatures difference trough the collectors increase with the decrease in the feed water flow rate, and it was the highest when the evacuated glass receiver is used.

2. The useful heat gain increases with the increase in the intensity of the beam radiation and the feed water flow rate. In addition, it was the highest when evacuated glass receiver is used.

3. The instantaneous thermal efficiency increases with the increase in the intensity of the beam radiation and the feed water flow rate. In addition, it was the highest when evacuated glass receiver is used.

4. The heat loss coefficient decreases with the increase in the feed water flow rate, and it was the lowest when the evacuated glass receiver is used.

5. The heat removal factor increases to unity with the increase in the feed water flow rate, and it was the highest when the evacuated glass receiver is used.

6. The collector efficiency is best at the high flow rate, and it were the highest at using the evacuated glass receiver.

Consequently, to improve the solar water heating systems efficiency (using PTC) the flow rate of the fluid should be increased.

6.2 Recommendations

The following recommendations can be considered for future researches.

1. The sun-tracking base can be developed for tracking the PTC system automatically.

2. The insulated flash-vessel can be fixed on the storage tank.

3. Different absorber coating materials can be tested to see their effects on the performance of the system.

4. PTC with a largest aperture width can also be tested with the system to see their effects on the performance.

5. Using steam flow meter to maintain a specific mass flow rate of steam produced by this experimental test rig in order to design a full scale of PTC system to satisfy any quantity of steam requirement.

References

[1]   Z. Sen, "Solar energy in progress and future research trends," *Prog. energy Combust. Sci.*, vol. 30, no. 4, pp. 367–416, 2004.

[2]   S. A. Kalogirou, "Solar thermal collectors and applications," *Prog. energy Combust. Sci.*, vol. 30, no. 3, pp. 231–295, 2004.

[3]   K. Sukhatme and S. P. Sukhatme, *Solar energy: principles of thermal collection and storage*. Tata McGraw-Hill Education, 1996.

[4]   T. Seblewongel, "Simulation of Parabolic Trough Concentrating Solar Power Generation System," phD. thesis. Addis Ababa University, 2014.

[5]   A. Fernández-Garc'\ia, E. Zarza, L. Valenzuela, and M. Pérez, "Parabolic-trough solar collectors and their applications," *Renew. Sustain. Energy Rev.*, vol. 14, no. 7, pp. 1695–1721, 2010.

[6]   W. Weiss and M. Rommel, "Solar heat for industrial processes: medium temperature collectors," *State Art within Task*, vol. 33, 2005.

[7]   "Amargosa Valley - Solar Millennium," 2009. [Online]. Available: http://www.basinandrangewatch.org/AV-SolarMill-scoping-Aug2009.html.

[8]   S. A. Kalogirou, *Solar energy engineering: processes and systems*, 2nd ed. Academic Press, 2013.

[9]   A. Press, "Storage Tank at Solar Power Plant in Desert Explodes; Immediate Area Is Evacuated," *Los Angeles Times*, 27-Feb-1999.

[10]   M. Eck and W.-D. Steinmann, "Direct steam generation in parabolic troughs: first results of the DISS project," *J. Sol. energy Eng.*, vol. 124, no. 2, pp. 134–139, 2002.

[11]   E. Zarza, M. E. Rojas, L. González, J. M. Caballero, and F. Rueda, "INDITEP: The first pre-commercial DSG solar power plant," *Sol.*

Energy, vol. 80, no. 10, pp. 1270–1276, 2006.

[12] S. D. Odeh, G. L. Morrison, and M. Behnia, "Modelling of parabolic trough direct steam generation solar collectors," *Sol. energy*, vol. 62, no. 6, pp. 395–406, 1998.

[13] E. Zarza, L. Valenzuela, J. León, H. Weyers, M. Eickhoff, M. Eck, and K. Hennecke, "The DISS Project: Direct Steam Generation in Parabolic Troughs: Operation and Maintenance Experience-Update on Project Status," *Sol. Eng.*, pp. 419–426, 2001.

[14] M. Geyer, E. Lüpfert, R. Osuna, A. Esteban, W. Schiel, A. Schweitzer, E. Zarza, P. Nava, J. Langenkamp, and E. Mandelberg, "Eurotrough-Parabolic trough collector developed for cost efficient solar power generation," *11th Int. Symp. Conc. Sol. power Chem. energy Technol.*, pp. 04–06, 2002.

[15] M. Eck, E. Zarza, M. Eickhoff, J. Rheinländer, and L. Valenzuela, "Applied research concerning the direct steam generation in parabolic troughs," *Sol. energy*, vol. 74, no. 4, pp. 341–351, 2003.

[16] M. Singh, B. Singh, and F. Sulaiman, "Designing A Solar Thermal Cylindrical Parabolic Trough Concentrator By Simulation.," *Int. Rio3 Congr.*, pp. 1–6, 2003.

[17] E. Zarza, L. Valenzuela, J. Leon, K. Hennecke, M. Eck, H.-D. Weyers, and M. Eickhoff, "Direct steam generation in parabolic troughs: Final results and conclusions of the DISS project," *Energy*, vol. 29, no. 5, pp. 635–644, 2004.

[18] M. J. Brooks and T. M. Harms, "Design, construction and testing of a parabolic trough solar collector for a developing-country application," *Proc. ISES Sol. World Congr. Orlando, FL*, vol. 605, pp. 6–12, 2005.

[19] M. Eck and E. Zarza, "Saturated steam process with direct steam generating parabolic troughs," vol. 80, pp. 1424–1433, 2006.

[20] A. V. Arasu and S. T. Sornakumar, "Performance characteristics of the solar parabolic trough collector with hot water generation system," *Therm. Sci.*, vol. 10, no. 2, pp. 117–167, 2006.

[21] M. Qu, D. H. Archer, and H. Yin, "A linear parabolic trough solar collector performance model," in *Energy Sustainability Conference*, 2007, pp. 663–670.

[22] D. Krüger, Y. Pandian, K. Hennecke, and M. Schmitz, "Parabolic trough collector testing in the frame of the REACt project," *Desalination*, vol. 220, no. 1, pp. 612–618, 2008.

[23] J. Folaranmi, "Design, construction and testing of a parabolic solar steam generator," *Leonardo Electron. J. Pract. Technol.*, vol. 14, pp. 115–133, 2009.

[24] N. R. Hau and M. A. E. Soberanis, "Efficiency of a parabolic trough collector as a water heater system in Yucatán, Mexico," *J. Renew. Sustain. Energy*, vol. 3, no. 6, p. 63108, 2011.

[25] S. Ruby, "Industrial Process Steam Generation Using Parabolic Trough Solar Collection," *Calif. Energy Comm. Publ. number CEC-500-2011-040*, 2012.

[26] L. Zhang, W. Wang, Z. Yu, L. Fan, Y. Hu, Y. Ni, J. Fan, and K. Cen, "An experimental investigation of a natural circulation heat pipe system applied to a parabolic trough solar collector steam generation system," *Sol. Energy*, vol. 86, no. 3, pp. 911–919, 2012.

[27] L. Valenzuela, D. Hernández-Lobón, and E. Zarza, "Sensitivity analysis of saturated steam production in parabolic trough collectors," *Energy

Procedia, vol. 30, pp. 765–774, 2012.

[28] E. Venegas-Reyes, O. A. Jaramillo, R. Castrejón-Garcia, J. O. Aguilar, and F. Sosa-Montemayor, "Design, construction, and testing of a parabolic trough solar concentrator for hot water and low enthalpy steam generation," *J. Renew. Sustain. Energy*, vol. 4, no. 5, p. 53103, 2012.

[29] L. Zhang, Z. Yu, L. Fan, W. Wang, H. Chen, Y. Hu, J. Fan, M. Ni, and K. Cen, "An experimental investigation of the heat losses of a U-type solar heat pipe receiver of a parabolic trough collector-based natural circulation steam generation system," *Renew. energy*, vol. 57, pp. 262–268, 2013.

[30] M. Alguacil, C. Prieto, A. Rodriguez, and J. Lohr, "Direct steam generation in parabolic trough collectors," *Energy Procedia*, vol. 49, pp. 21–29, 2014.

[31] B. T. Chiad, F. A. H. Mutlak, M. Al-ansari, and A. A. Ahmed, "Improving the Solar Concentrator for Hot Water Generation," *Int. J. Appl. or Innov. Eng. Manag.*, vol. 3, no. 7, pp. 313–319, 2014.

[32] J. Al Asfar, O. Ayadi, and A. Al Salaymeh, "Design and performance assessment of a parabolic trough collector," *Jordan J. Mech. Ind. Eng.*, vol. 8, no. 1, 2014.

[33] M. G. Tayade, R. E. Thombre, and S. Dutt, "Performance Evaluation of Solar Parabolic Trough," *Int. J. Nano Dimens.*, vol. 5, no. 3, pp. 233–240, 2014.

[34] I. H. Yilmaz, H. Hayta, R. Yumrutas, and M. S. Söylemez, "Performance testing of a parabolic trough collector array," in *The 6th International Congress of Energy and Environment Engineering and Management (CIIEM15), Paris, France*, 2015, pp. 22–24.

[35] F. Jamadi, "experimental investigation of effect of oil mass flow changes on parabolic trough collector efficiency in a solar water heater system," *Int. J. "Technical Phys. Probl. Eng.*, vol. 8, no. 26, pp. 88–94, 2016.

[36] J. A. Duffie and W. A. Beckman, *Solar engineering of thermal processes*, vol. 3. Wiley New York, 2013.

[37] O. Garcia-Valladares and N. Velázquez, "Numerical simulation of parabolic trough solar collector: Improvement using counter flow concentric circular heat exchangers," *Int. J. Heat Mass Transf.*, vol. 52, no. 3, pp. 597–609, 2009.

[38] E. Jacobson, N. Ketjoy, S. Nathakaranakule, and W. Rakwichian, "Solar parabolic trough simulation and application for a hybrid power plant in Thailand," *Sci. Asia*, vol. 32, no. 2, pp. 187–199, 2006.

[39] N. Janotte, S. Meiser, D. Krüger, E. Lüpfert, R. Pitz-Paal, S. Fischer, and H. Müller-Steinhagen, "Quasi-dynamic analysis of thermal performance of parabolic trough collectors," in *SolarPACES 2009 Conference Proceedings*, 2009.

[40] A. Architectural, "aluminium composite materials." [Online]. Available: new alucobond solar_ light reflectivity values.pdf.

[41] L. Ma, Z. Lu, J. Zhang, and R. Liang, "Thermal performance analysis of the glass evacuated tube solar collector with U-tube," *Build. Environ.*, vol. 45, no. 9, pp. 1959–1967, 2010.

[42] H. P. Garg and others, *Solar energy: fundamentals and applications*. Tata McGraw-Hill Education, 2000.

[43] F. A. Al-Sulaiman, "Energy and sizing analyses of parabolic trough solar collector integrated with steam and binary vapor cycles," *Energy*,

vol. 58, pp. 561–570, 2013.

[44] S. Kalogirou, "Parabolic trough collector system for low temperature steam generation: design and performance characteristics," *Appl. Energy*, vol. 55, no. 1, pp. 1–19, 1996.

[45] O. A. Jaramillo, E. Venegas-Reyes, J. O. Aguilar, R. Castrejón-Garcia, and F. Sosa-Montemayor, "Parabolic trough concentrators for low enthalpy processes," *Renew. energy*, vol. 60, pp. 529–539, 2013.

[46] A. V. Arasu and T. Sornakumar, "Performance Characteristics of ParabolicTrough Solar Collector System forHot Water Generation," *Int. Energy J.*, vol. 7, no. 2, 2006.

[47] A. V. Arasu and T. Sornakumar, "Design, manufacture and testing of fiberglass reinforced parabola trough for parabolic trough solar collectors," *Sol. Energy*, vol. 81, no. 10, pp. 1273–1279, 2007.

Appendix [A]

Design Drawings of PTC System
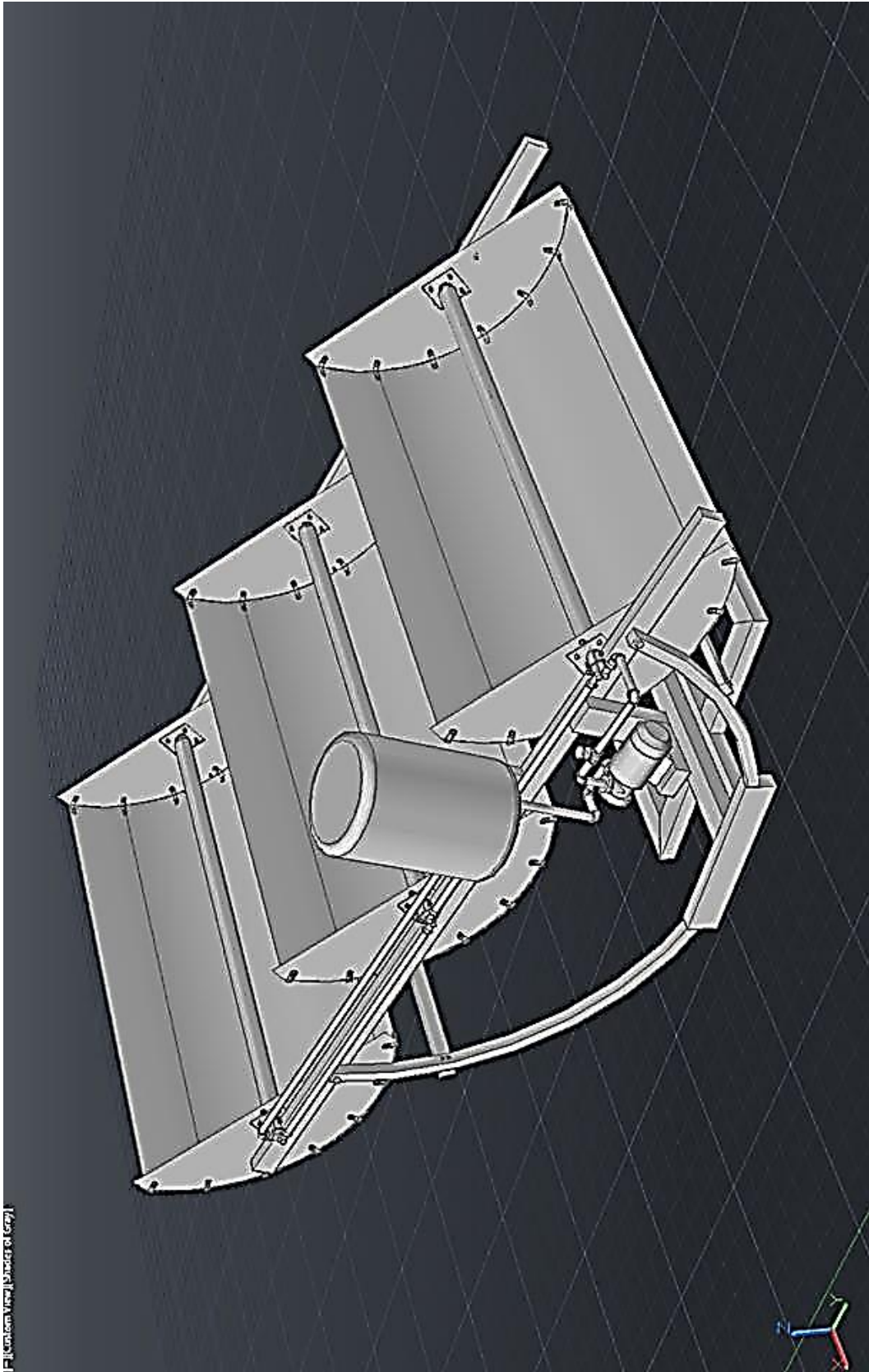
Figure (A.1): PTC system
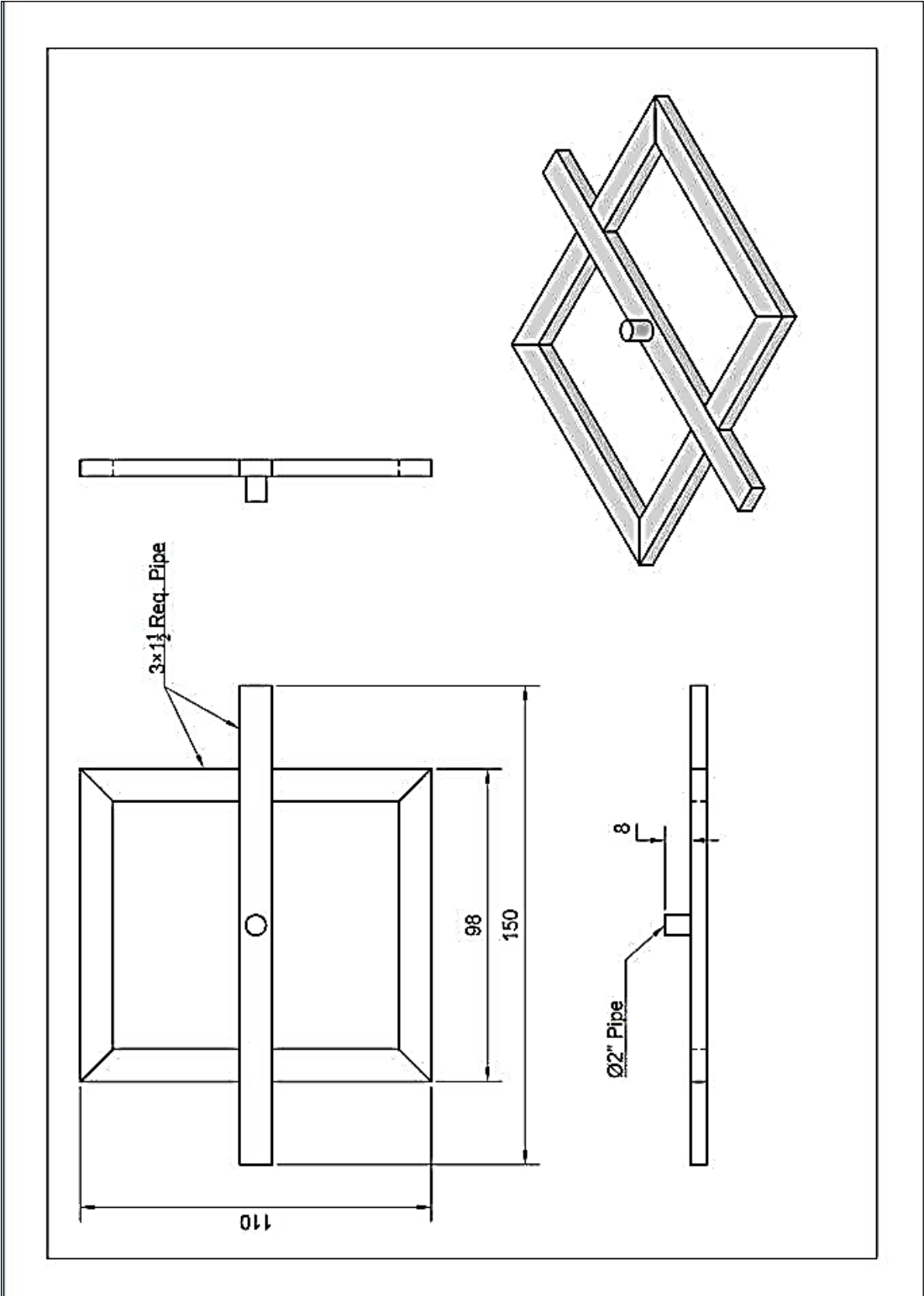
Figure (A.2): Dimensioned Diagram of the Stationary Base
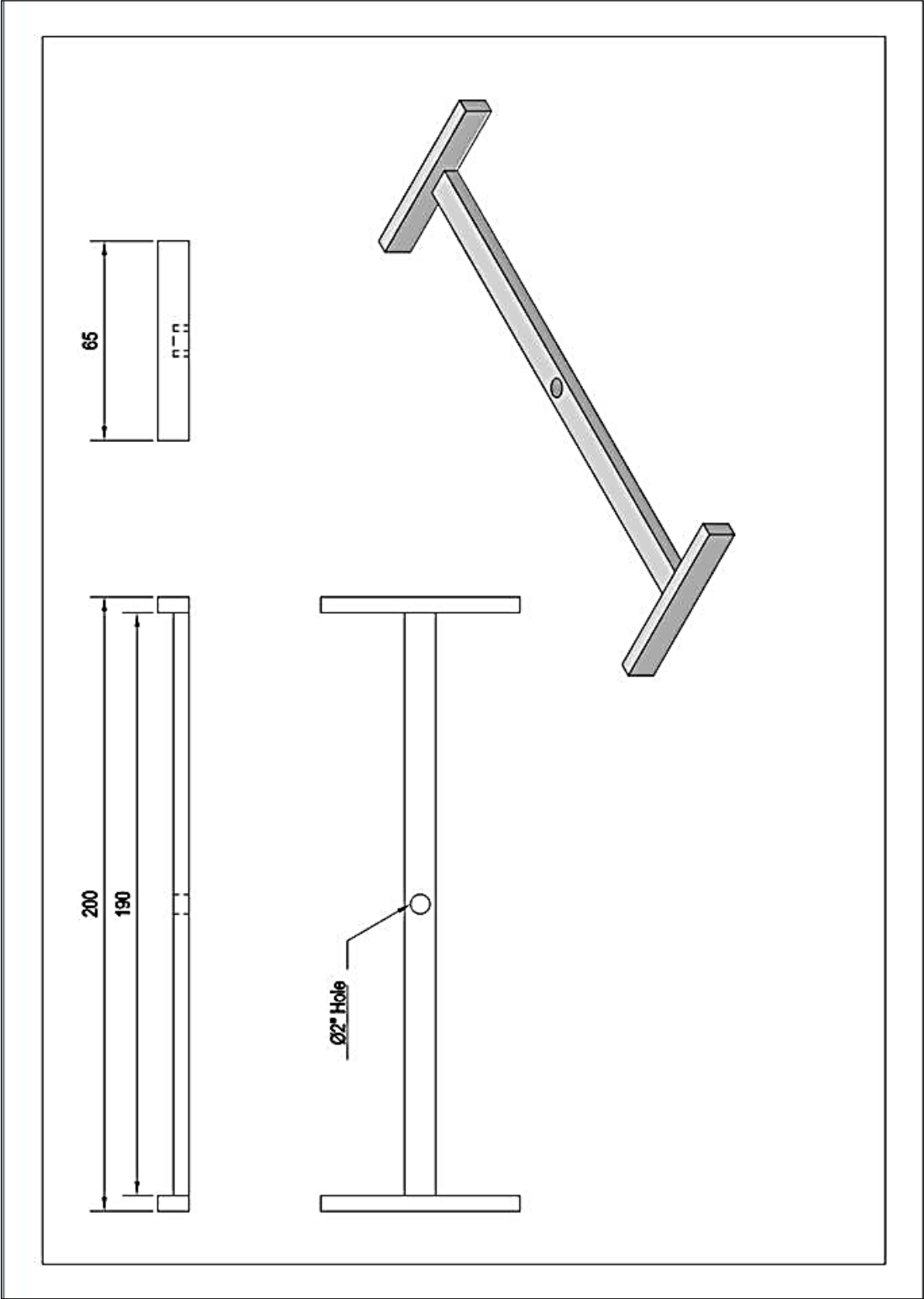
Figure (A.3): Dimensioned Diagram of the Axial Motion Base
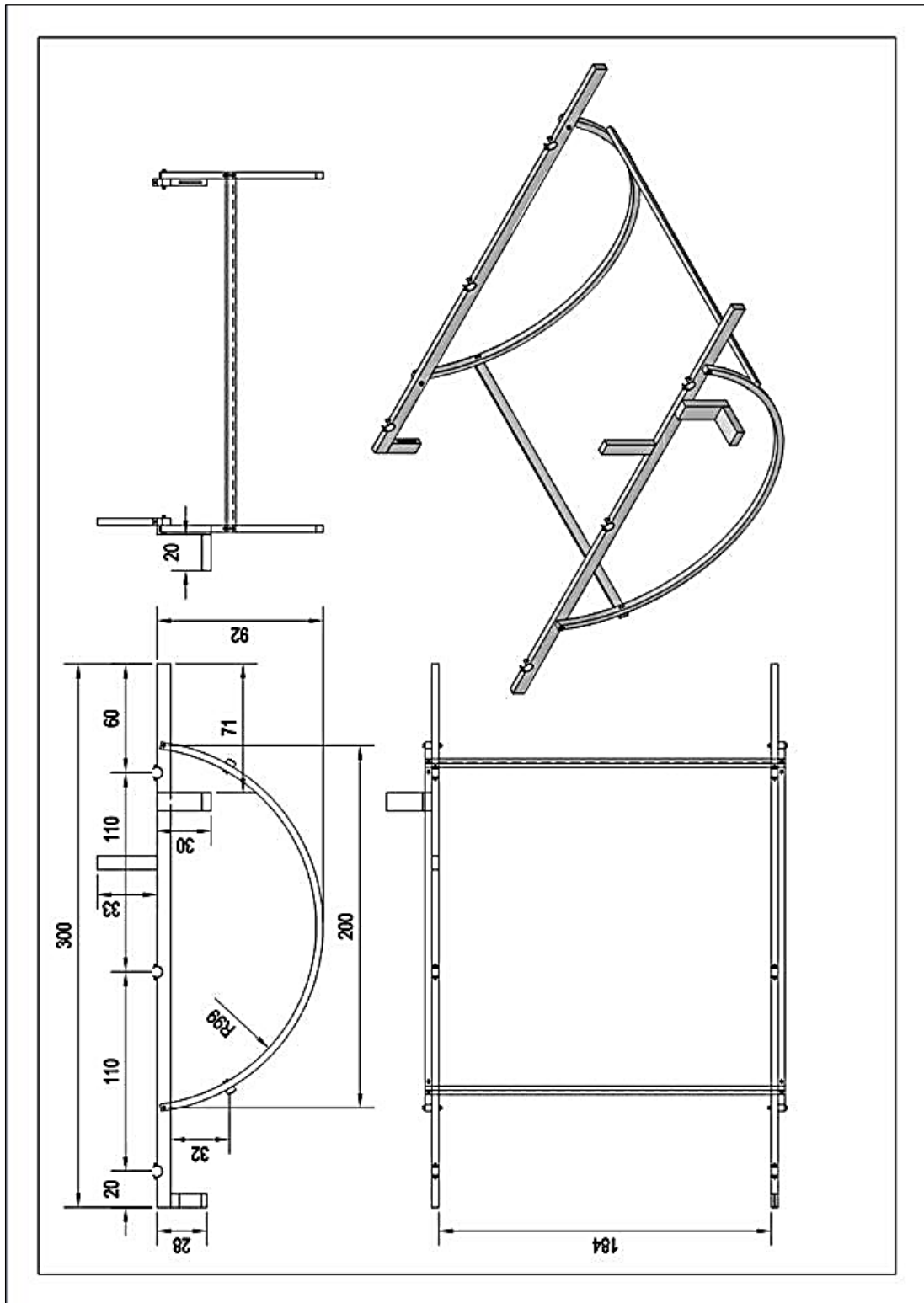
Figure (A.4): Dimensioned Diagram of the Tilting Motion Base
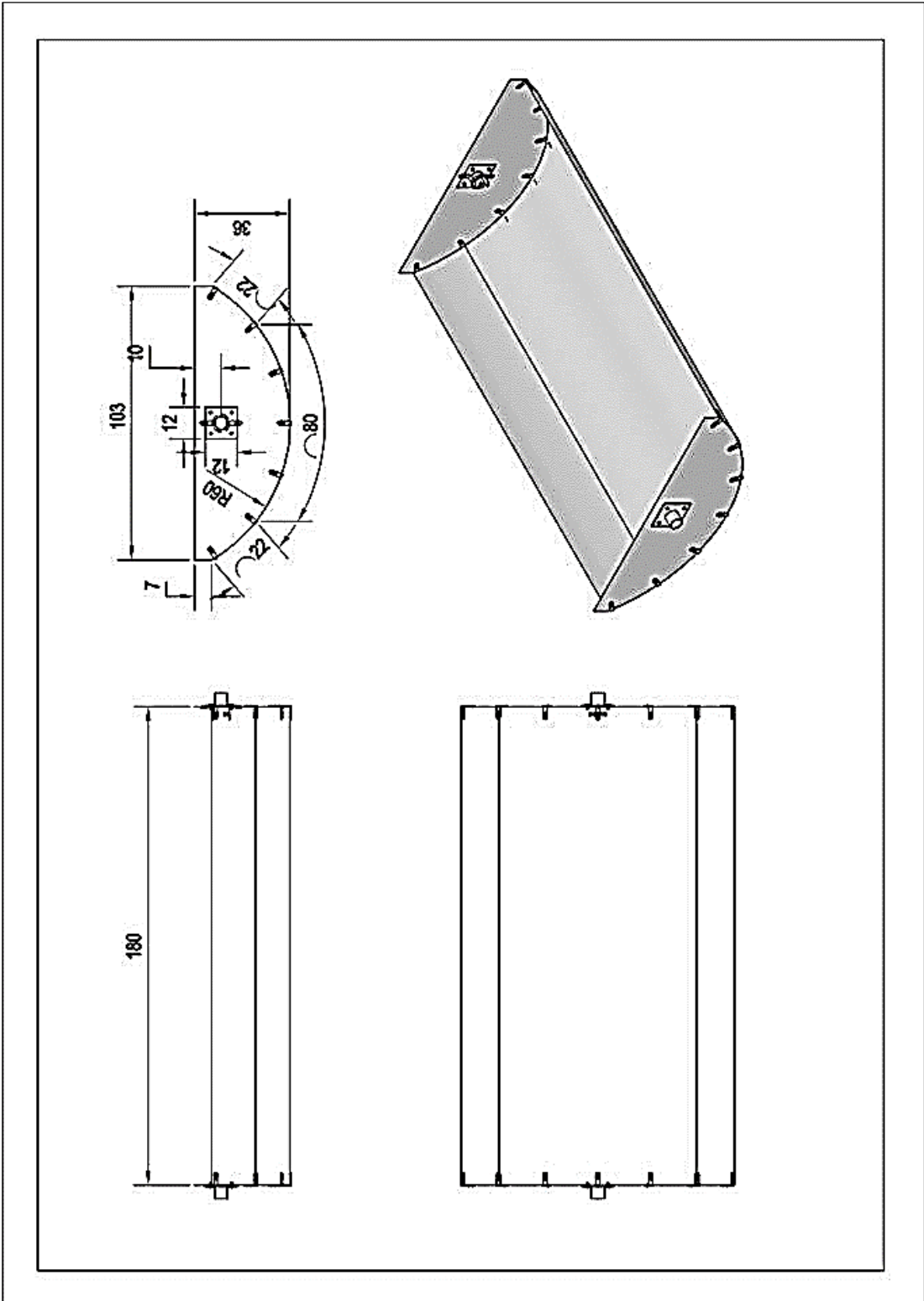
Figure (A.5): Dimensioned Diagram of the PTC
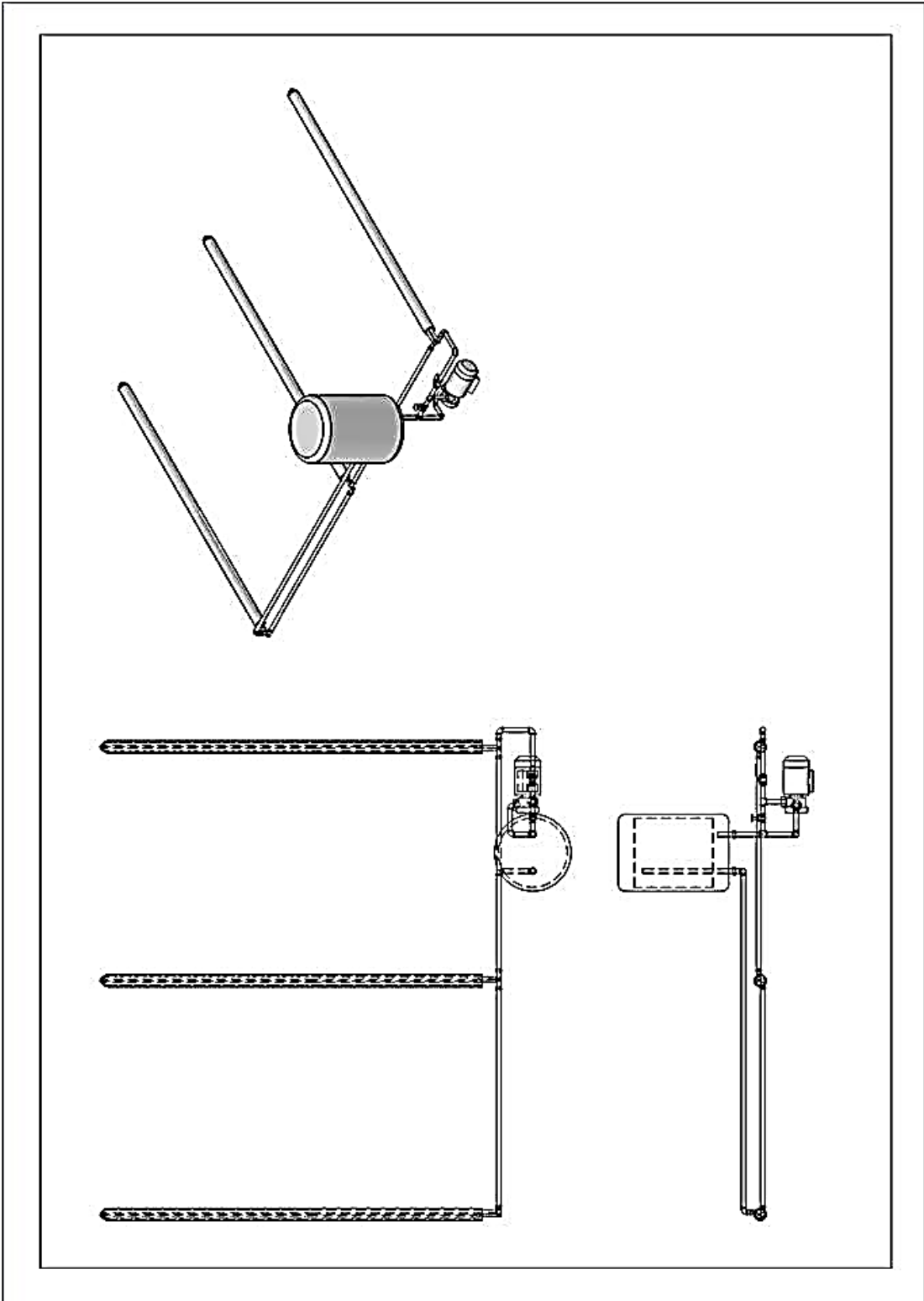
Figure (A.6): Pipeline Grid of PTC System

Appendix (B-Tables)   No. of day =217   δ= 16.83º   ϕ =32.02º L_{loc} =44.33º

Table (B.1): Experimental Data for Evacuated Glass Receiver During 5th August 2016   Flow rate : 100L/hr.

Time	T_1^* (ºC)	T_2 (ºC)	T_3 (ºC)	T_4^* (ºC)	T_5 (ºC)	T_6 (ºC)	T_7 (ºC)	T_a (ºC)	Pressure of tank (barG)	Beam radiation, I_b (w/m^2)	Wind speed (m/s)	Cp (kJ/kg k)	Q_u (W)	η_{thi} (%)	$T_{in}-T_a/I_b$
09:00	40.5	40.8	41.0	41.2	41.1	40.7	40.6	40.8	0	880	0.4	4.18	81	2.5	0.000
09:15	45.4	46.9	48.3	49.4	49.3	47.1	45.5	41.1	0	884	0.3	4.18	465	14.1	0.005
09:30	51.1	53.0	54.6	55.5	55.3	52.9	51.2	41.5	0.4	889	0.2	4.18	511	15.4	0.011
09:45	56.3	58.3	59.8	60.9	60.7	58.5	56.5	41.8	0.7	893	0.3	4.18	535	16.0	0.016
10:00	62.6	65.4	66.9	67.4	67.2	64.8	63.1	42.1	1	897	0.2	4.18	558	16.7	0.023
10:15	68.7	71.4	73.5	74.0	73.8	71.3	69.2	42.5	1.4	900	0.1	4.19	617	18.4	0.029
10:30	74.4	76.7	78.8	79.6	79.4	77.1	74.9	42.7	1.8	903	0.2	4.19	606	18.0	0.035
10:45	79.6	82.0	84.4	85.0	84.8	82.4	80.1	43.1	2.2	907	0.2	4.20	630	18.6	0.040
11:00	84.5	87.6	89.5	90.3	90.0	87.4	85.1	43.6	2.7	911	0.3	4.20	677	19.9	0.045
11:15	89.7	92.5	94.9	95.7	95.5	92.8	90.2	44	3.1	915	0.2	4.21	702	20.5	0.050
11:30	94.7	97.5	100.0	101.0	100.7	97.9	95.3	44.5	3.6	917	0.7	4.21	738	21.5	0.055
11:45	99.8	102.9	105.4	106.3	106.0	103.1	100.4	44.9	4	918	0.6	4.22	762	22.2	0.060
12:00	104.8	107.9	110.7	111.6	111.3	108.3	105.4	45.4	4	920	0.7	4.23	799	23.3	0.065
12:15	109.6	112.6	115.5	116.6	116.2	113.1	110.2	45.8	4	921	0.6	4.23	824	24.0	0.069
12:30	114.7	117.9	120.6	121.7	121.3	118.4	115.4	46.2	4	920	0.7	4.24	826	24.0	0.074
12:45	119.5	122.7	125.3	126.3	125.9	123.1	120.1	46.6	4	919	0.5	4.25	804	23.4	0.079
13:00	123.9	127.0	129.6	130.6	130.2	127.7	124.6	46.8	4	917	0.6	4.26	793	23.2	0.084

T_1^*/ T_4^* represent the inlet temperatures to the first collector and outlet temperatures from the last collector, respectively.

Table (B.2): Experimental Data for Evacuated Glass Receiver During 6th August 2016   Flow rate : 650 L/hr.

Time	$T_1{}^*$ (ºC)	T_2 (ºC)	T_3 (ºC)	$T_4{}^*$ (ºC)	T_5 (ºC)	T_6 (ºC)	T_7 (ºC)	T_a (ºC)	Pressure of tank (barG)	Beam radiation, I_b (w/m^2)	Wind speed (m/s)	Cp (kJ/kg k)	Q_u (W)	η_{thi} (%)	T_{in}-T_a/I_b
09:00	40.5	40.7	40.8	40.9	40.9	40.6	40.5	40.7	0	892	0.7	4.18	302	9.1	0.000
09:15	47.9	48.4	48.8	49.1	49.0	48.7	48.0	41	0	897	0.9	4.18	906	27.0	0.008
09:30	55.3	56.0	56.4	56.7	56.6	56.1	55.4	41.2	0.4	901	0.8	4.18	1057	31.4	0.016
09:45	62.7	63.3	63.9	64.3	64.2	63.6	62.8	41.6	0.7	906	0.4	4.18	1209	35.7	0.023
10:00	70.3	71.0	71.5	71.8	71.7	71.3	70.4	42.1	1.1	909	0.8	4.19	1135	33.4	0.031
10:15	77.5	78.3	78.8	79.2	79.1	78.5	77.6	42.5	1.6	913	0.9	4.19	1295	38.0	0.038
10:30	85.4	86.1	86.7	87.2	87.0	86.4	85.5	43	2.2	916	0.6	4.20	1366	39.9	0.046
10:45	92.0	92.8	93.3	93.8	93.7	93.1	92.1	43.4	2.8	919	0.5	4.21	1375	40.1	0.053
11:00	98.3	99.2	99.7	100.4	100.3	99.4	98.4	43.7	3.4	922	0.8	4.21	1599	46.4	0.059
11:15	104.9	105.6	106.3	106.9	106.8	106.1	105.1	43.9	4	924	0.6	4.22	1541	44.6	0.066
11:30	111.9	112.7	113.4	114.0	113.9	113.2	112.1	44.2	4	925	0.4	4.23	1606	46.5	0.073
11:45	118.6	119.3	120.0	120.7	120.6	119.9	118.8	44.7	4	927	0.3	4.24	1610	46.5	0.080
12:00	125.2	126.1	126.7	127.4	127.2	126.5	125.4	45.1	4	929	0.3	4.26	1693	48.8	0.086
12:15	131.8	132.7	133.3	134.0	133.8	133.1	132.0	45.5	4	929	0.5	4.27	1735	50.0	0.093
12:30	138.3	139.2	139.9	140.5	140.3	139.7	138.5	46	4	928	0.4	4.28	1702	49.1	0.099
12:45	144.5	145.3	145.9	146.6	146.4	145.9	144.7	46.3	4	927	0.2	4.30	1630	47.1	0.106
13:00	150.6	151.5	152.1	152.7	152.5	152.3	150.9	46.6	4	925	0.3	3.36	1274	36.9	0.112

$T_1{}^*$/ $T_4{}^*$ represent the inlet temperatures to the first collector and outlet temperatures from the last collector, respectively.

Appendix (B-Tables)   No. of day =220 δ= 15.96° ϕ =32.02° L_{loc} =44.33°

Table (B.3): Experimental Data for Evacuated Glass Receiver During 8th   August 2016   Flow rate : 300 L/hr.

Time	T_1^* (ºC)	T_2 (ºC)	T_3 (ºC)	T_4^* (ºC)	T_5 (ºC)	T_6 (ºC)	T_7 (ºC)	T_a (ºC)	Pressure of tank (barG)	Beam radiation, I_b (w/m²)	Wind speed (m/s)	Cp (kJ/kg k)	Q_u (W)	η_{thi} (%)	T_{in}-T_a/I_b
09:00	40.3	40.5	40.7	40.8	40.7	40.4	40.3	40.6	0	886	0.2	4.18	174	5.3	0.000
09:15	43.7	44.4	44.6	45.1	45.0	45.3	43.8	41	0	891	0.1	4.18	481	14.4	0.003
09:30	50.2	51.2	51.8	52.4	52.3	52.4	50.3	41.6	0.2	896	0.3	4.18	759	22.7	0.010
09:45	56.8	58.0	58.9	59.5	59.4	59.0	56.9	42.1	0.5	900	0.3	4.18	934	27.8	0.016
10:00	64.3	65.8	66.8	67.4	67.3	66.2	64.4	42.7	0.8	904	0.6	4.19	1074	31.8	0.024
10:15	71.4	72.8	73.8	74.8	74.7	73.0	71.5	43.2	1.3	908	0.3	4.19	1180	34.8	0.031
10:30	78.0	79.6	80.7	81.6	81.5	79.9	78.2	43.7	1.8	911	0.2	4.19	1252	36.8	0.038
10:45	84.7	86.3	87.5	88.2	88.0	86.7	84.8	44	2.3	914	0.6	4.20	1218	35.7	0.045
11:00	91.3	93.0	94.2	95.1	94.9	93.4	91.5	44.5	2.8	918	0.8	4.21	1326	38.7	0.051
11:15	97.8	99.3	100.5	101.5	101.3	100.1	98.0	44.8	3.4	921	1.1	4.22	1293	37.6	0.058
11:30	104.3	105.7	107.1	108.1	107.9	106.7	104.5	45.2	3.9	923	0.9	4.22	1331	38.6	0.064
11:45	110.6	112.3	113.5	114.5	114.5	113.2	110.9	45.6	4	926	1.1	4.23	1369	39.6	0.070
12:00	117.2	119.0	120.2	121.2	121.0	119.7	117.4	45.9	4	927	1.3	4.24	1408	40.7	0.077
12:15	123.5	125.2	126.7	127.7	127.4	126.2	123.8	46.3	4	927	1.2	4.26	1483	42.8	0.083
12:30	129.8	131.6	132.9	133.9	133.6	132.6	130.1	46.6	4	926	1	4.27	1451	42.0	0.090
12:45	136.0	137.6	139.0	139.9	139.5	138.9	136.3	46.9	4	925	1	4.28	1388	40.2	0.096
13:00	142.1	143.6	144.9	145.9	145.4	145.1	142.4	47.1	4	923	1.1	4.29	1357	39.4	0.103

T_1^*/ T_4^* represent the inlet temperatures to the first collector and outlet temperatures from the last collector, respectively.

Appendix (B-Tables)   No. of day =221   δ= 15.66° ϕ =32.02° L_{loc} =44.33°

Table (B.4): Experimental Data for Evacuated Glass Receiver During 9th   August 2016   Flow rate: 500 L/hr.

Time	T_1^* (°C)	T_2 (°C)	T_3 (°C)	T_4^* (°C)	T_5 (°C)	T_6 (°C)	T_7 (°C)	T_a (°C)	Pressure of tank (barG)	Beam radiation, I_b (w/m²)	Wind speed (m/s)	Cp (kJ/kg k)	Q_u (W)	η_{thi} (%)	T_{in}-T_a/I_b
09:00	40.2	40.4	40.5	40.6	40.6	40.4	40.3	40.5	0	887	0.2	4.18	232	7.01	0.000
09:15	46.2	46.9	47.3	47.5	47.4	47.2	46.3	40.8	0	891	0.1	4.18	755	22.67	0.006
09:30	53.2	54.0	54.6	54.8	54.7	54.2	53.3	41.1	0.3	894	0.3	4.18	929	27.82	0.014
09:45	60.4	61.3	61.9	62.2	62.1	61.6	60.5	41.5	0.6	897	0.4	4.18	1046	31.22	0.021
10:00	67.8	68.7	69.3	69.7	69.6	69.0	67.9	41.8	0.9	901	0.3	4.19	1105	32.84	0.029
10:15	74.4	75.3	76.0	76.5	76.4	75.7	74.5	42.2	1.4	904	0.2	4.19	1223	36.21	0.036
10:30	81.1	82.1	82.8	83.4	83.3	82.4	81.2	42.5	1.9	907	0.3	4.20	1341	39.58	0.043
10:45	88.1	89.0	89.8	90.4	90.3	89.5	88.2	42.9	2.5	910	0.4	4.20	1343	39.51	0.050
11:00	95.4	96.4	97.2	97.8	97.7	96.8	95.5	43.4	3.1	913	0.5	4.21	1404	41.17	0.057
11:15	101.3	102.4	103.2	103.6	103.4	102.7	101.4	43.8	3.6	915	0.2	4.22	1348	39.44	0.063
11:30	108.0	109.0	109.8	110.4	110.2	109.5	108.1	44.1	4	918	0.3	4.23	1409	41.11	0.070
11:45	114.2	115.4	116.1	116.6	116.4	115.8	114.4	44.5	4	921	0.2	4.24	1413	41.07	0.076
12:00	121.0	122.0	122.9	123.5	123.4	122.6	121.1	44.9	4	924	0.1	4.25	1476	42.76	0.082
12:15	127.8	128.9	129.8	130.4	130.2	129.6	128.0	45.3	4	925	0.1	4.26	1539	44.55	0.089
12:30	134.4	135.6	136.4	137.0	136.8	136.2	134.6	45.6	4	925	0.2	4.28	1544	44.69	0.096
12:45	141.1	142.2	143.0	143.7	143.5	142.9	141.3	45.9	4	924	0.1	4.29	1520	44.04	0.103
13:00	147.5	148.6	149.3	149.9	149.7	149.5	147.8	46.1	4	922	0.1	4.31	1460	42.38	0.110

T_1^*/ T_4^* represent the inlet temperatures to the first collector and outlet temperatures from the last collector, respectively.

Table (C.1): Experimental Data for Non-evacuated Glass Receiver During 10th   August 2016   Flow rate : 500 L/hr.

Time	T_1^* (°C)	T_2 (°C)	T_3 (°C)	T_4^* (°C)	T_5 (°C)	T_6 (°C)	T_7 (°C)	T_a (°C)	Pressure of tank (barG)	Beam radiation, I_b (w/m^2)	Wind speed (m/s)	Cp (kJ/kg k)	Q_u (W)	η_{thi} (%)	T_{in}-T_a/I_b
09:00	40.7	40.8	40.9	41.0	41.0	40.8	40.7	40.9	0	896	0.3	4.18	174	5.2	0.000
09:15	47.7	48.0	48.0	48.1	48.0	47.9	47.8	41.2	0	901	0.2	4.18	219	6.5	0.007
09:30	54.3	54.5	54.7	54.8	54.7	54.6	54.4	41.4	0.3	906	0.2	4.18	283	8.4	0.014
09:45	59.6	59.8	60.0	60.0	59.9	59.9	59.7	41.7	0.5	911	0.3	4.18	232	6.8	0.020
10:00	64.9	65.1	65.3	65.4	65.3	65.2	65.0	42	0.7	915	0.2	4.19	291	8.5	0.025
10:15	69.8	70.1	70.3	70.4	70.3	70.1	69.9	42.4	1	918	0.1	4.19	349	10.2	0.030
10:30	74.3	74.7	74.9	75.0	74.9	74.6	74.4	42.8	1.3	921	0.2	4.19	429	12.5	0.034
10:45	78.3	78.7	78.9	79.1	79.0	78.6	78.4	43.2	1.6	925	0.3	4.19	494	14.3	0.038
11:00	82.2	82.6	82.8	83.0	82.9	82.5	82.3	43.6	1.9	927	0.2	4.20	466	13.5	0.042
11:15	85.8	86.3	86.5	86.7	86.6	86.2	86.0	44	2.2	930	0.1	4.20	518	14.9	0.045
11:30	89.7	90.1	90.3	90.6	90.4	90.1	89.8	44.3	2.5	934	0.7	4.20	514	14.7	0.049
11:45	93.4	93.9	94.1	94.4	94.3	93.8	93.5	44.6	2.8	937	0.3	4.21	555	15.9	0.052
12:00	97.1	97.7	97.9	98.1	97.9	97.5	97.2	45	3.1	940	0.4	4.21	614	17.5	0.055
12:15	100.7	101.1	101.5	101.8	101.6	101.2	100.9	45.4	3.4	943	0.1	4.22	627	17.8	0.059
12:30	104.1	104.5	104.8	105.1	104.9	104.6	104.3	45.7	3.8	941	0.5	4.22	586	16.7	0.062
12:45	107.3	107.7	108.0	108.2	108.0	107.8	107.5	45.9	4	939	0.3	4.23	528	15.1	0.065
13:00	110.3	110.7	110.9	111.1	110.9	110.8	110.5	46.2	4	938	0.2	4.23	470	13.4	0.068

T_1^*/ T_4^* represent the inlet temperatures to the first collector and outlet temperatures from the last collector, respectively.

Table (C.2): Experimental Data for Non-evacuated Glass Receiver During 11th August 2016   Flow rate : 300 L/hr.

Time	T$_1$* (°C)	T$_2$ (°C)	T$_3$ (°C)	T$_4$* (°C)	T$_5$ (°C)	T$_6$ (°C)	T$_7$ (°C)	T$_a$ (°C)	Pressure of tank (barG)	Beam radiation, I$_b$ (w/m^2)	Wind speed (m/s)	Cp (kJ/kg k)	Q$_u$ (W)	η_{thi} (%)	T$_{in}$-T$_a$/I$_b$
09:00	40.2	40.4	40.5	40.6	40.6	40.3	40.2	40.6	0	897	0.5	4.18	139	4.2	0.000
09:15	44.7	45.0	45.1	45.2	45.1	45.0	44.8	40.9	0	901	0.9	4.18	170	5.1	0.004
09:30	50.0	50.4	50.7	50.6	50.5	50.5	50.1	41.2	0	905	1.1	4.18	205	6.1	0.010
09:45	55.3	55.8	55.9	55.9	55.8	55.7	55.4	41.6	0.3	909	0.9	4.18	240	7.1	0.015
10:00	60.5	61.0	61.1	61.2	61.1	61.0	60.6	42.1	0.5	912	0.5	4.18	240	7.0	0.020
10:15	65.8	66.3	66.5	66.6	66.5	66.4	65.9	42.5	0.8	916	0.8	4.19	275	8.0	0.025
10:30	70.6	71.2	71.5	71.6	71.5	71.3	70.8	43	1.1	919	0.7	4.19	345	10.0	0.030
10:45	75.2	75.9	76.2	76.3	76.1	75.8	75.3	43.5	1.4	923	1.3	4.19	363	10.5	0.034
11:00	79.9	80.5	80.8	81.0	80.9	80.6	80.1	44	1.7	926	0.9	4.20	415	12.0	0.039
11:15	84.7	85.3	85.8	86.0	85.8	85.5	84.9	44.4	2	930	1.3	4.20	450	13.0	0.043
11:30	88.4	89.1	89.5	89.7	89.5	89.2	88.6	44.8	2.4	933	1.2	4.20	469	13.5	0.047
11:45	91.8	92.5	92.9	93.2	92.9	92.8	92.1	45.3	2.7	935	1.5	4.21	469	13.4	0.050
12:00	95.5	96.2	96.6	97.0	96.7	96.5	95.8	45.7	3	938	0.8	4.21	505	14.4	0.053
12:15	98.5	99.1	99.6	100.0	99.7	99.4	98.8	46.1	3.3	939	0.9	4.21	534	15.2	0.056
12:30	101.5	102.2	102.6	103.0	102.7	102.5	101.8	46.3	3.6	938	0.8	4.22	523	14.9	0.059
12:45	104.0	104.6	105.0	105.4	105.1	105.1	104.3	46.5	3.9	936	0.7	4.22	510	14.6	0.061
13:00	107.2	107.9	108.3	108.6	108.3	108.3	107.5	46.7	4	934	1.1	4.23	492	14.1	0.065

T$_1$*/ T$_4$* represent the inlet temperatures to the first collector and outlet temperatures from the last collector, respectively.

Table (C.3): Experimental Data for Non-evacuated Glass Receiver During 12th   August 2016   Flow rate : 650 L/hr.

Time	$T_1{}^*$ (ºC)	T_2 (ºC)	T_3 (ºC)	$T_4{}^*$ (ºC)	T_5 (ºC)	T_6 (ºC)	T_7 (ºC)	T_a (ºC)	Pressure of tank (barG)	Beam radiation, I_b (w/m²)	Wind speed (m/s)	Cp (kJ/kg k)	Q_u (W)	η_{thi} (%)	T_{in}-T_a/I_b
09:00	40.8	40.9	41.0	41.1	41.1	40.9	40.8	41	0	886	1.3	4.18	226	6.8	0.000
09:15	47.0	47.2	47.3	47.4	47.3	47.0	46.8	41.2	0	890	0.9	4.18	302	9.1	0.007
09:30	53.3	53.5	53.6	53.8	53.7	53.5	53.3	41.6	0.3	893	0.7	4.18	377	11.3	0.013
09:45	59.2	59.3	59.6	59.7	59.6	59.4	59.2	42	0.5	897	0.6	4.18	378	11.3	0.019
10:00	64.3	64.6	64.7	64.9	64.8	64.6	64.4	42.4	0.7	900	0.4	4.18	469	14.0	0.024
10:15	68.9	69.1	69.4	69.5	69.4	69.2	69.0	42.6	1	903	0.5	4.19	454	13.5	0.029
10:30	73.7	74.0	74.2	74.4	74.3	74.0	73.8	42.9	1.3	905	0.1	4.19	500	14.8	0.034
10:45	78.5	78.8	79.0	79.1	79.0	78.8	78.6	43.3	1.6	909	0.2	4.19	486	14.3	0.039
11:00	82.8	83.1	83.3	83.5	83.4	83.1	82.9	43.7	1.9	913	0.5	4.20	494	14.5	0.043
11:15	87.3	87.6	87.9	88.1	88.0	87.7	87.5	44	2.3	916	0.6	4.20	569	16.6	0.047
11:30	91.2	91.5	91.7	92.0	91.9	91.6	91.3	44.4	2.6	917	1	4.21	577	16.9	0.051
11:45	95.0	95.3	95.6	95.8	95.7	95.4	95.1	44.7	2.9	919	0.7	4.21	570	16.6	0.055
12:00	98.8	99.2	99.4	99.7	99.6	99.2	98.9	45.1	3.2	921	0.5	4.21	647	18.8	0.058
12:15	102.0	102.3	102.6	102.9	102.8	102.5	102.2	45.4	3.6	922	0.3	4.22	648	18.8	0.061
12:30	105.4	105.7	106.0	106.3	106.2	105.8	105.5	45.8	4	921	0.4	4.22	648	18.8	0.065
12:45	108.5	108.7	109.0	109.3	109.2	109.0	108.7	46	4	920	0.6	4.23	589	17.1	0.068
13:00	111.5	111.7	112.0	112.2	112.0	112.2	111.8	46.3	4	918	0.3	4.23	535	15.6	0.071

$T_1{}^*$/ $T_4{}^*$ represent the inlet temperatures to the first collector and outlet temperatures from the last collector, respectively.

Appendix (C-Tables)   No. of day =225   δ= 14.42º ϕ =32.02º L_{loc} =44.33º

Table (C.4): Experimental Data for Non-evacuated Glass Receiver During 13th August 2016   Flow rate : 100 L/hr.

Time	T_1^* (ºC)	T_2 (ºC)	T_3 (ºC)	T_4^* (ºC)	T_5 (ºC)	T_6 (ºC)	T_7 (ºC)	T_a (ºC)	Pressure of tank (barG)	Beam radiation, I_b (w/m^2)	Wind speed (m/s)	Cp (kJ/kg k)	Q_u (W)	η_{thi} (%)	T_{in}-T_a/I_b
09:00	40.0	40.2	40.3	40.4	40.3	40.1	40.0	40.5	0	894	0.1	4.18	46	1.4	-0.001
09:15	45.0	45.4	45.6	45.8	45.71	45.61	45.1	40.7	0	899	0.2	4.18	93	2.8	0.005
09:30	50.3	50.8	51.1	51.3	51.12	50.92	50.2	41.2	0.1	905	0.5	4.18	116	3.4	0.010
09:45	55.5	56.0	56.3	56.6	56.53	56.23	55.6	41.6	0.3	909	0.3	4.18	128	3.8	0.015
10:00	60.5	61.1	61.5	61.8	61.64	61.44	60.7	41.9	0.5	913	0.4	4.18	151	4.4	0.020
10:15	65.4	66.1	66.5	66.8	66.55	66.25	65.5	42.3	0.7	916	0.3	4.19	163	4.8	0.025
10:30	69.6	70.3	70.7	71.1	70.86	70.56	69.8	42.7	1	920	0.6	4.19	175	5.1	0.029
10:45	73.7	74.4	74.9	75.3	75.07	74.77	73.9	43.1	1.3	923	0.5	4.19	186	5.4	0.033
11:00	77.7	78.5	79.1	79.5	79.18	78.88	77.9	43.4	1.6	925	0.3	4.19	210	6.1	0.037
11:15	81.1	82.1	82.7	83.1	82.89	82.29	81.4	43.7	1.9	928	0.2	4.20	233	6.7	0.040
11:30	84.8	85.8	86.4	87.0	86.70	86.00	85.0	44	2.2	930	0.4	4.20	257	7.4	0.044
11:45	88.2	89.4	90.0	90.6	90.31	89.51	88.5	44.2	2.5	933	0.5	4.20	280	8.0	0.047
12:00	92.0	93.2	94.0	94.5	94.22	93.42	92.3	44.6	2.8	934	0.3	4.21	292	8.4	0.051
12:15	95.2	96.4	97.3	97.9	97.63	96.73	95.5	44.9	3.1	936	0.4	4.21	316	9.0	0.054
12:30	98.1	99.3	100.1	100.7	100.44	99.64	98.5	45.3	3.4	935	0.2	4.21	305	8.7	0.057
12:45	101.2	102.3	103.1	103.7	103.25	102.65	101.5	45.5	3.7	934	0.3	4.22	293	8.4	0.060
13:00	103.9	105.0	105.7	106.3	105.86	105.36	104.3	45.8	4	932	0.2	4.22	282	8.1	0.062

T_1^*/ T_4^* represent the inlet temperatures to the first collector and outlet temperatures from the last collector, respectively.

Appendix [D]

Error Analysis

The accuracy of obtaining experimental results depends upon two factors: the accuracy of measurements and the nature of rig design. The last factor can be affected by the following:

1. Solar radiation angles.
2. The type of thermocouple and method of fixing it on the surface.

There is no doubt that, the maximum portion of errors in calculations referred essentially to the errors in the measured quantities. Hence, to calculate the error in the obtained results **Kline and McClintock, (1953)** method is used in this field.

Let the result R be a function of n independent variables: e_1, e_2 ....., e_n.

$$R = R(e_1, e_2 \ldots\ldots e_n) \qquad\qquad \ldots\ldots\ldots\ldots\ldots\ldots\ldots\ldots\ldots\ldots\ldots\ldots (D.1)$$

For small variations in the variables, this relation can be expressed in linear form as:

$$\delta R = \frac{\partial R}{\partial e_1}\delta e_1 + \frac{\partial R}{\partial e_2}\delta e_2 + \cdots + \frac{\partial R}{\partial e_n}\delta e_n \qquad \ldots\ldots\ldots\ldots\ldots\ldots\ldots\ldots\ldots\ldots\ldots (D.2)$$

Hence, the uncertainty interval (w) in the result can be given as:

$$w_R = \left[\left(\frac{\partial R}{\partial e_1}w_1\right)^2 + \left(\frac{\partial R}{\partial e_2}w_2\right)^2 + \cdots + \left(\frac{\partial R}{\partial e_n}w_n\right)^2\right]^{1/2} \qquad \ldots\ldots\ldots\ldots\ldots\ldots (D.3)$$

Or;

$$w_R = \left[\sum_{i=1}^{n}\left(\frac{\partial R}{\partial e_i}w_i\right)^2\right]^{1/2} \qquad \ldots\ldots\ldots\ldots\ldots\ldots\ldots\ldots\ldots\ldots\ldots\ldots\ldots\ldots (D.4)$$

Eq. (D.3) is greatly simplified upon dividing by Eq. (D.2) to nondimensionalize:

$$\frac{w_R}{R} = \left[\left(\frac{\partial R}{\partial e_1}\frac{w_1}{R}\right)^2 + \left(\frac{\partial R}{\partial e_2}\frac{w_2}{R}\right)^2 + \cdots + \left(\frac{\partial R}{\partial e_n}\frac{w_n}{R}\right)^2\right]^{1/2} \quad \dots \dots \dots \dots \dots \text{(D.5)}$$

Or;

$$\frac{w_R}{R} = \left[\sum_{i=1}^{n}\left(\frac{w_i}{e_i}\right)^2\right]^{1/2} \quad \dots \dots \dots \dots \dots \dots \dots \dots \text{(D.6)}$$

Hence, the experimental errors that may be happen in the independent parameters are given in the following table which is taken from measuring devices as follows:

Independent parameter (e)	Uncertainty (W)
Temperature (T)	$\pm 0.1 \ ^\circ C$
Solar radiation (I)	$\pm 10 \ W/m^2$
Mass flow rate ($\dot{m}$)	± 0.0004 kg/s
pressure gauge (bar)	± 0.001 bar

The thermal collector efficiency Eq. (3.28) can be written as follows:

$$\eta_{th} = \frac{Q_u}{I_b A_a} = \frac{\dot{m}_w * C_p * (T_{f,o} - T_{f,i})}{I_b A_a} = \frac{\dot{m}_w * C_p * \Delta T}{I_b A_a} \quad \dots \dots \dots \dots \dots \text{(D.7)}$$

The experimental error in the thermal collector efficiency calculation can be expressed in the following manner:

$$\frac{\partial \eta_{th}}{\partial \Delta T} = \frac{\dot{m}_w * C_p}{I_b A_a} \quad \dots \dots \dots \dots \dots \dots \dots \dots \dots \text{(D.8)}$$

$$\frac{\partial \eta_{th}}{\partial I_b} = -\frac{\dot{m}_w * C_p * \Delta T}{I_b^2 A_a} \quad \dots \dots \dots \dots \dots \dots \dots \dots \text{(D.9)}$$

$$\frac{\partial \eta_{th}}{\partial \dot{m}_w} = \frac{C_p \, \Delta T}{I_b \, A_a} \quad \dotfill \text{(D.10)}$$

Thus;

$$w_{\eta_{th}} = \left[\left(\frac{\partial \eta_{th}}{\partial \Delta T} w_{\Delta T} \right)^2 + \left(\frac{\partial \eta_{th}}{\partial I_b} w_{I_b} \right)^2 + \left(\frac{\partial \eta_{th}}{\partial \dot{m}_w} w_{\dot{m}_w} \right)^2 + \right]^{1/2} \dotfill \text{(D.11)}$$

Example: (At 11:00 AM on the 6th of August)

I_b=922 W/m², $\dot{m}_w$=0.1805 kg/s, C_p=4210 j/kg.K, $T_{f,i}$=98.3 ºC, $T_{f,o}$= 100.4 ºC , ΔT= 2.1 ºC , A_a=3.73 m² , η_{th}=0.464

$$w_{\eta_{th}} = \left[(0.220962 * 0.1)^2 + (-5.032 * 10^{-4} * 10)^2 + (2.57 * 0.0004)^2 \right]^{1/2}$$

$$= 0.0226852$$

Thus;

$$\frac{w_{\eta_{th}}}{\eta_{th}} = 0.0488905$$

<div align="center">

Appendix [E]

Calculation Procedures

</div>

As a sample for calculations, one of the experimental tests that carried out has been adopted to clarify experimental calculations.

E.1 Thermal Instantaneous Efficiency

For the experimental test that carried on the 6th of August, the data processed at 12:00 PM for the solar collector with evacuated glass receiver, was as below:

$$m^{\cdot} = 650\frac{L}{hr.} = 0.18\frac{kg}{s} \ , \ Cp = 4260\frac{J}{kg.k} \ , \ T_{f,i} = 125.2 \ °C \ , \ T_{f,o} =$$
127.4 °C

I_b =929 W/m^2 , A_a =3.73m^2

Now, recall Eq. (3.28)

$$\eta_{th} = \frac{m^{\cdot} \ C_p(T_{f,o} - T_{f,i})}{A_a I_b} = \frac{0.1805*4260*(127.4 - 125.2)}{3.73*929} = 48.8\%$$

E.2 Heat Removal Factor and Heat Loss Coefficient

From the figure (5.9 a) for the solar collector with evacuated glass receiver and 650L/hr. flow rate, the thermal collector efficiency that evaluated by using linear curve fitting across the heat loss parameters $(\Delta T/I_b)$, was as below:

$$\eta_{th} = 0.522 - 2.205\ (\Delta T/I_b)$$

This equation has the form of the Eq. (3.29), which can help to experimentally obtain the heat removal factor F_R and the overall heat loss coefficient U_L.

 Where

$F_R U_L/C$ represents the slope of the line $= 2.205$ ……………………. (E.1)

and, $F_R\ \eta_o$ represents the y-intercept $= 0.522$ ………………………….(E.2)

From (E.2) at $\eta_o = 0.55$ ⟶ $F_R = 0.95$

From (E.1) at $F_R = 0.95,\ C = 4.68$ ⟶ $U_L = 10.8$ W/m² k

Appendix [F]

Calibration of Apparatuses
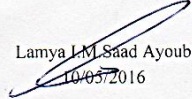
Calibration Certificate

Central Organization for Standardization and Quality
Control (COSQC)

Metrology Department

P.O. Box13032 Algeria street, Baghdad ,Tel:7765180   E-Mail : cosqc@yahoo.com

Certificate No.: PH   403 / 2016

Date of issue :   09/05/2016

Customer	
Name:	وزارة التعليم العالي والبحث العلمي / جامعة كربلاء / كلية الهندسة
Address:	العراق

Item under calibration	
Description:	PORTABLE MULTI THERMOMETER + TC (K)
Manufacturer:	YOKOGAWA / JAPAN
Model:	2423 A
Serial number:	1
Other identification:	(0 -------- 170) °C
Date of reception:	05/05/2016
Condition of reception:	GOOD

Standard(s) used in the calibration			
Description:	Thermometer readout	PT100	Water bath
Manufacturer:	Fluke / USA	Fluke / USA	Hetogfrig / Danmark
Model:	1529	5615	———
Serial number:	B2C801	10860	———
Other identification:	———	———	———

Calibration information	
Date of calibration:	09/05/2016
Place of calibration:	Temperature measurement lab
Method(s) of calibration:	Calibration method using Working Thermometer - Calibration Procedure 2008
Calibrated quantity:	Temprature / Celcius / ℃
Results of calibration:	Attached a complete result in Annex 1 of this certificate
Measurement uncertainty:	There ported expanded uncertainty is based on GUM Standard and the standard Uncertainty multiplied by coverage factor k=2 to give confidence level of 95%
Metrological traceability:	The traceability of measurement results to the SI units is assured by theNational standard maintained at Central Organization for standardization and Quality Control through calibration at :- - COSQC/ Electrical lab (Cert. 028/2016/E) - Temp. measurement lab. (Cert. PH - 01-124-00) - NVLAB (REPORT NO. B3114057)
Environmental conditions of calibration:	Temp. (25 °C): ±1°C R. H.(50%) ±5%
Observations, opinions or recommendations:	

Performed by :

MUSTAFA + NEDAL
10/05/2016

Approved by:

Lamya J.M. Saad Ayoub
10/05/2016

1of 1

Figure (F.2):Calibration Certificate of Thermometer

Calibration Certificate

Central Organization for Standardization and Quality
Control (COSQC)

Metrology Department

P.O. Box13032 Algeria street, Baghdad ,Tel:7765180

E-Mail : cosqc@yahoo.com

Certificate No.: PH   403 / 2016

Date of issue :   09/05/2016

Results

Set Value C°	Reference Value C°	Indicate Value C°	Correction C°	ERROR C°	Uncertainty
35	35.7538	36.06	-0.3062	0.3062	0.612444608
100	99.8478	96.26	3.5878	-3.5878	0.615600078
170	171.0298	168.6	2.4298	-2.4298	0.629085091

Performed by:

MUSTAFA + NEDAL

Reviese by:

JAMAL

Approved by:

Lamya I.M.Saad Ayoub

2of 1

Figure(F.1): contd.

Calibration certificate

Central Organization for Standardization and Quality
Control (COSQC)
Metrology Department

P.O. Box13032 Aljadria street,Baghdad ,Tel:7765180   E-Mail :   cosqc@yahoo.com

Certificate No: PRE/472/2016
Date of issue: 8/5/2016

Customer	
Name:	جامعة كربلاء/ كلية الهندسة
Address:	

Item under calibration			
Description:	Pressure gauge		
Manufacturer:	HERDE		
Model:	Bourdon Tube		
Serial number:	/		
Other identification:	Rang = 10 bar	d = 0.2 bar	Tolerance= 1.6
Date of reception:	4/ 5 /2016		
Condition of reception:	New		

Standard(s) used in the calibration			
Description:	Portable pressure calibrator		
Manufacturer:	Jofra Instrument		
Model:	AMETEK		
Serial number:	9894005		
Other identification:	Rang = 20 bar	d = 0.001 bar	

Calibration information	
Date of calibration:	8/5/2016
Place of calibration:	Pressure Lab
Method(s) of calibration:	Calibration method using aportable pressure calibrator accuracy (1%) from full scall Base down DKD-6
Calibrated quantity:	Pressure
Results of calibration:	Attached a complete result in Annex 1 of this certificate
Measurement uncertainty:	The reported expanded uncertainty is based on GUM Standard and the standard Uncertainty multiplied by coverrage factor k=2 to give confidence level of 95
Metrological traceability:	The traceability of measurement to the SI units is assured by the National Standard maintained at centeral organization for standardization and quality control through calibration certificat issued from COFRAC accreditation No. 2.37
Environmental conditions of calibration:	Temp.: 23 ^{0}C ±2 R. H.(%) Pressure (mbar)
Observations, opinions or recommendations:	The results are within the tolerance according to DKD-6

Performed by:
Ahmed Salman

Approved by: Hanan A.J.Al-Moudares
Head of Mass & pressure section
8 /5 /2016

Page (1) of (2)

Figure (F.3): Calibration Certificate Of Gauge Pressure

F-3

Calibration certificate

Central Organization for Standardization and Quality Control (COSQC)
Metrology Department

P.O. Box13032 Aljadria street,Baghdad ,Tel:7765180

E-Mail : cosqc@yahoo.com

Certificate No: PRE/472/2016
Date of issue: 8/5/2016

Results

Applied Pressure Bar	Reference Reading		Mean Reading bar	Deviation bar	Error %	Uncertainty ± bar
	Upward bar	Downward bar				
0	0.0	0.0	0.0	0.0	0.0	0.001
2	1.9	1.9	1.9	0.1	1.0	0.001
4	4.0	4.0	4.0	0.0	0.0	0.001
6	6.0	6.0	6.0	0.0	0.0	0.001
8	8.0	8.0	8.0	0.0	0.0	0.002
10	9.9	9.9	9.9	0.1	1.0	0.002

Performed by:
Ahmed Salman

Approved by:
Hanan A.J.Al-Moudares
Head of Mass & pressure section

8/5/2016

Page (2) of (2)

This certificate is issued in accordance with the laboratory accrediation requirements.It provides tracibility of measurement to recognized national standards,and to the units of measurement realized at the COSQC or other recognized national standards laboratories. This certificate may not be reproduced other than in full by photographic process.This certificate refers only to the particular item submitted for calibration.

Figure (F.2): Contd.

الخلاصة

تم بناء وتشغيل واختبار ثلاثة مجمعات شمسية حوضية ذات قطع مكافئ من اجل توليد الماء الساخن والبخار عند درجة حرارة متوسطة. في هذه الدراسة تم تقديم بحث عملي لاختبار أداء ال PTC (مساحة الفتحة الكلية $3.73\ m^2$). النموذج تم تصنيعه باستخدام مواد محلية المصدر ويشتمل على أسطح عاكسة، هيكل تثبيت يعمل كمعقب يدوي للشمس وكذلك أنابيب امتصاص. تم تصنيع المجمعات من الألمنيوم لخفة وزنة ومقامته للظروف المناخية. تصميم المجمعات كان على أساس أن تكون المستلمات بدون تظليل حيث تم تطوير معقب شمسي يدوي (بمحورين) لتعقب الإشعاع الشمسي المباشر. الاختبارات العملية نفذت تحت الظروف المناخية لمدينة النجف الأشرف ($32.02^o\ N$ و $44.33^o\ E$) خلال أيام مختارة من شهر أغسطس. البيانات المقاسة تم جمعها لثمانية أيام (6,5 و8 إلى 13 أغسطس 2016). الاختبارات نفذت باستخدام القياسات الخارجية لحساب الكسب الحراري المفيد والكفاءة الحرارية اللحظية. في تحليل أداء أل(PTC) تم بحث تأثير درجة حرارة الدخول، الظروف المحيطة، حالتين للمستلم الزجاجي والتغير في معدل جريان مائع التشغيل. تم حساب الأداء الحراري لل(PTC) طبقا ل (Standard ASHRAE 93-1986) وتم إيجاد منحني الكفاء لل(PTC). ذروة الكفاءات المستحصلة كانت (50%، 18.8%) للمجمعات الشمسية مع المستلم المفرغ وغير المفرغ على التوالي عند معدل الجريان الأعلى. تم توليد بخار بدرجة حرارة تفوق ($152\ ^0C$) عند ضغط (4barG). معادلة كفاءة المجمع المستحصلة في العمل الحالي تمت مقارنتها مع بحوث أخرى. النتائج النهائية تبين بان تقنية استخدام ال(PTC) تكون قابلة للتطبيق للتطبيقات التي تتطلب درجات حرارة تصل إلى ($152\ ^0C$).

وزارة التعليم العالي والبحث العلمي

جامعة كربلاء ـ كلية الهندسة

قسم الهندسة الميكانيكية

بناء واختبار مجمع حوضي ذو قطع مكافئ لتوليد البخار

رسالة مقدمة إلى كلية الهندسة ـ جامعة كربلاء كجزء من متطلبات نيل درجة الماجستير في الهندسة الميكانيكية

من قبل

احمد عبد الرزاق شهيد

بكالوريوس 2005

بإشراف

أ.م.د محمد حسن عبود

أ.م.د رؤوف محمد راضي

كانون الثاني 2017

ربيع الآخر 1439هـ